VLADIMIR I. GUREVICH

RECENT SEDIMENTOGENESIS AND ENVIRONMENT ON THE ARCTIC SHELF OF WESTERN EURASIA

MEDDELELSER NR. 131
OSLO 1995

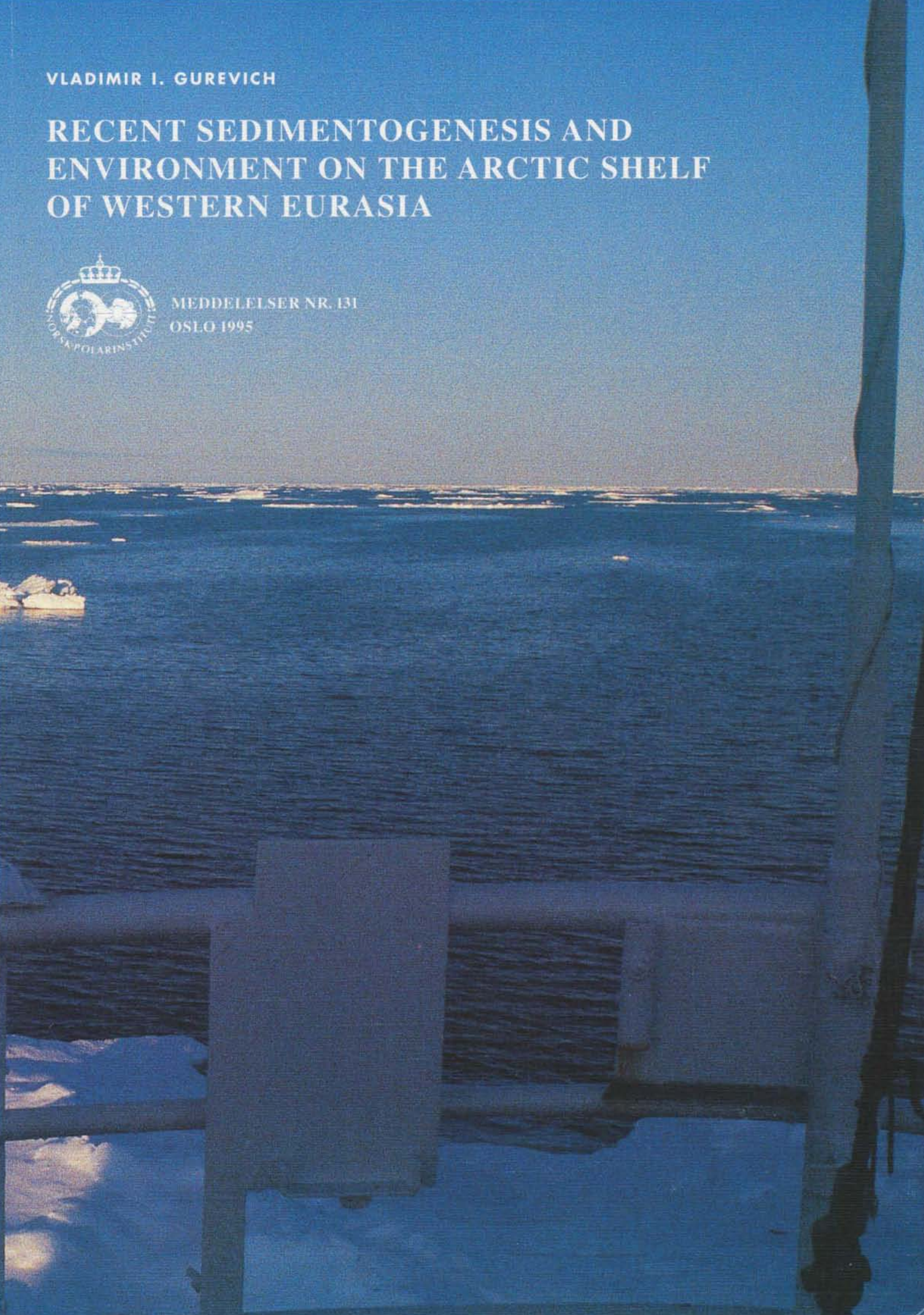

Vladimir I. Gurevich

RECENT SEDIMENTOGENESIS AND ENVIRONMENT ON THE ARCTIC SHELF OF WESTERN EURASIA

MEDDELELSER NR. 131
OSLO 1995

Vladimir I. Gurevich († 1994)
VNIIOkeangeologia
St. Petersburg
Russia

Editor of text and illustrations: Annemor Brekke
Cover photo: Anders Solheim: Scenary in the Northern Barents Sea
Grapich design/production: Grimshei Grafiske, Lørenskog, Norway
Printet in October 1995
ISBN 82-7666-071-1

CONTENTS

PREFACE

In June 1989, the Norwegian Research Council for Science and the Humanities (NAVF) and the Russian State Committee for Science and Technology signed a general agreement on Cooperation within Arctic research. As a result of this agreement, a programme concerned with Arctic geology was established - *Geological Correlation and Evolution of the Eastern Svalbard – Franz Josef Land Region: The Northern Barents Sea Geotraverse* – with participation from the Russian Scientific Research Institute for Geology and Mineral Resources of the World Ocean (VNII-Okeangeologia), the University of Oslo, and the Norwegian Polar Institute. Although the data base for the present study was not acquired as a part of this progamme, its publication is a direct result of this cooperation.

An initial phase of the *Northern Barents Sea Geotraverse* consisted of a compilation of already existing, available data from the region. The present study forms an important part of this compilation, combining results from 25 years of work in a series of maps. Despite their small scale, some of the maps are based on several thousands of observations. They therefore represent an important body of background information which should be considered before more detailed and specific observation programmes are carried out.

The observations and analyses presented here span a wide range of scientific topics and are mostly presented on maps on a scale of 1:15 mill. Therefore, individual investigators possessing detailed information on specific topics, or in localised areas, may find discrepancies between their own data and the present publication. However, this work is not intended to be detailed on local scales; its unique value lies in presenting such a wide variety of parameters as comparable, regional maps.

Some terms used in this publication may be attributed a slightly different meaning from that traditionally applied in western countries. Despite the work done on the English translation of the manuscript, we have tried not to alter the text significantly from its original version as the interpretations and conclusions are representative of the author's view, and not necessarily of the view of the Norwegian Polar Institute. We believe, however, that the present publication will be of value to those working on related issues in the same region. We also believe it will prove important as background material for the planning and conduction of further investigations.

It was a shock to learn that Dr. Vladimir Gurevich died suddenly in the summer of 1994, before he could see the present publication printed. It is our sincere hope that this paper, as well as his many other publications, will be read and appreciated by many. In that way it can be said that Vladimir Gurevich has made a significant contribution to a better understanding of the dynamic physical systems of the Arctic seas, an area of great international interest today.

Anders Solheim

INTRODUCTION

The Western Arctic Shelf of Eurasia is the world's largest shelf, extending across the entire Barents Sea, White Sea and Kara Sea. The author has been systematically studying modern sedimentogenesis and environmental problems on this shelf since 1967. However, most publications dealing with these matters have been written in Russian and are inaccessible to our European and American colleagues. A brief overview of the research is therefore presented in this publication.

To achieve maximum brevity, the author was inspired by the Chinese proverb "better to look once than listen a thousand times". The primary data and conclusions are therefore mainly presented in tables and on 1:15,000,000 scale maps. The maps are mainly based on data acquired from 1967 to 1991, but an attempt has been made to utilise relevant material from our forerunners as well as other present-day workers, especially from the Russian Scientific Research Institute for Geology and Mineral Resources of the World's Oceans (VNIIOkeangeologia) where this manuscript has been prepared.

1. SEDIMENTOLOGICAL STUDIES

The White Sea and Barents Sea are the "cradle" of Russian marine geology, and have been considerably more studied than the Kara Sea. Figures 1.1–1.3 summarise the present extent of our research in these areas, and Table 1.1 shows the data that form the basis for our interpretations.

The thicknesses of Upper Cenozoic deposits given in Table 1.1 are based on our own published data (see references) and those obtained by Norwegian scientists (Solheim & Kristoffersen 1984, A. Elverhøi, pers. comm.), as well as other Russian work (V.E. Melnitsky, R.R. Murzin, D.A. Kostin, V.M. Zakharenko, M.I. Kniazev, R.B. Krapivner, I.I. Gritsenko, V.I. Bondarev, N.A. Spiridonov, N.A. Devdariany, Yu.A. Pavlidis and others, pers. comm.). Data from maps compiled by M.L. Verba, V.E. Volk, A.K. Bogolepov and others (pers. comm.) have been used to analyse the conformity of structural planes. To supplement our own material concerning the study and mapping of recent deposits we have used data from Klenova (1960), Nevesskiy (in Nevesskiy, Medvedev & Kalinenko 1977), and I.K. Avilov, V.D. Dibner, D.S. Yashin, N.N. Lapina, Yu. G. Samoilovitch and others (pers. comm.).

The maps published here have been reduced to 1:15,000,000 from base maps constructed on a scale of 1:2,500,000 using the Gauss-Krüger conical projection. The author hopes that this scale is at least adequate for the amount of detail shown.

Table 1.1 Geological investigations on the Western Arctic Shelf

Type of investigation	*Unit*	*White Sea*	*Shelf Barents Sea*	*Kara Sea*	*Entire Western Arctic*
Area	million km²	0.078	1.52	0.74	2.50
Shallow-seismic profiling					
low-frequency	km	3275	69 920	9708	82 903
high-frequency	"	1700	6050	792	21 070
Echo sounding	"	890	9200	300	10 390
Bore holes					
onshore	hole	45	226	30	301
offshore	"	10	81	7	98
Satellite imagery	thousand km²	6.47	3.20	9.10	18.8
Gravity cores	sites				
excavated Holocene bed	"	21	511	90	622
nonexcavated "	"	272	1396	260	1928
Dredge	sites	1466	7985	6919	18 628
Lithological-geochemical analysis	sites				
granulometric	"	830	4100	1200	6130
carbonate determin.	"	860	1778	367	3005
organic carbon and bituminoids	"	344	1146	443	2078
gas analysis	"	130	700	220	1050
pollen analysis	"	40	433	149	622
mineralogical analysis of heavy suite	"	140	1135	135	1420
clay mineral determin.	"	90	765	220	1075
petrographical analysis of gravel fraction	"	20	499	50	569
heavy metal determin.	"	120	835	110	1065
radiocarbon dating	"	69	25	3	97
determin. of density and humidity	"	115	620	76	811
Hydrological study of near-bottom layer	sites	71	367	127	565
Study of benthos	sites				
quantitative collections	"	190	870	43	1103
qualitative collections (with trawl)	"	37	2460	35	2532
submarine photography	"	1148	489	30	1667
Geo-ecological investigation	sites				
determination of antibiotic activity of sporogenous bacteria	"	45	150	–	195
determination of radionuclides (^{134}Cs, ^{137}Cs, others)	"	–	252	174	426

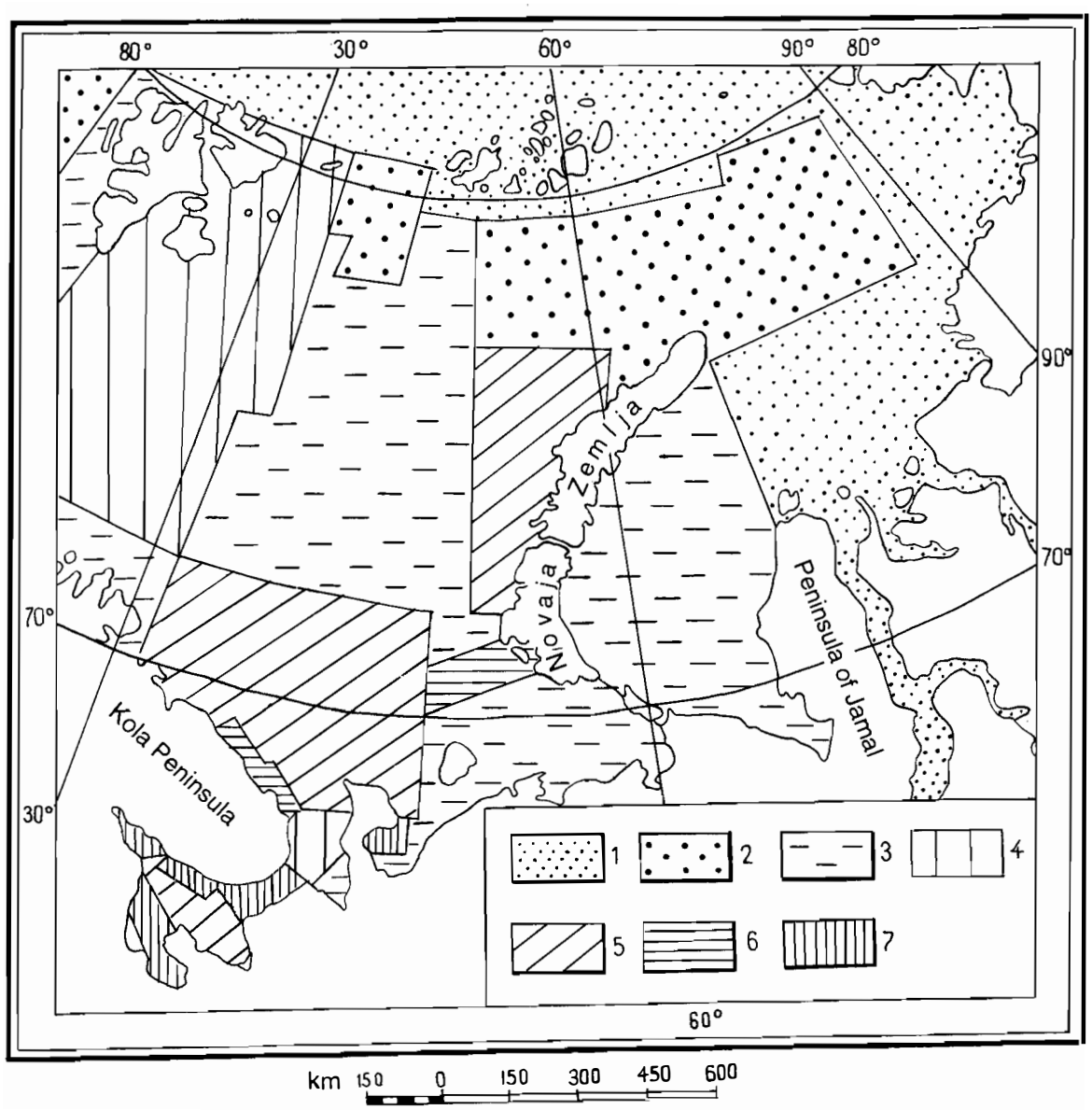

Fig. 1.1 Shallow seismic coverage of the Western Arctic Shelf at the beginning of 1992. 1. no shallow seismic, 2. scattered regional profiles; 3. series of regional profiles on a scale of 1:2,500,000; 4. survey grid of profiles on a scale of 1:1,500,000; 5. survey grid of profiles on a scale of 1:1,000,000; 6. survey and reconnaissance grids on a scale of 1:500,000; 7. survey grid on a scale of 1:200,000.

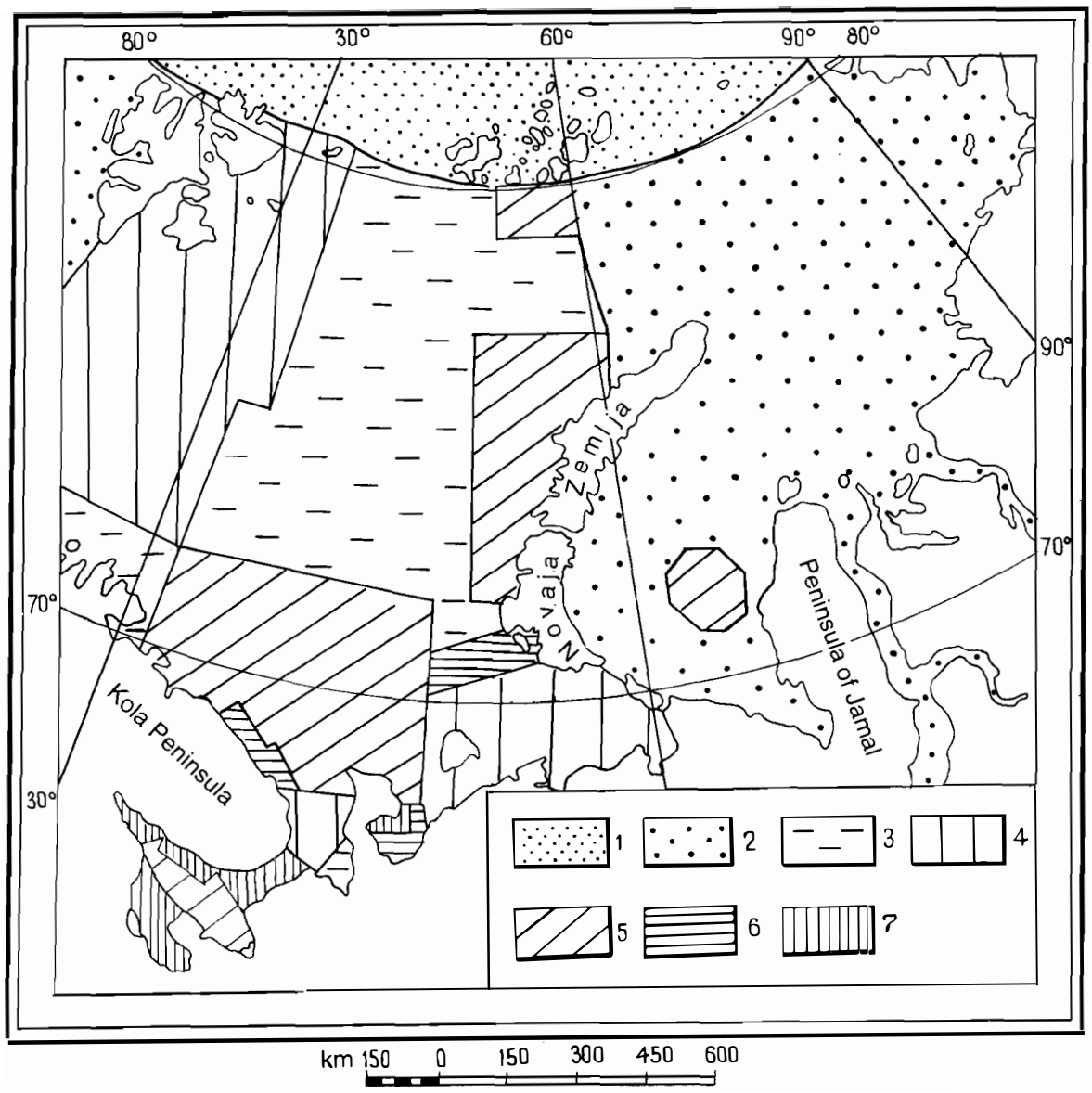

Fig. 1.2 Investigation of the modern deposits of the Western Arctic Shelf by the beginning of 1992. 1. regional, sporadic work with average sampling density on a scale of 1:5,000,000; 2. regional non-systematic work with average sampling density on a scale of 1:2,500,000; 3. regional syste-matic work along profiles with average sampling density on a scale of 1:2,000, 000, 4. regional systematic work in specific areas, with average sampling density on a scale of 1:1,500,000; 5. small-scale surveying with sampling density on a scale of 1:1,000,000; 6. small-scale reconnaissance and surveying with sampling density on a scale of 1:500,000; 7. medium-scale surveying with sampling density on a scale of 1:200,000; or larger.

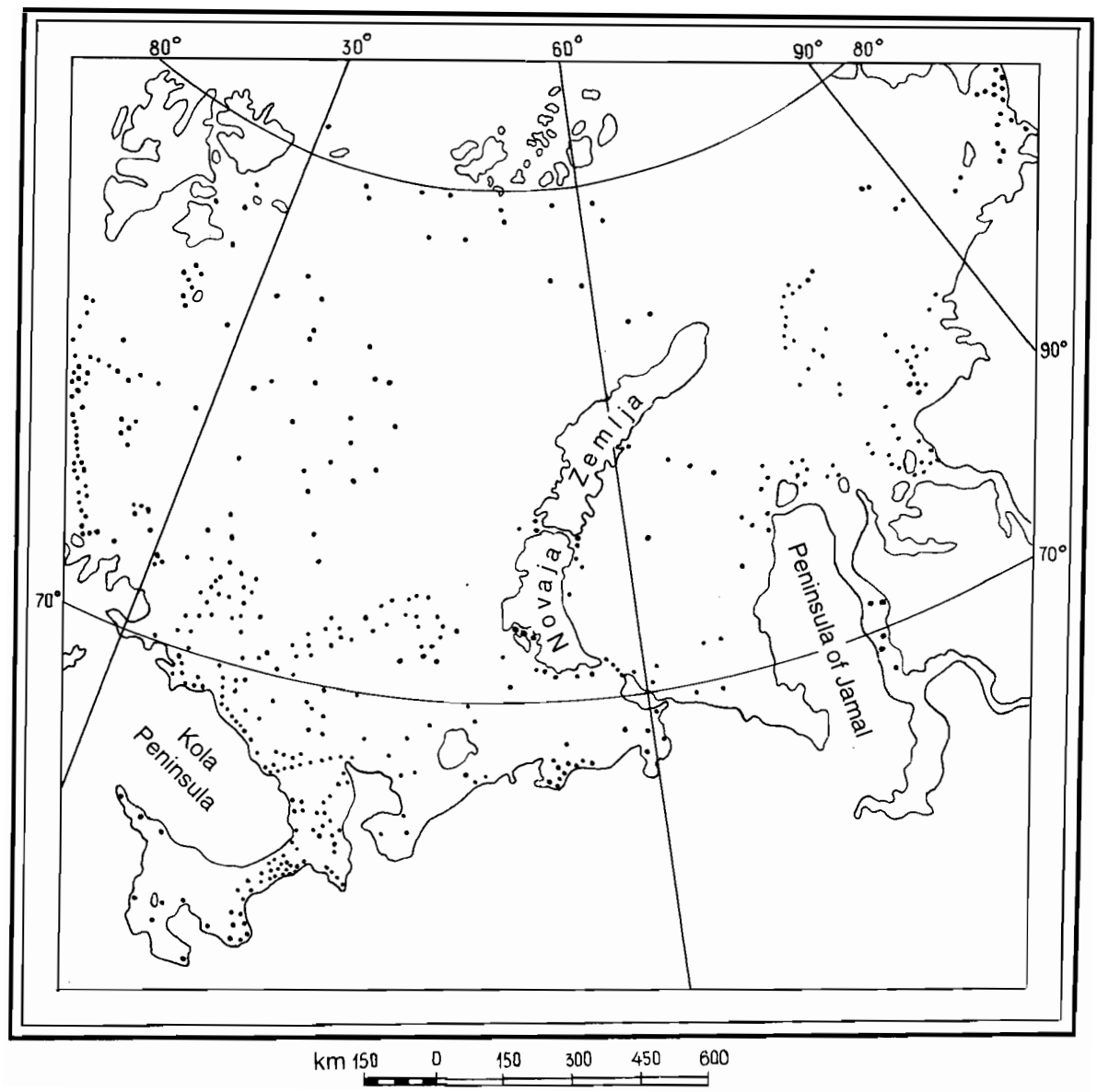

Fig. 1.3 Positions of near-bottom current measurements on the Western Arctic Shelf.

2. DEPOSITIONAL CONDITIONS

Recent sedimentation on the Western Arctic Shelf is influenced by many factors. In our opinion, the most important ones are the conformity of structural planes, the sedimentary regime, hydrological conditions in the near-bottom layer of water, and facies zonation.

2.1 Conformity of structural planes

The vast quantities of deep- and shallow-seismic profiling data obtained in recent years have permitted the preparation of structural maps based on the principal reflectors of the sedimentary basins. These reflectors are:

- E_2 – the sea floor
- E_1 – a bed of Holocene age
- D_{1-2} – a bed of Pliocene-Quaternary age
- B – the upper surface of Jurassic rocks
- A – a bed of Triassic rocks
- III (IV) – the upper surface of deformed basement.

The initial primary data base for analysing this in three dimensions was obtained by selecting 1232 points of equal orthogonal framework from 1:2,500,000 scale maps, the points being 2 cm squares. Secondary data fed into the data base were the following calculated data on thicknesses:

- E_2-E_1 – thickness of Holocene deposits
- E_1-D_{1-2} – thickness of Pliocene-Pleistocene deposits, etc.

Conformity (i.e. the degree of inheritance of structural planes) has been traced by correlational analysis (Gurevich & Musatov 1988) (Table 2.1).

Table 2.1 Co-efficients of correlation between depths of reflectors from the sedimentary cover and thickness

Reflectors,	*thickness*	E_2	E_1	D_{1-2}	*B*	*A*
E_1	0.99	–	–	–	–	
D_{1-2}	0.96	0.96	–	–	–	
B	0.18	0.18	0.23	–	–	
A	0.20	0.20	0.24	0.77	–	
III (IV)	0.16	0.16	0.17	0.49	0.75	
E_2-E_1	0.33	0.34	0.34	0.18	0.10	
E_1-D_{1-2}	–	‹	0.32	0.37	0.19	

The positive sign and the homogeneous exchange of the co-efficients of correlation show that most of the structural planes are successively inherited. Recent deposition is first and foremost shown by the depth to the pre-Pliocene surface (0.96). The thickness of Holocene deposits chiefly depends upon the position of Recent, pre-Holocene and pre-Quaternary surfaces, i.e. the depth from the modern structural plane (0.34). The thickness of the Pliocene-Quaternary deposits, on the other hand, does not quite correlate with the recent relief, but is related to the position of the pre-Pliocene surface and the upper surface of the Jurassic (0.32 and 0.37). This suggests that partial structuro-tectonic and sedimentary reconstruction has taken place during the Late Cenozoic. This supposition is supported by the graphs showing correlations between the thickness of the Upper Cenozoic and the major reflectors, obtained by the "sliding window" technique applied along latitude 74°N (Fig. 2.1). Hence, the thickness of modern deposits in the Barents Sea depends essentially on the position of the pre-Pliocene and Jurassic surfaces. Almost no correlation exists on Novaya Zemlya and the adjacent shelf. The thickness of modern deposits in the Kara Sea closely correlates with Jurassic and Triassic surfaces, less so with the pre-Neogene relief, but well-defined inverse relationships support the notion of inversion of relief.

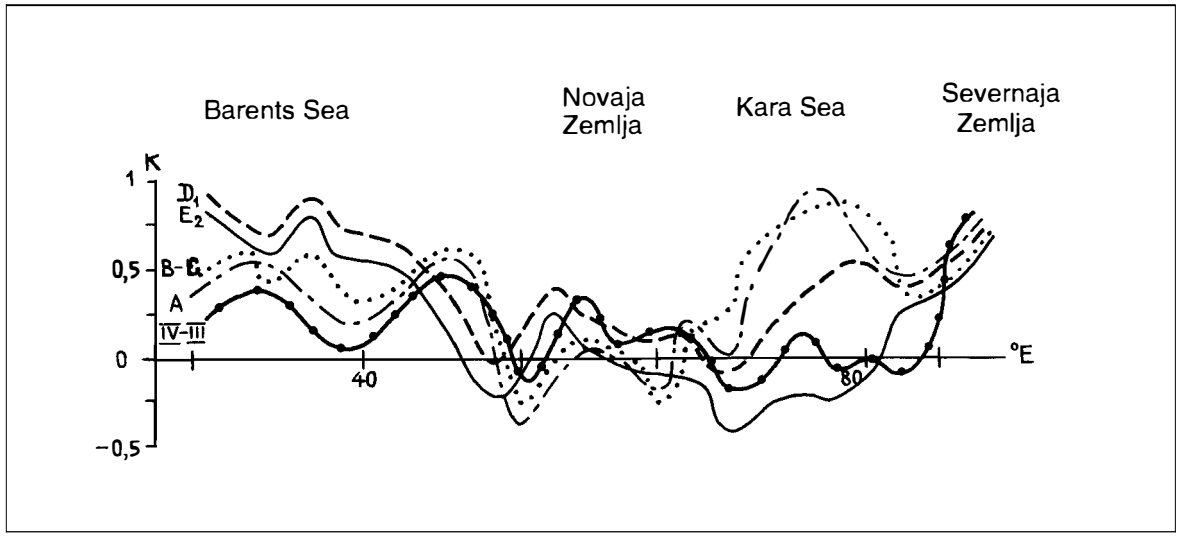

Fig. 2.1 Correlations between the thickness of Upper Cenozoic deposits and the position of major seismic reflectors in the depositional veneer of the Western Arctic Shelf. Major reflectors: III–IV. surface of folded basement, A. base of Triassic, B–C. base of Jurassic, D_1. base of Pliocene, E_2. surface of recent sea floor.

R-factor (correlational) analysis establishing the conformity of structural planes and sedimentation shows that the chief factors determining thickness are the degree of non-compensation for subsidence caused by sedimentation (load 0.84), the direction and intensity of present-day movement (load 0.29) and the common inheritance of structural planes (0.13). These three principal factors account for 80 % of the system and mostly determine the sedimentary regime (see section 8.1).

Cluster analysis of the factors determining the matrix of Phanerozoic sedimentation in the 1232 squares contours homogeneous clusters which have been used to produce a map of the depositional provinces on the Western Arctic Shelf (see section 8.5).

2.2 Hydrological conditions

Hydrodynamic and other hydrological parameters of the near-bottom water layer characterise the labile components of the sea-floor landscape. Two very important parameters of this kind are the maximum velocity of near-bottom currents (Fig. 2.2) and their horizontal gradients (Fig. 2.3). The greatest near-bottom hydrodynamic activity is found in the White Sea (Table 2.2).

Near-bottom current velocities and the amplitude of their changes determine the dynamic character of recent deposits and many other lithological-geochemical and biotic parameters (section 8.2). A map of the near-bottom horizontal temperature gradient (Fig. 2.4) fixes the position of frontal zones and determines much of the distribution of shelf benthos and the biogenic components of recent deposits (see section 5.2).

2.3 Facies zonation

The facies of marine deposits is usually related to bathymetric factors and circumcontinental zonation. A classification scheme based on these parameters is proposed in Table 2.3 for the Western Arctic Shelf and its continental slope (Fig. 2.5).

The distribution of various types of facies among the recent sediments on the Western Arctic Shelf is shown in Table 2.4.

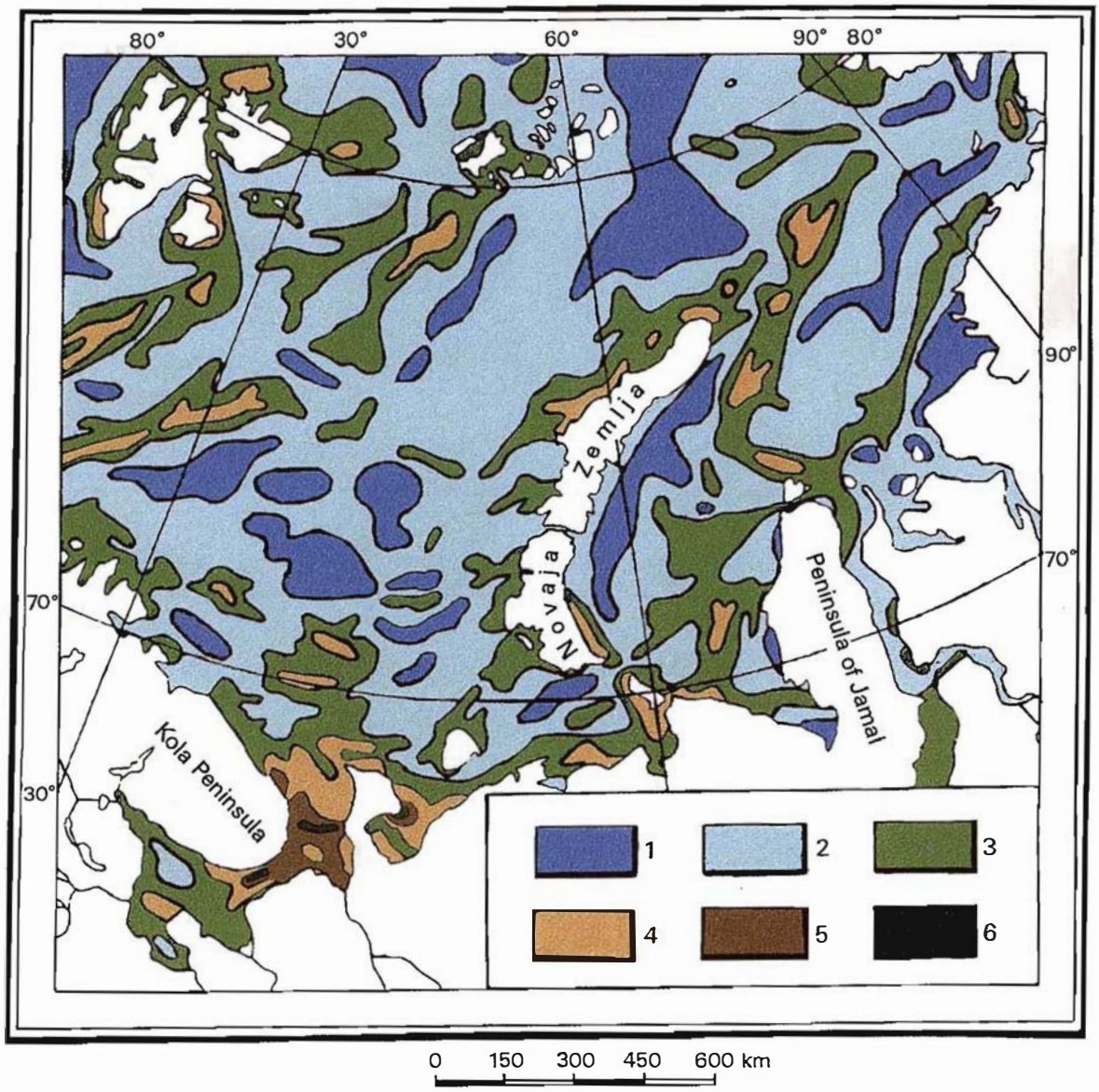

Fig. 2.2 Maximum velocities of near-bottom currents on the Western Arctic Shelf in m/s: 1. < 0.1; 2. 0.1 to 0.3; 3. 0.3 to 0.5; 4. 0.5 to 1; 5. 1 to 1.5; 6. > 1.5.

Table 2.2 Distribution of near-bottom current velocities

Velocity m/s	*Shelf % area*			
	White Sea	*Barents Sea*	*Kara Sea*	*Entire Western Arctic*
< 0.1	–	14.6	14.5	18.4
0.1 – 0.2	–	26.0	28.8	25.6
0.2 – 0.3	–	29.2	30.4	26.8
0.3 – 0.5	13.2	25.0	21.0	21.8
0.5 – 1.0	30.8	5.0	5.2	5.5
1.0 – 1.5	16.6	0.2	–	0.6
> 1.5	2.0	0.02	–	0.07

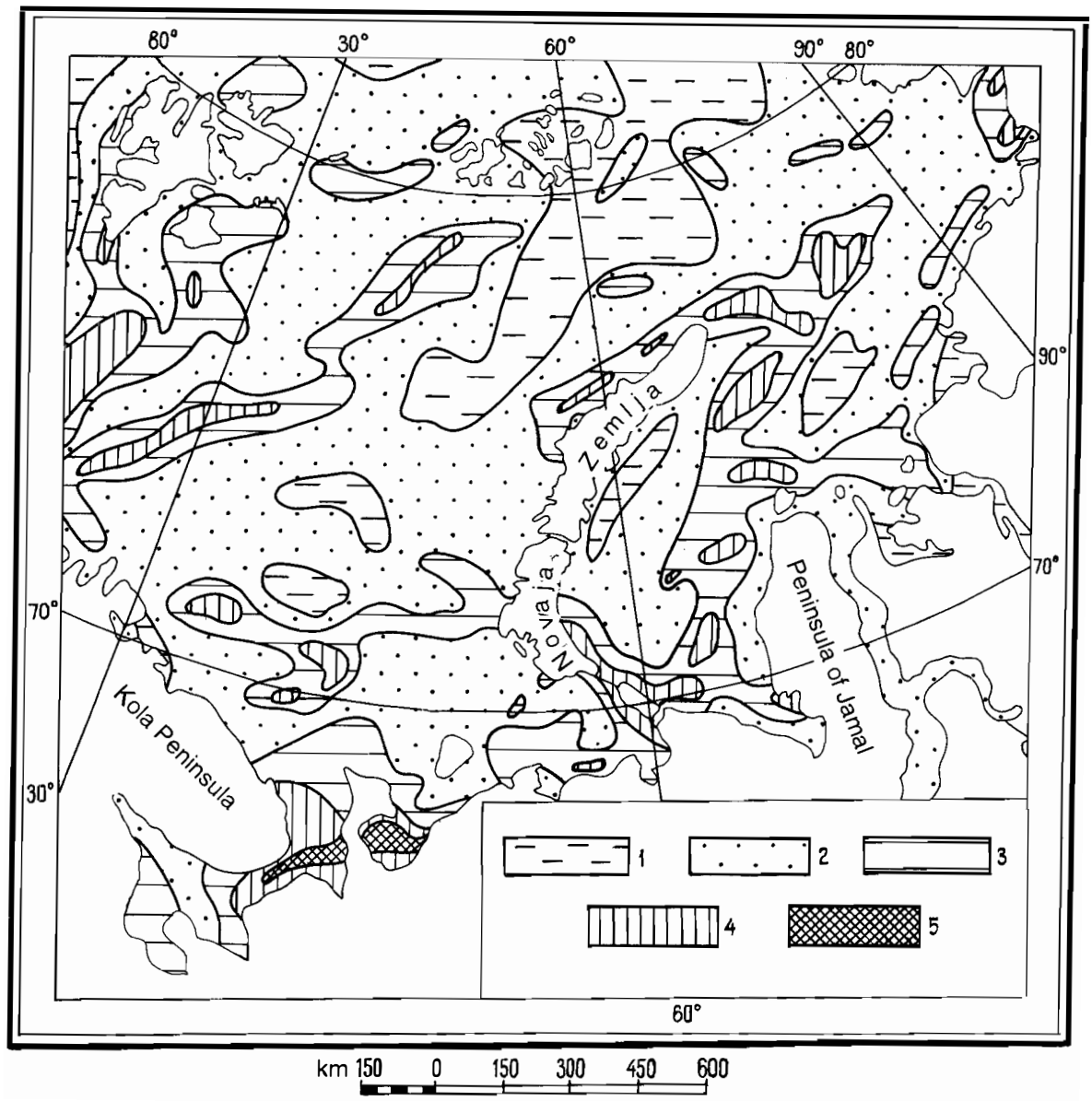

Fig. 2.3 Horizontal gradient of near-bottom velocities on the Western Arctic Shelf in m/s per 100 linear km: 1. < 0.1; 2. 0.1 to 0.5; 3. 0.5 to 1; 4. 1 to 2; 5. > 2.

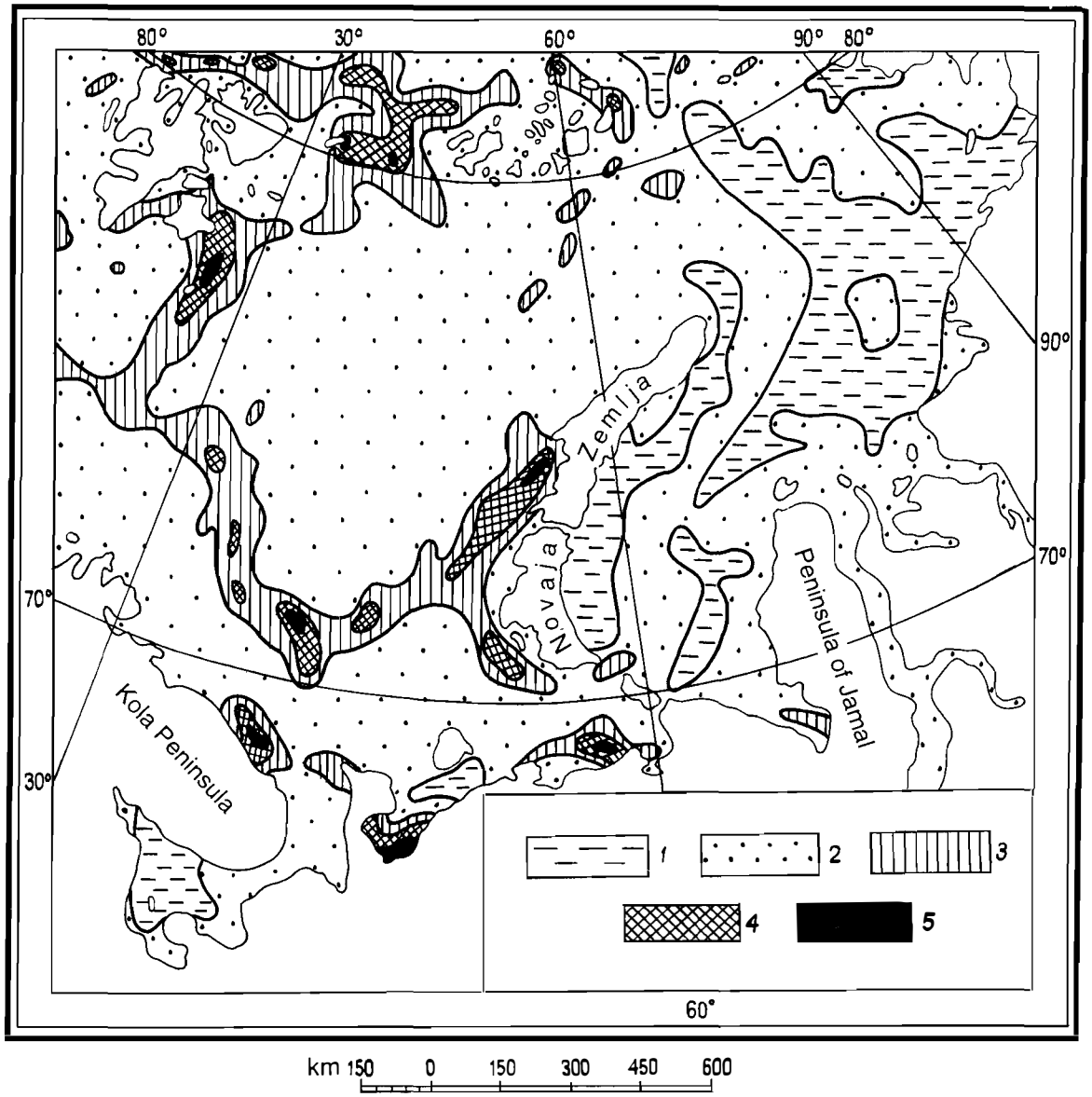

Fig. 2.4 Gradient of horizontal changes of near-bottom temperature on the Western Arctic Shelf in °C per 100 km: 1. < 0.5; 2. 0.5 to 3; 3. 3 to 4; 4. 4 to 5; 5. > 5.

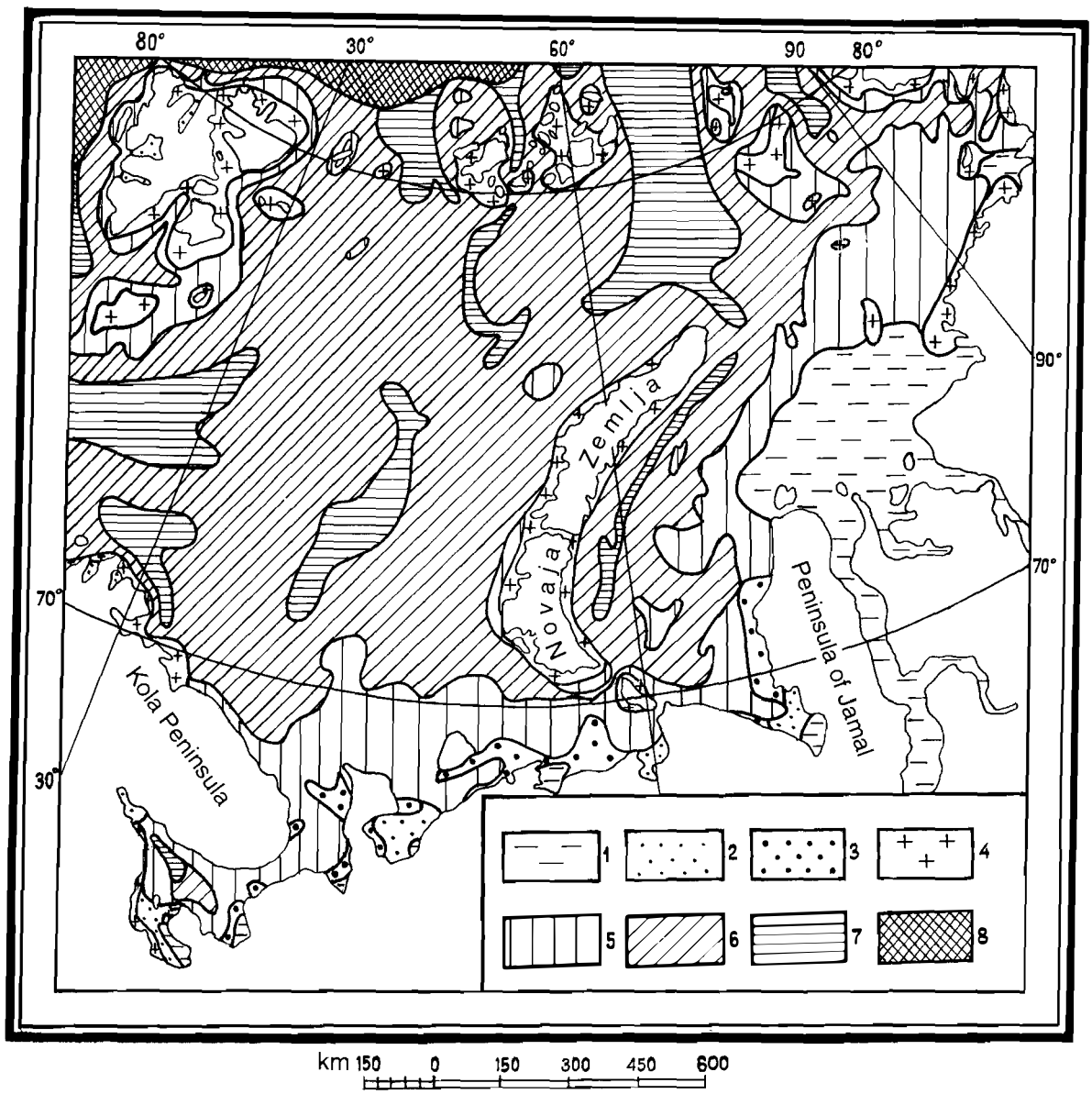

Fig. 2.5 Facies zonation of modern deposits on the Western Arctic Shelf. The deposits are: 1. deltas and estuaries; 2. bays and lagoons; 3. bars and barrier islands; 4. skerries and banks; 5. shallow-water plains; 6. deep-water plains; 7. depressions and troughs; 8. continental slope.

Table 2.3 Facies classification for the Western Arctic Shelf and adjacent continental slope

Bathymetric regions	*Depth*	*Shore zone*	*Circumcontinental zonation* *Neritic zone* *offshore*	*inner shelf*	*outer shelf*	*Continental slope*
Supralittoral	Onshore, wave affected	Deposits of superaquatic basins, storm deposits	–	–	–	–
Littoral	Tide-dependent	Deposits of relict lakes	Beach deposits; deposits of tidal marshes and emerged shoals	–	–	–
Upper sublittoral	0 – 50 m	–	Deltaic and estuarine deposits; deposits in bays & lagoons, on bars & barrier islands	Deposits of skerries, underwater rises & shallow-water plains	–	–
Lower sublittoral	50–100 m shelf break	–	–	–	Deposits of deep-water plains, shelf depressions & troughs	–
Epiba-Shelf thyal	– break 1000 m	–	–	–	Deposits of continental slopes	

Table 2.4 Distribution of the facies of recent deposits on the Western Arctic Shelf (numerator – % area, denominator – % volume)

Types of facies	*White Sea*	*Barents Sea*	*Kara Sea*	*Entire Western Arctic*
Deltas & estuaries	6.8 15.3	0.3 1.1	16.7 18.3	6.2 8.9
Bays & lagoons	9.4 7.7	1.1 1.5	0.4 0.3	1.1 1.5
Bars & barrier islands	6.3 11.7	0.8 3.0	1.1 4.6	1.1 4.4
Skerries & banks	4.1 0.7	4.1 0.4	6.7 1.2	5.0 0.7
Shallow-water plains	61.5 46.4	11.9 13.4	26.2 10.0	18.3 15.1
Deep-water plains	7.3 9.5	60.4 50.8	30.6 30.7	48.5 39.5
Depressions & troughs	4.6 8.7	11.6 16.8	11.9 22.6	11.5 18.3
Continental slopes	– –	9.8 13.0	6.4 12.3	8.3 11.6

Appropriate locations to prospect for sand for the construction industry would be deltas and estuaries, and bars and barrier islands. The predicted resources of these facies are about 28 billion m^3 on the Barents Sea Shelf, about 14 billion m^3 on the White Sea Shelf, and about 5 billion m^3 on the Kara Sea Shelf.

3. INTENSITY OF SEDIMENTATION AND GRANULAR COMPOSITION OF SEDIMENTS

3.1 Late Cenozoic sedimentation

With the assistance of E.E. Musatov, an isopach map of the Upper Cenozoic (Pliocene-Quaternary) deposits has been prepared for the Western Arctic Shelf (Fig. 3.1) based on a large volume of generalised data (see Table 1.1), chiefly marine shallow-seismic profiling and evaluation of onshore bore-hole data, as well as satellite imagery (Gurevich et al. 1984). The average seismic velocity used for the unconsolidated deposits was 1650 m/sec.

Table 3.1 Distribution of the thickness (m) of Pliocene-Quaternary deposits on the Western Arctic Shelf and adjacent land areas

Regions	*Occurrence, % of area*					*Average weighted thickness*
	0–5 m	*5–10 m*	*10–50 m*	*50–200 m*	*>200 m*	
Offshore regions						
White Sea	14	28	48	10	–	23.6
Barents Sea	10	22	51	17	–	30.9
Kara Sea	6	24	49	20	1	38.5
Norwegian-Greenland Sea, continental slope	–	–	–	28	62	266
Arctic Ocean slope	–	–	–	61	39	195
Adjacent land						
Baltic Shield	54	25	19	1	–	7.8
Northern part of Russian Plate	4	20	54	22	–	33.6
Northern part of Timan-Pechora province	1	1	5	63	29	155
Pay-Khoy, Vaigatch, Novaya Zemlya	42	27	29	2	–	12.0
Yamal	–	–	3	32	65	207
Svalbard & Franz Josef Land	77	21	2	–	–	3.9

On the whole, the distribution of the thickness of Upper Cenozoic deposits on the Western Arctic Shelf reflects the inherited pattern of basinal sedimentation. Anomalous increases in thickness offshore from the Kola peninsula, northern Norway, the northern island of Novaya Zemlya and the Svalbard archipelago conform to the model of minimum ice dispersion.

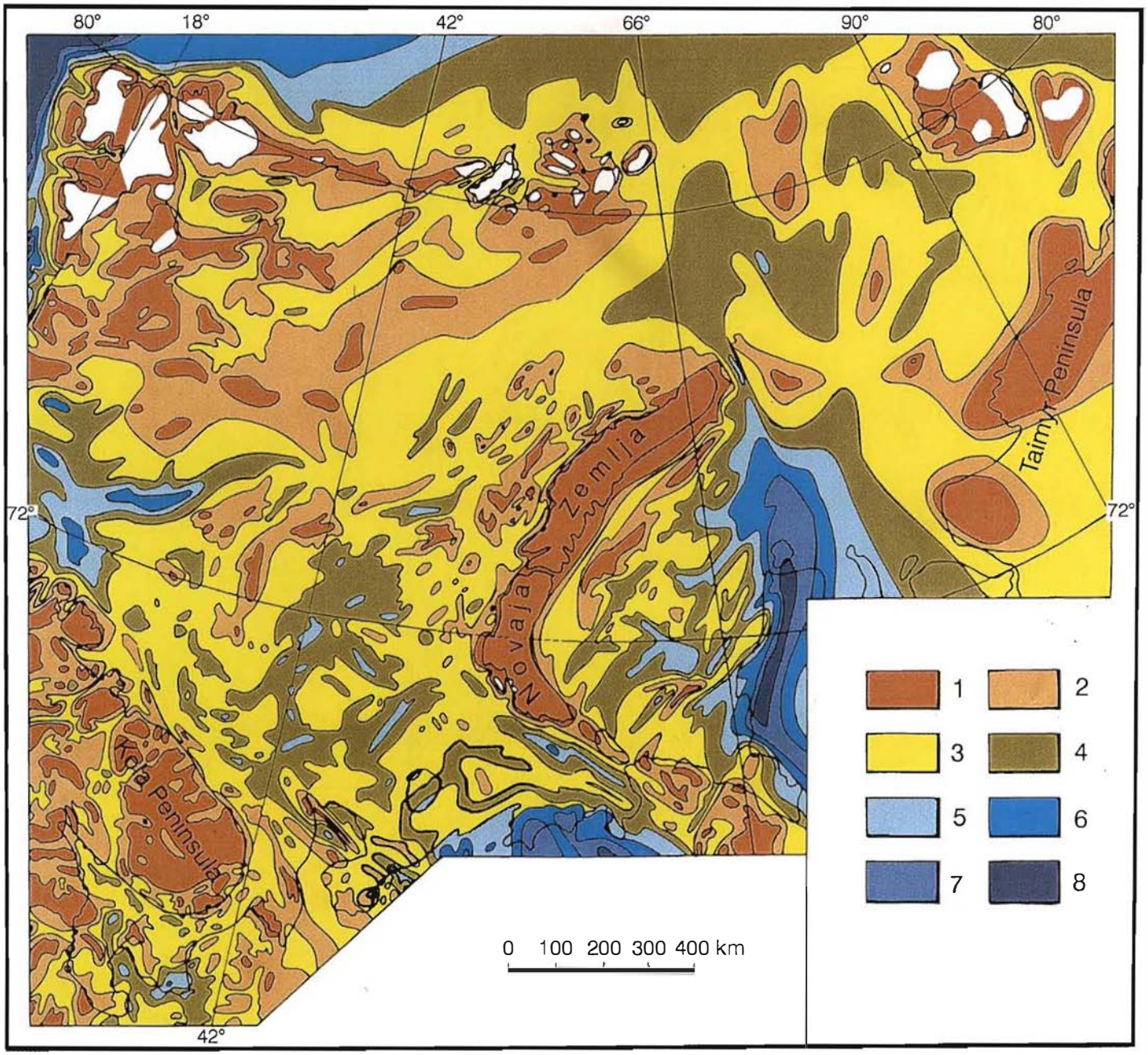

Fig. 3.1 Thickness of Pliocene-Quaternary deposits on the Western Arctic Shelf in metres: 1. < 5; 2. 5 to 10; 3. 10 to 50; 4. 50 to 100; 5. 100 to 150; 6. 150 to 200; 7. 200 to 250; 8. > 250.

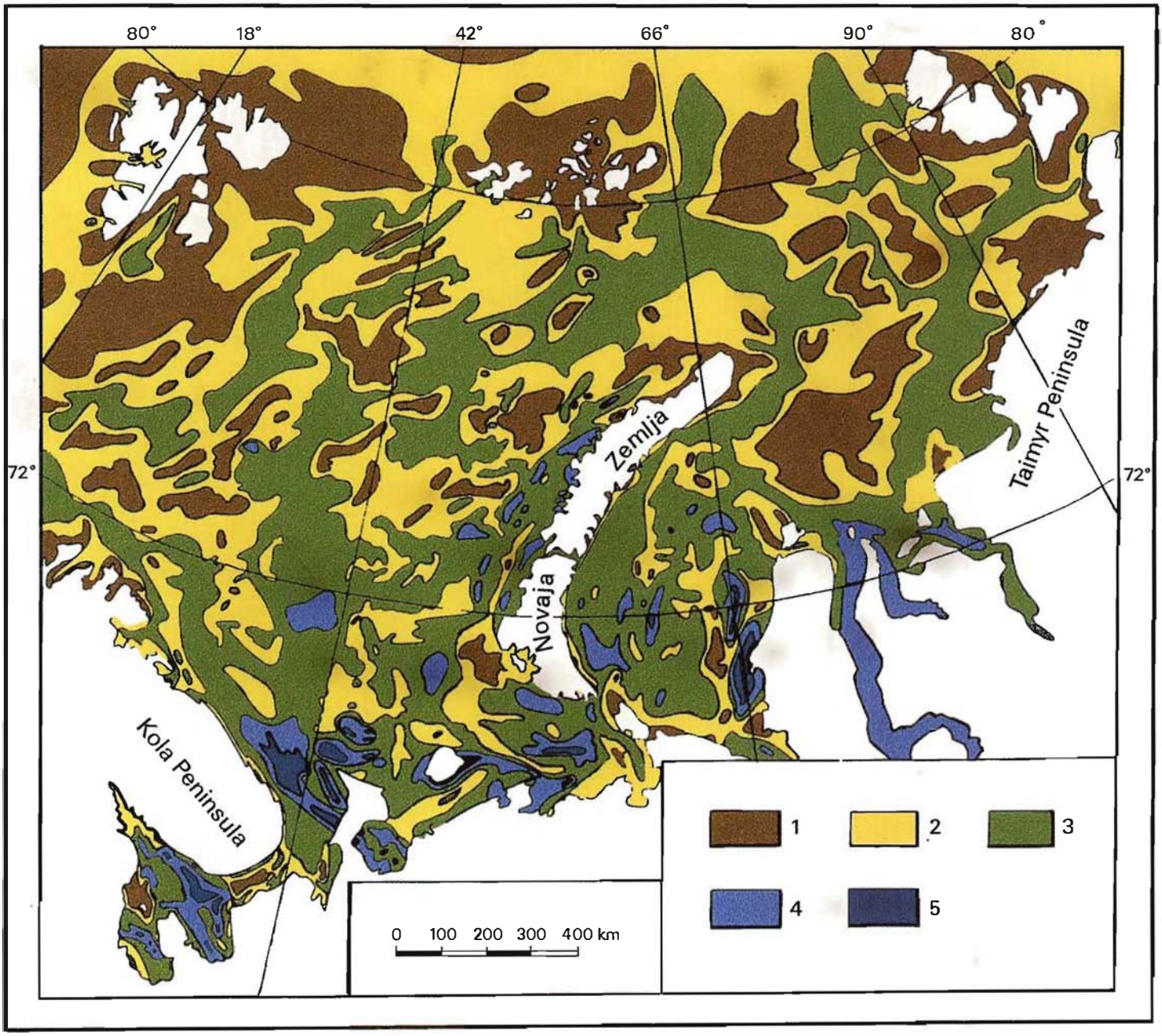

Fig. 3.2 Thickness of Holocene deposits on the Western Arctic Shelf in metres: 1. < 0.1; 2. 0.1 to 1; 3.1 to 5; 4. 5 to 10; 5. > 10.

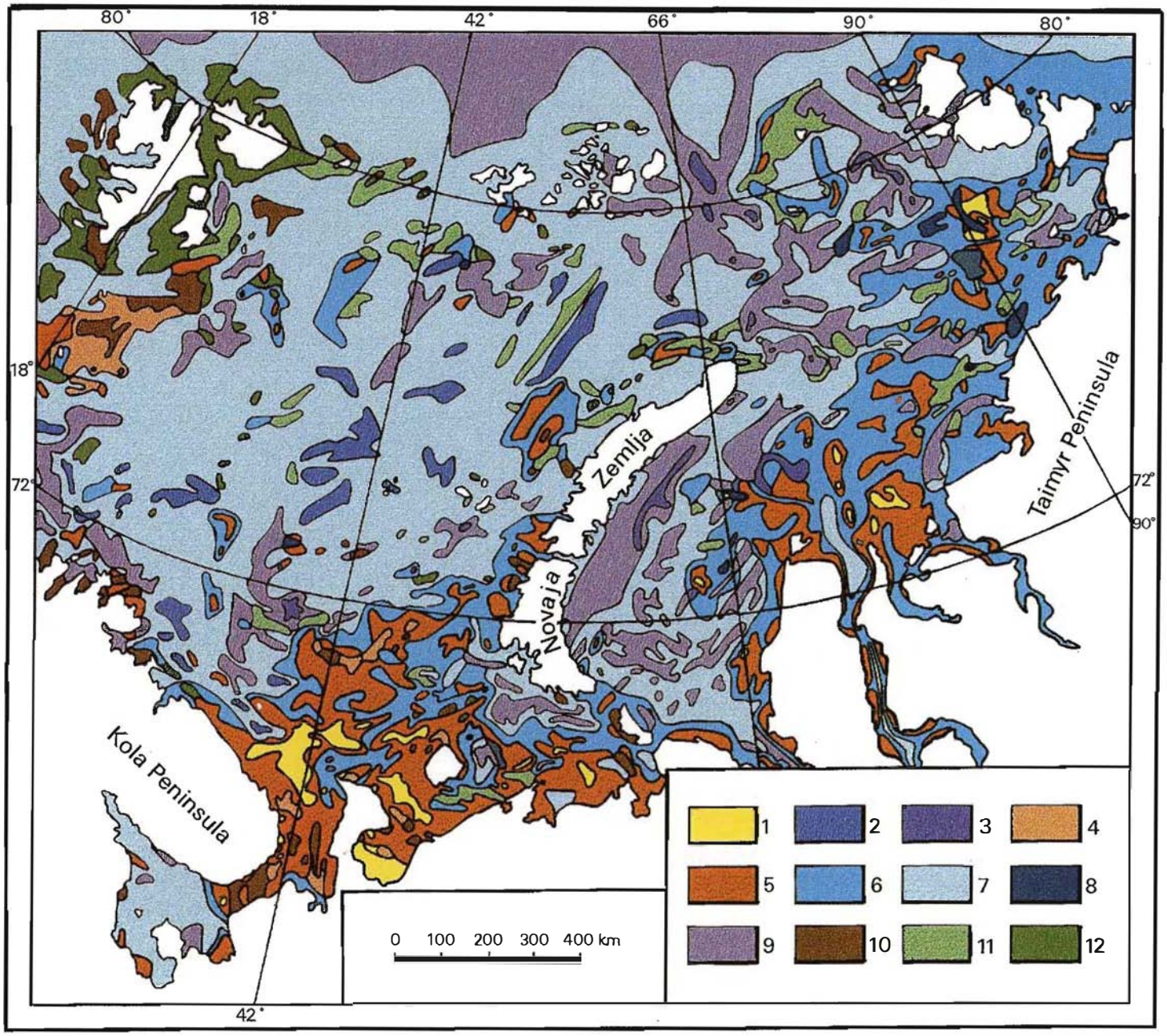

Fig. 3.3 The modern Western Arctic Shelf deposits classified granulometrically: 1. pure sand; 2. pure silt; 3. pure clay; 4. gravelly sand; 5. silty sand; 6. sandy silt; 7. clayey silt; 8. sandy clay; 9. silty clay; 10. sand-cobble-pebble mixtite; 11. sand silty-clayey mixtite; 12. cobble-pebble-silty-clayey polymixtite (diamicton).

3.2 Holocene sedimentation

The isopach map of Holocene deposits (Fig. 3.2) is based on data from gravity cores, drill cores, dredging, echo-sounding, high-frequency shallow-seismic profiling, satellite imagery and submarine photography (see Table 1.1). This map offers the first opportunity to appreciate the scale of recent sedimentation on the western Eurasian Arctic shelf by applying the technique of absolute mass. The thickness data, bulk density and granular composition of the sediments were calculated (Table 3.3).

3.3 Granular composition of sediments

The categories of all recent deposits based on their grain size distribution were determined using a specially designed granulometric classification (Gurevich 1986, 1990) shown in Figure 8.9. The distribution of granulometric grades in the White Sea, Barents Sea and Kara Sea forms the basis for a lithological map of the recent deposits (Fig. 3.3). Table 3.3 also shows an assessment of the total mass arranged according to decreasing average bulk density.

This table shows that the occurrence of monogranular or pure deposits (containing more than 75 % sand, silt or clay) does not exceed 1 %, either by space or mass. As regards total mass, the figures for bigranular or transitionary deposits, especially those having a relatively silty composition, are: sandy silt SSi – > 10 %, silty sand SiS – > 12 %, silty clay SiC – > 17 %, clayey silt CSi - nearly 47 %. Trigranular or mixed sand-silt-clay mixtite SSiC, practically absent from the White Sea, is widespread in northern parts of the Barents Sea and the Kara Sea. Polygranular boulder-pebbly and gravelly polymixtites (BPbSSi and GrSSi, respectively) are only present in appreciable quantities in the Barents Sea, mainly in areas that have suffered Pleistocene sea-floor glaciomarine and glacial erosion.

The total mass of the recent deposits on the Western Arctic Shelf is estimated to be 6760 billion tons, the White Sea Shelf accounting for 650, the Barents Sea Shelf 3550 and the Kara Sea Shelf 2560 billion tons. A systematic error in calculating the depositional mass (about ± 15 % relative error) is first and foremost caused by variations in the thickness of Holocene sediments. The volume of recent sedimentation cannot be explained by fluvial transport and shore abrasion alone, and strongly supports the hypothetical role of sea-floor erosion, and perhaps increases the importance of the autochthonous-palimpsestic component in recent arctic shelf sedimentogenesis.

3.4 Colour of sediments

A standardised description of the predominant colour of the bottom deposits, based on samples from 7500 sites, is shown in Figure 3.4. The dominant colours are brown and green (46.7 % and 32.6 % of the sites, respectively), rarely grey and yellow (8.9 and 9.5 %, respectively); sites with pink, black and blue deposits do not exceed 0.1 % of squares. The oxidation state and the content of basic chromophores – mobile forms of iron and manganese in the deposits – determine the colour and its intensity. The colour sequence of pink-brown-yellow-green-grey-black-blue is a response to the decreasing Redox potential of deposits from + 450–400 to – 150 mV and less (Gurevich & Pavlova 1974). Natural, lateral changes of colour generally reflect the influence of circumcontinental, climatic and facies zonations. Down-core changes of colour usually indicate the stage of diagenesis reached.

3.5 Lithogenetic consolidation

Lithogenetic consolidation takes place through the successive transitional stages of lithogenesis, diagenesis, catagenesis and metamorphogenesis. Differences in the density parameters of Holocene deposits (numerator) and the bedding of Upper Pleistocene deposits (denominator) illustrate this (Table 3.5).

Table 3.3 Holocene sedimentation on the Western Arctic Shelf

Granulometric types	*Index*	*Bulk density, t/m3*	*White Sea*	*Barents Sea*	*Kara Sea*	*% sq.*	*Western vol. km³*	*Arctic mass bill.*	*Shelf % mass t.*
			mass, bill. t.						
Boulders, pebbles with sand	SBPb	1.78	32.4	54.1	–	1.81	48.6	86.5	1.3
Bouldery -pebbly poly-mixtite	BPbSC	1.76	–	20.2	0.5	0.80	11.8	20.8	0.3
Gravelly sand	GrS	1.70	26.7	31.3	–	1.08	34.1	58.0	0.9
Sand	S	1.63	47.4	216.3	14.0	1.28	170.4	277.7	4.1
Gravelly polymix-tite	GrSSiC	1.45	–	24.8	0.4	1.84	17.4	25.2	0.4
Silty sand	SiS	1.40	150.4	424.2	276.3	9.98	607.8	850.9	12.6
Sandy silt	SSi	1.31	–	359.7	340.0	10.88	534.1	699.7	10.3
Silt	Si	1.27	–	91.9	70.5	2.78	127.9	162.4	2.4
Clayey sand	CS	1.25	–	–	64.6	1.00	51.7	64.6	1.0
Sandy clay	SC	1.24	–	–	26.3	0.61	21.2	26.3	0.4
Clayey silt	CSi	1.23	373.4	1849.7	952.0	51.28	2581.4	3175.1	46.9
Sandy-silty clayey mixtite	SSiC	1.21	–	67.3	33.8	2.93	88.5	101.0	1.5
Silty clay	SiC	1.12	18.0	405.0	737.0	13.19	1035.7	1160.0	17.1
Clay	C	1.05	–	6.3	48.4	0.53	52.1	54.7	0.8
Sum	–	648.3	3550.8	2563.8	100.0	5377.7	6763.0	100.0	

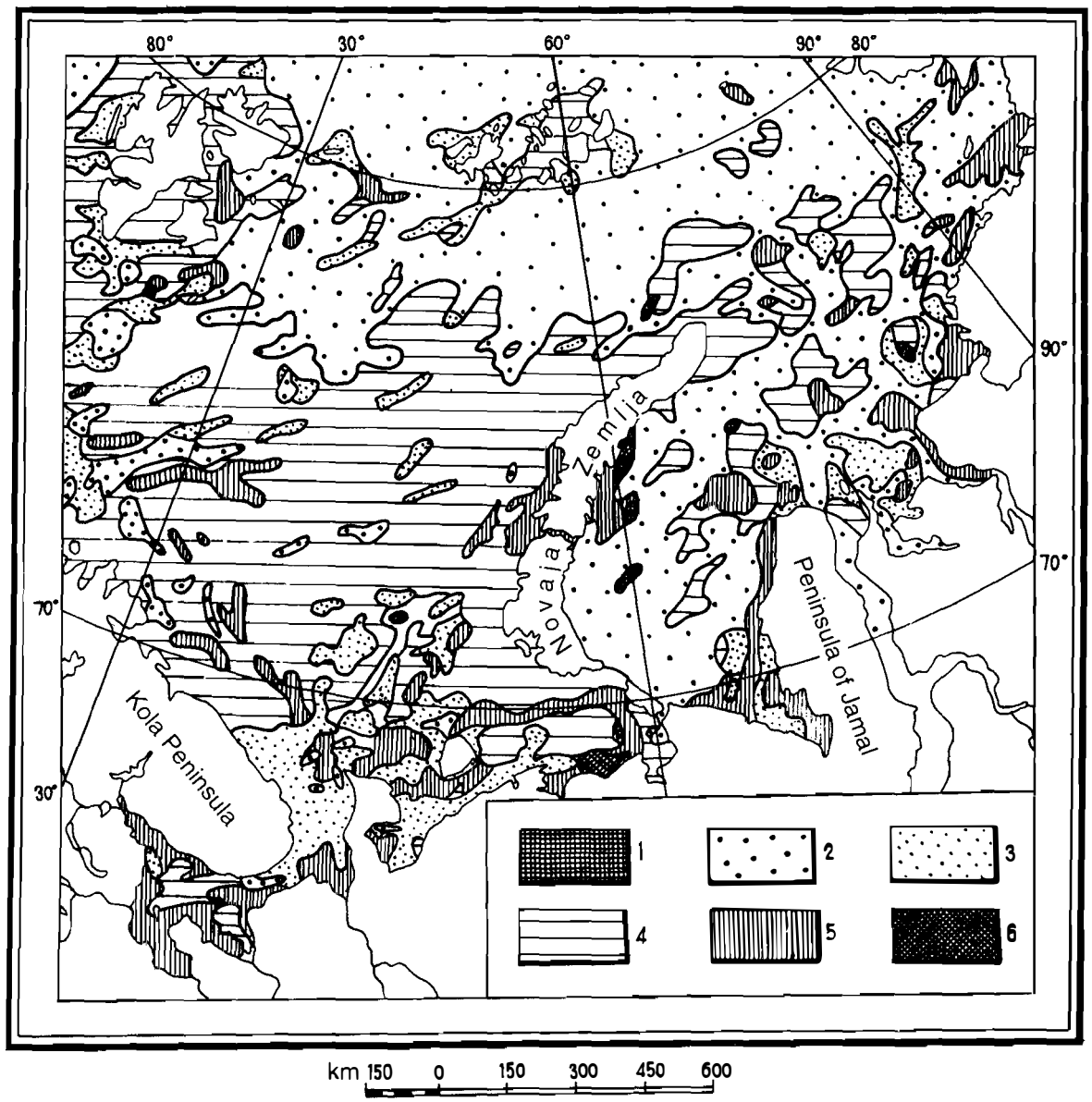

Fig. 3.4 Colour of the sea-floor surface layer of modern deposits on the Western Arctic Shelf: 1. red, pink; 2. brown; 3. yellow; 4. green; 5. grey; 6. blackish-blue, black.

Plots of bulk density versus median diameter (Fig. 3.5) show that despite a large range of granulometrical fractions, the points fall into four groups, approximately determined by the formula:

$$\lg \rho o = a \lg \bar{d} + b$$

Index a characterises the degree of consolidation of deposits at different stages of lithogenesis and is as follows:

- sedimentation a = 0.094 b = 0.208
- early diagenesis a = 0.080 b = 0.232
- diagenesis a = 0.050 b = 0.318
- catagenesis a = 0.018 b = 0.410

Thus, using the Western Arctic Shelf as a model, a probable reliable indicator for lithogenetic consolidation was established for granulometrically different terrigenic formations at a single stage of lithogenesis (Gurevich 1990).

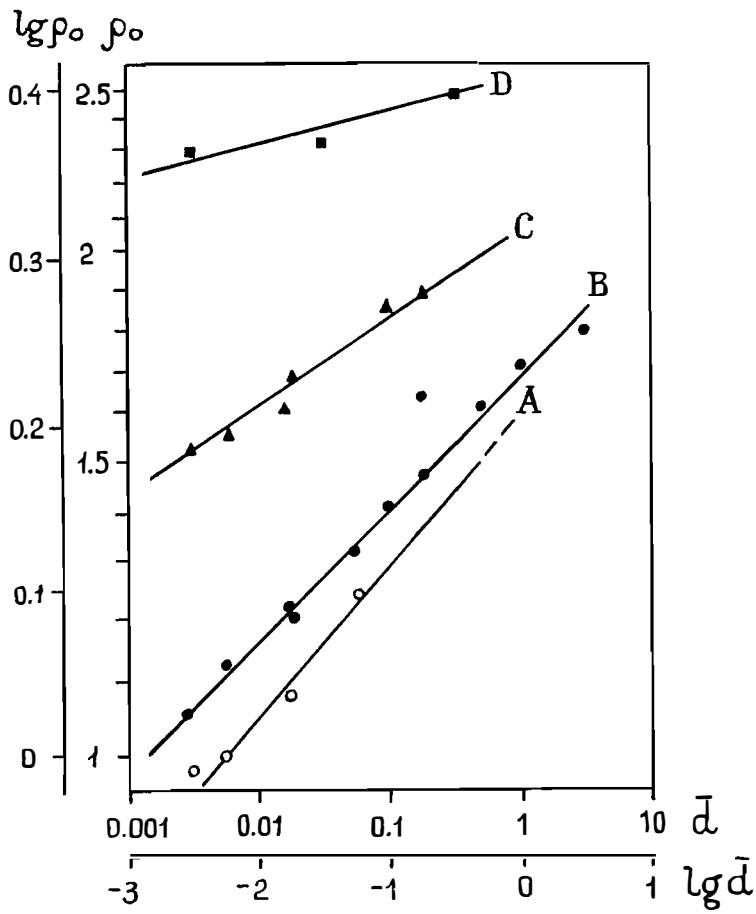

Fig. 3.5 Diagram showing the relationship between bulk density (ρ_O, gm/cm^3) and size of median diameter (d, mm) for terrigenic deposits at various stages of consolidation. A. modern deposits of active (sea floor) layer (depositional stage); B. Holocene deposits (early diagenesis); C. Upper Pleistocene deposits; D. Mesozoic deposits (catagenic stage).

Table 3.5 Water content, porosity and density of bottom deposits on the Western Arctic Shelf

Granulometric composition	*No. of samples*	*Water content, w, (% of wet wt.)*	*Porosity n, %*	*Dry bulk density* P_o *g/cm³*
Gravel with boulders, pebbles and sand	35 –	19.6 –	34.2 –	1.78 –
Gravelly sand	18 –	22.3 –	37.1 –	1.70 –
Coarse- and medium-grained sand	102 –	23.9 –	38.8 –	1.61 –
Fine-grained sand	91 5	23.1 17.3	36.8 32.0	1.65 1.90
Gravelly polymixtite	30 16	36.0 24.7	43.5 36.3	1.45 1.76
Silty sand	36 6	32.3 17.1	44.1 31.2	1.40 1.87
Sandy-clayey-silty mixtite	170 10	43.1 19.4	50.9 34.6	1.21 1.69
Sandy silt	85 8	37.1 22.0	47.4 35.9	1.31 1.67
Clayey silt	75 24	41.4 25.5	49.7 40.1	1.23 1.61
Silty clay	92 8	49.3 26.2	53.9 40.1	1.12 1.57
Clay	70 7	52.8 20.6	54.1 30.8	1.05 1.53
Average	804 84	36.9 22.9	46.3 36.4	1.35 1.68

4. TERRIGENIC COMPONENTS

Components of marine deposits are terrigenic, biogenic, chemogenic, volcanogenic, cosmogenic and technogenic (section 8.4). Terrigenic siliciclastic and clayey components dominate on the Western Arctic Shelf. The percentage of the mass of sediment that is insoluble in HCl gives a broad quantitative estimate of the general composition of the sediments. Figure 4.1 illustrates the distribution of the terrigenic siliciclastic component on the Western Arctic Shelf.

Their granulometrical size shows that terrigenic units include clayey, silty and sandy fractions, as well as coarse, angular clastic material.

4.1 Rudaceous fragments

Boulders and pebbles are rare in modern deposits on the Western Arctic Shelf; areas with gravelly sediment are much more common (Fig. 4.2). A.P. Lisitsyn believes the pebbles and gravel on the shelf originate from floating ice, whereas Klenova (1960), Dibner (1978), and the author attribute them to abrasion of the bottom (Gurevich & Hasankaev 1974). Evidence supporting this opinion

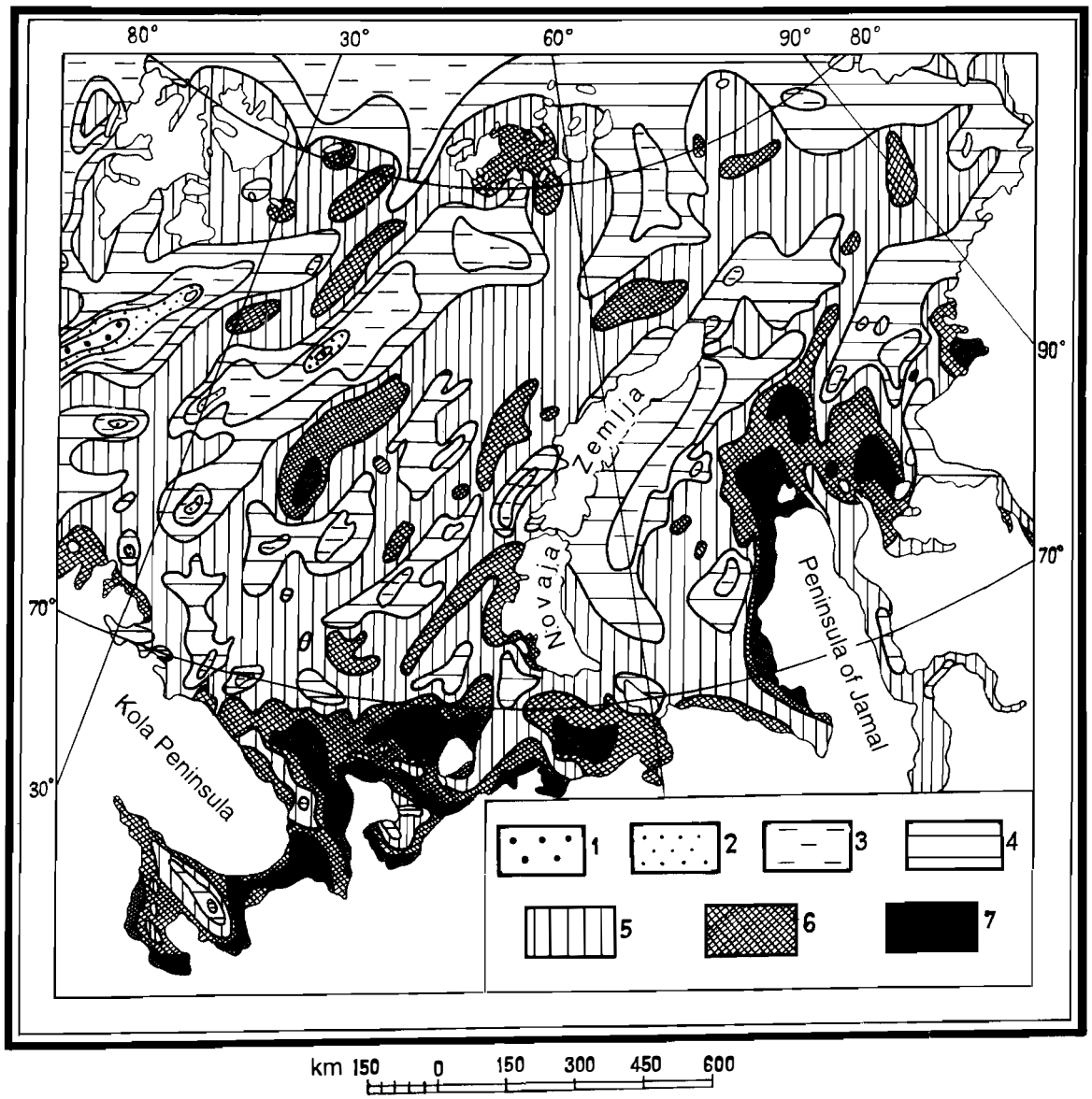

Fig. 4.1 Distribution of terrigenic siliciclastic components in the modern deposits of the Western Arctic Shelf, insoluble remains (%): 1. < 50; 2. 50 to 60; 3. 60 to 75; 4. 75 to 80; 5. 80 to 90; 6. 90 to 95; 7. > 95.

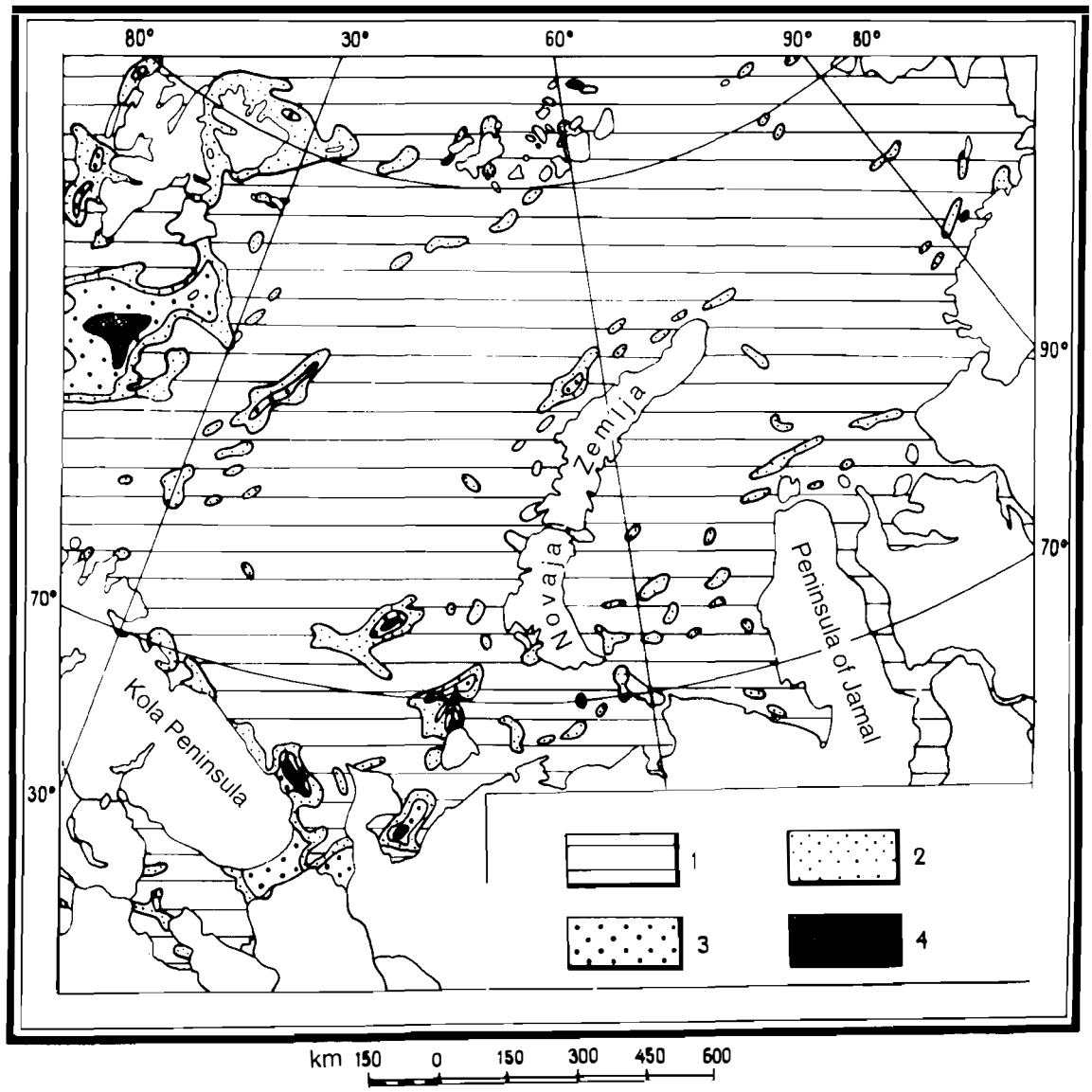

Fig. 4.2 Distribution of the gravel fraction in the modern deposits of the Western Arctic Shelf (%): 1. < 5; 2. 5 to 25; 3. 25 to 50; 4. > 50.

may be found on the map showing the petrological associations of clastic components, based on analysis of samples of the fine gravelly fraction from 499 stations (Fig. 4.3). When regional cartographical surveys are being undertaken, a strong correlation can usually be seen between the rock type forming the coarse clastic fraction of modern sediments and underlying pre-Quaternary strata, especially in areas with only a thin veneer of Quaternary sediment (5–10 m or less). This provides some justification for our concept (Gurevich & Yakovleva 1976, Gurevich & Vlasova 1983, Gurevich 1990, Lopatin & Gurevich 1990) of widespread autochthonous and palimpsestic units on the Western Arctic Shelf.

4.2 Light fraction minerals

The sand fraction of marine sediments is richest in light minerals, the distribution being shown in Figure 4.4. Mixed chlorite-quartz-feldspar (26 % of the total area of the Western Arctic Shelf), feldspar-quartz (52 %) and quartz (about 21 %) compositions are usually dominant. Pure quartz sands (quartz content > 90 %) are common in hydrodynamically active areas of the northern White Sea (Fig. 4.5).

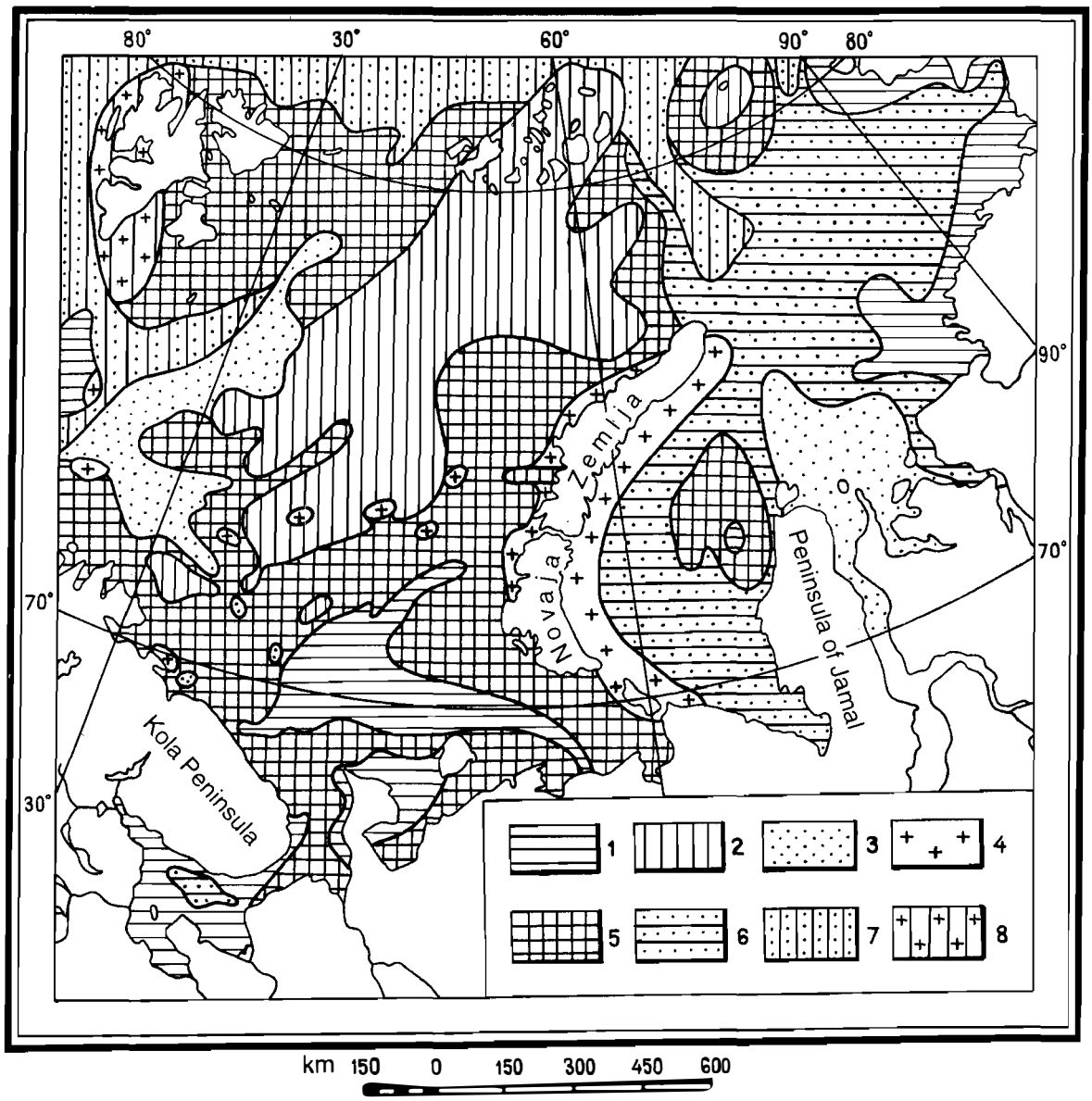

Fig. 4.3 Petrographical associations of coarse sand and fine gravel in the modern deposits of the Western Arctic Shelf: 1. association M (sum of metamorphic rock fragments – quartzites, schists and amphibolites - exceeds 50 %); 2. association F (sum of Phanerozoic sedimentary rock fragments – sandstones, shales, siltstones – exceeds 50 %); 3. association Q (sum of recent sediment fragments – clay aggregates, silts, clay - exceeds 50 %); 4. association A (sum of igneous rock fragments – granites, granodiorites, syenites, gneisses - 25–50 %); 5. mixed association MF; 6. mixed association QM; 7. mixed association QF; 8. mixed association AF.

4.3 Heavy fraction minerals

Most heavy minerals in marine sediments are concentrated in the silt fraction. The distribution of silt is shown in Figure 4.6.

The map showing mineral associations (Fig. 4.7) was compiled on the basis of mineralogical investigations of compositions of heavy minerals at 1420 stations, and the distributions of the heavy fraction of modern sediments (Fig. 4.8) and stable utility minerals (Figs. 4.9–4.11) were also taken into account. Comparison of these maps shows that areas with high concentrations essentially coincide. These areas follow zones which have high hydrodynamic activity in the near-bottom water layer and a high velocity gradient in the near-bottom currents (Figs. 2.3 and 2.4). High con-centrations of stable heavy minerals simultaneously coincide with ancient river valleys.

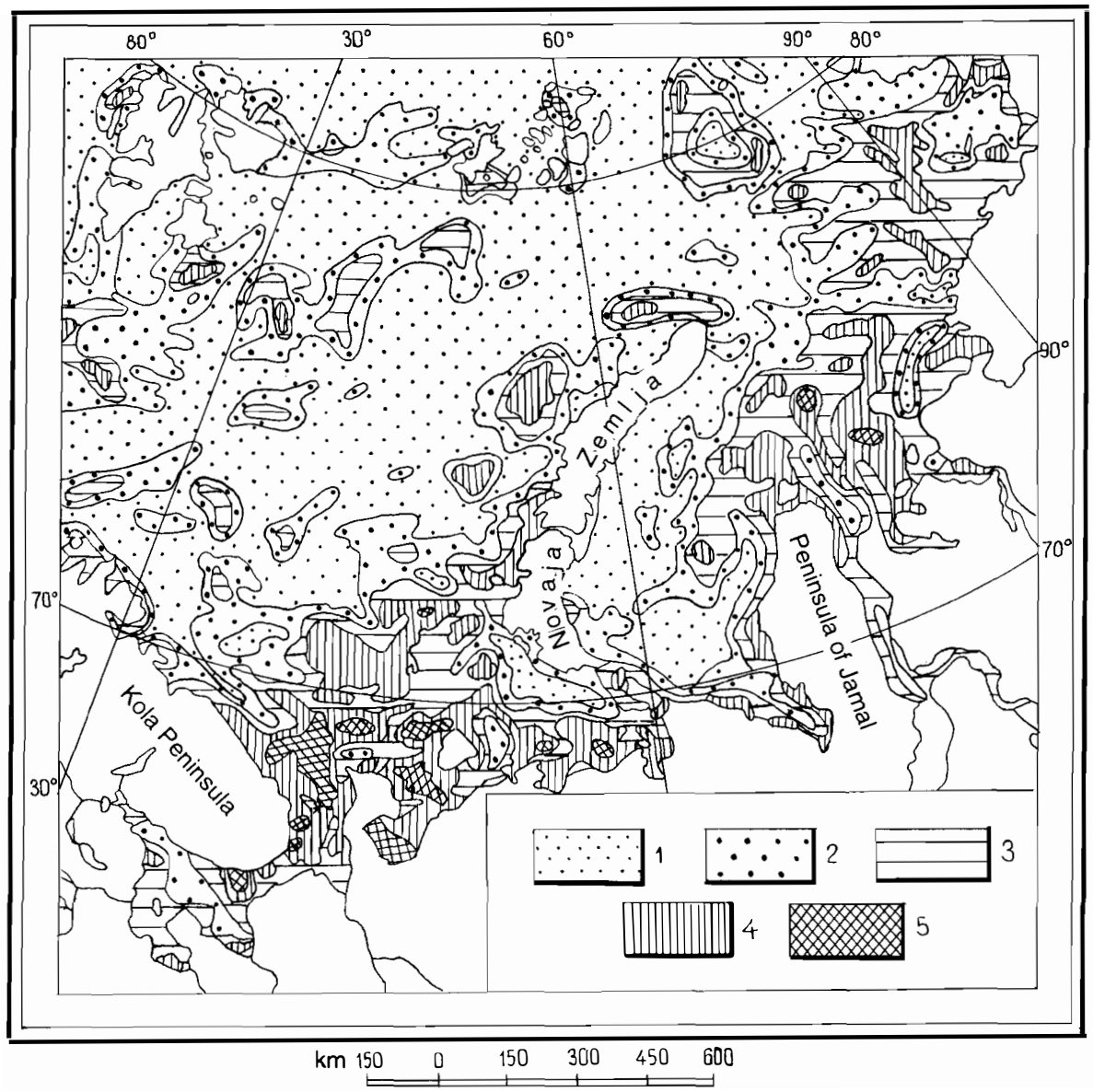

Fig. 4.4 The content (%) of the sand fraction of modern deposits on the Western Arctic Shelf: 1. < 10, 2. 10 to 25; 3. 25 to 50; 4. 50 to 75; 5. > 75.

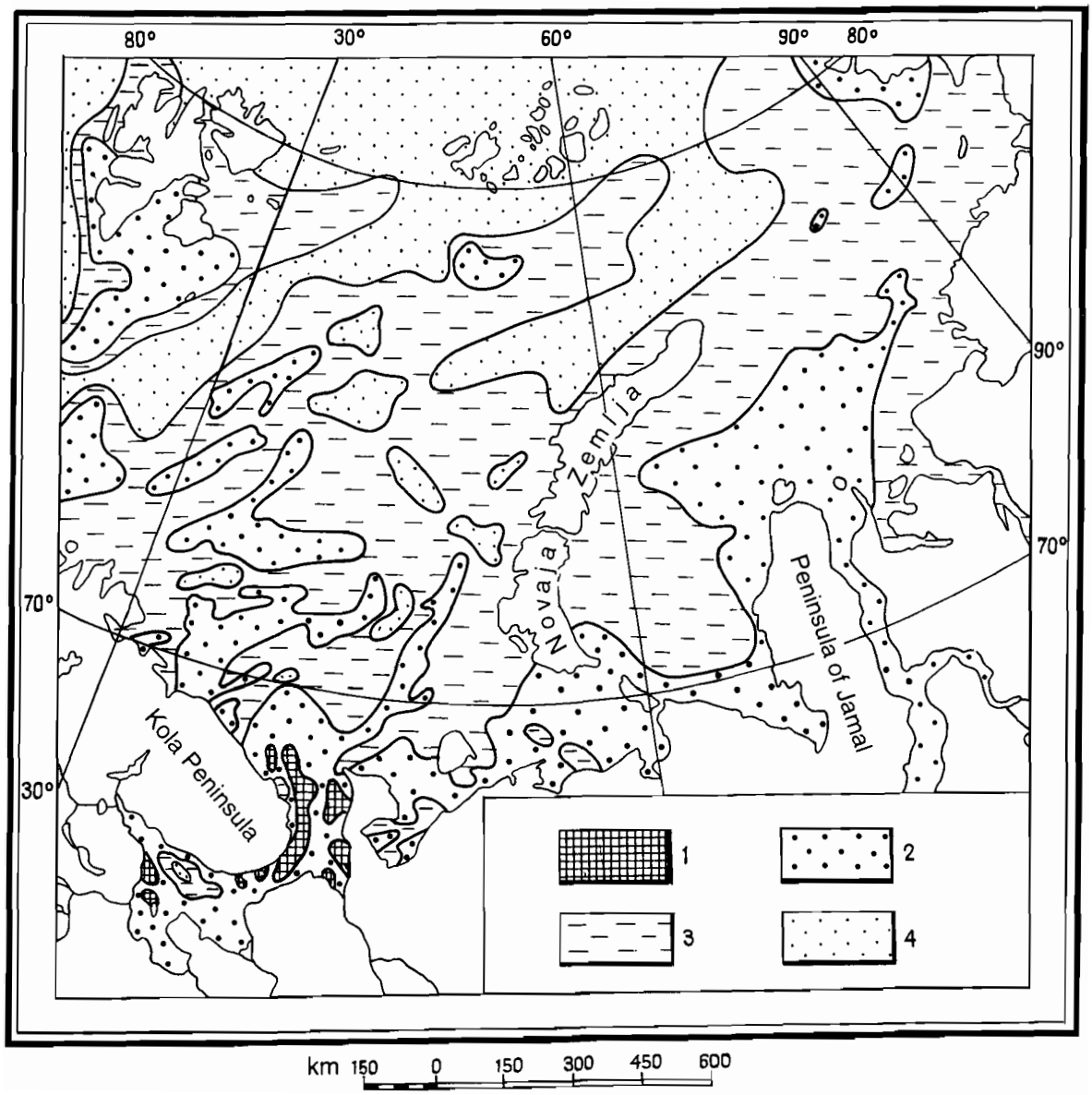

Fig. 4.5 Mineral composition of the light fraction of the modern deposits of the Western Arctic Shelf:
1. pure quartz (> 90 % qu); 2. essential quartz (75 to 90 % qu); 3. quartzo-feldspathic (50 to 75 % qu, > 25 % fsp); 4. mixed composition (< 50 % qu).

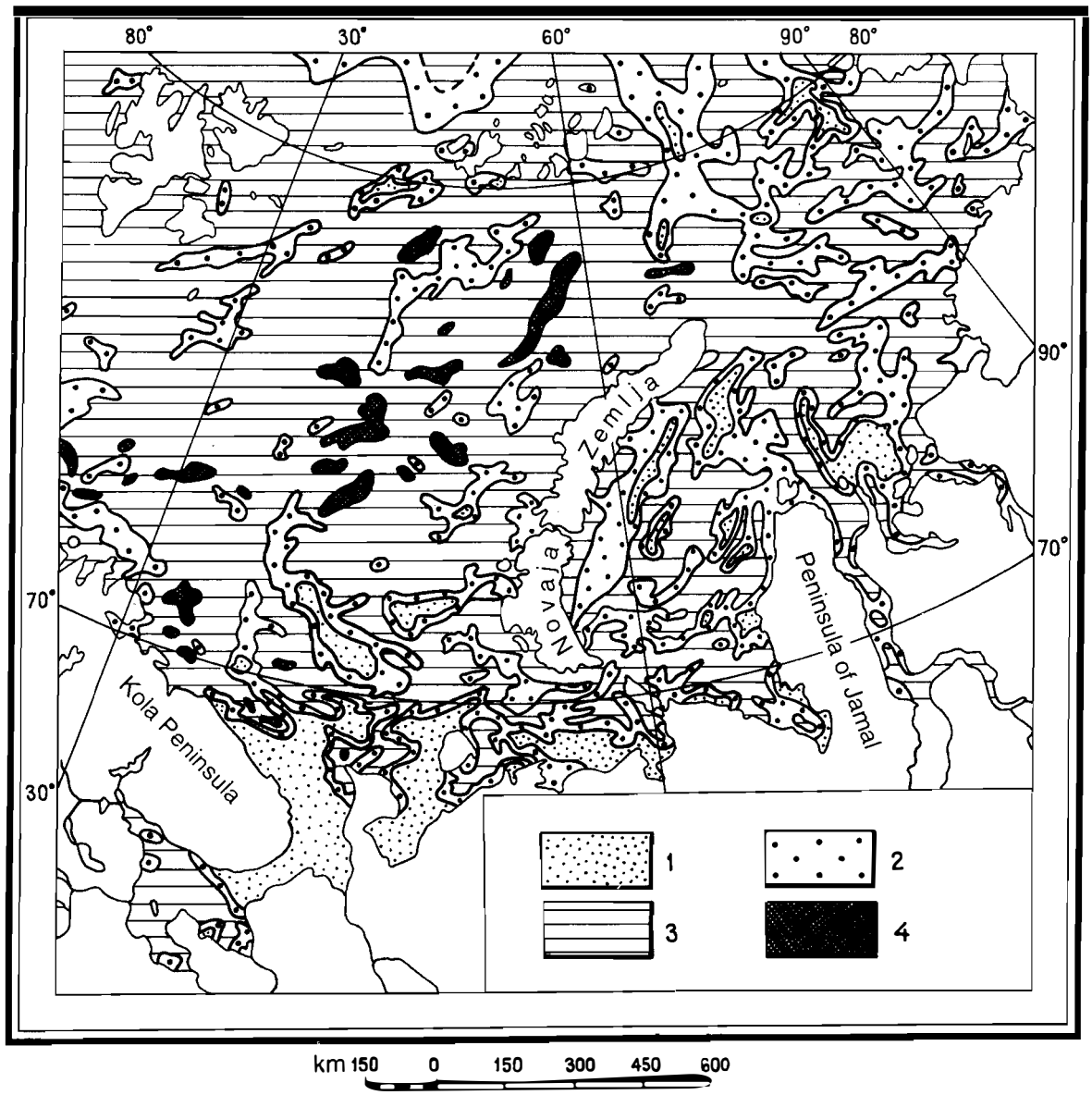

Fig. 4.6 The content (%) of the silty fraction of the modern deposits of the Western Arctic Shelf: 1. < 25; 2. 25 to 50; 3. 50 to 75; 4. > 75.

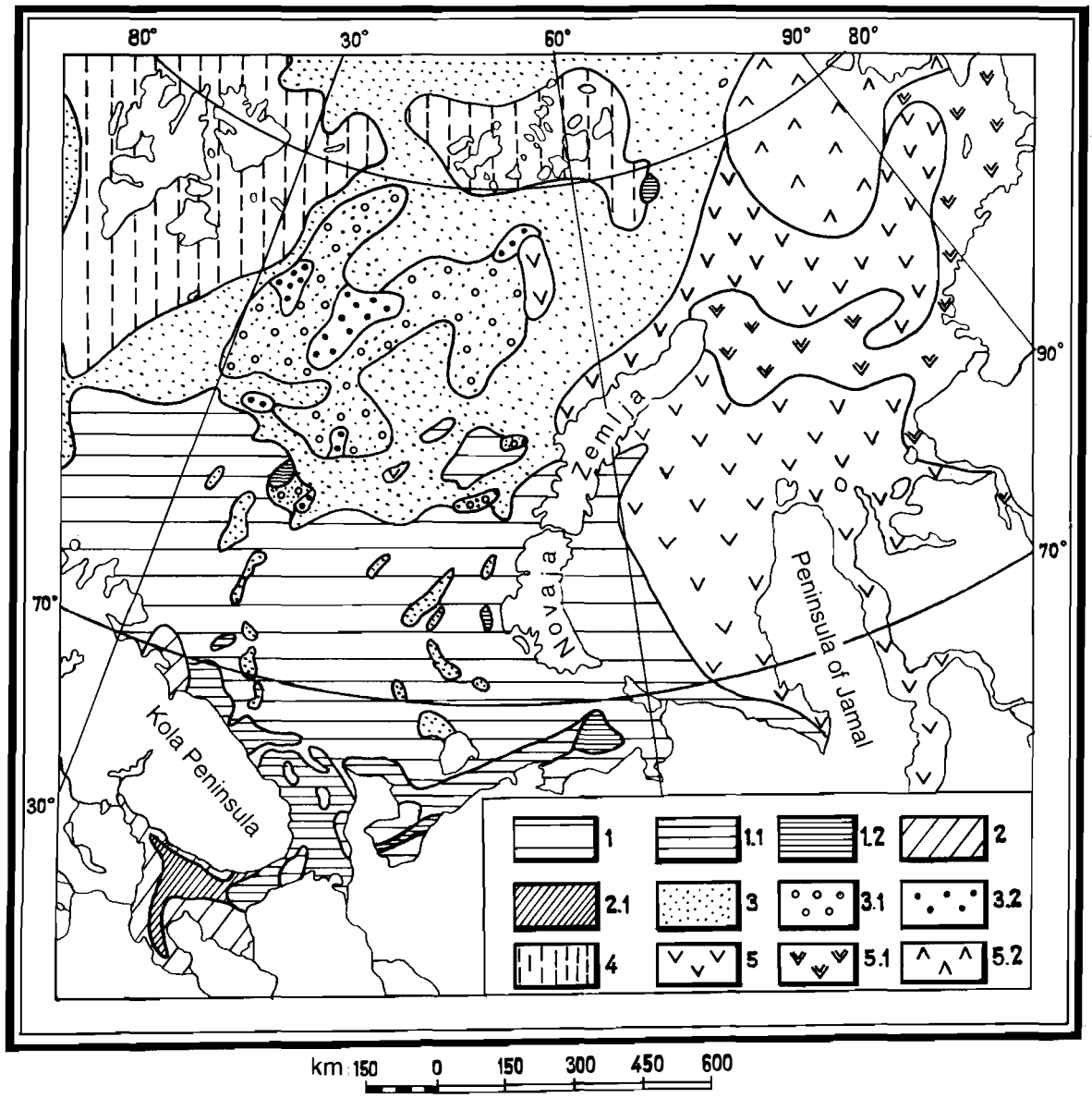

Fig. 4.7 Mineral composition of the heavy fraction of the modern deposits of the Western Arctic Shelf: 1. epidote-garnet-ore-hornblende association, South Barents type, including 1.1. non-epidote offshore subtype (ep < 10 %); 1.2. sphene-zircon subtype (sph, zr > 10 %). 2. epidote-garnet- hornblende association, Belomorian type, including 2.1. essential hornblende basin subtype (hbl > 50 %). 3. epidote-garnet-ore association, Central Barents type, with authigenic ferriferous mineralisation (> 10 %), including 3.1. non- epidote subtype; 3.2. sphene-leucoxene-apatite subtype (sph, leu, ap > 10 %). 4. chlorite-hornblende-ore-pyroxene association, Svalbard type. 5. epidote-pyroxene-ore-hornblende association, Kara type, including. 5.1. non-epidote Siberian subtype (ep < 10 %); 5.2. garnet Severozemelian subtype (ga > 10 %).

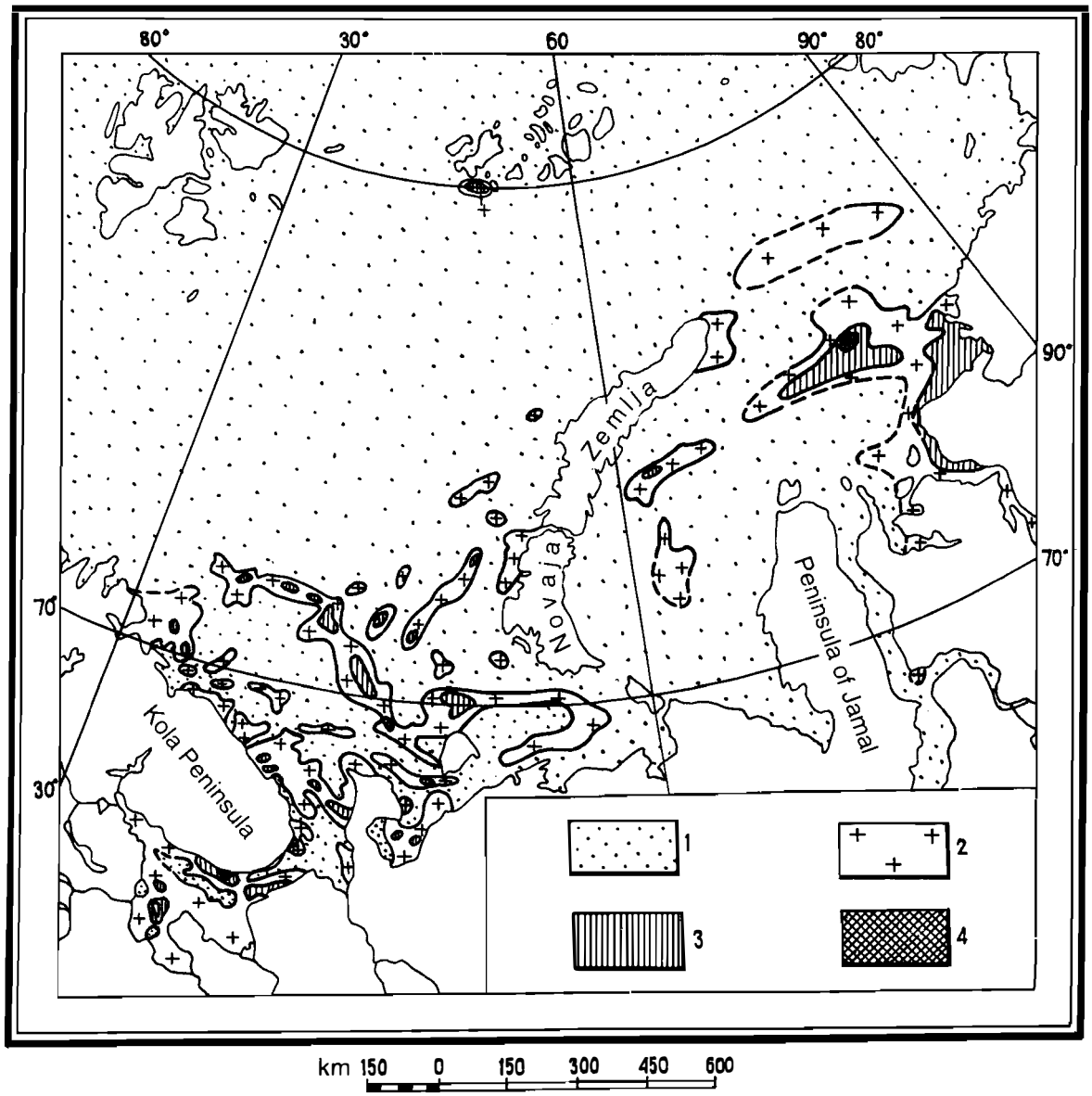

Fig. 4.8 The content (%) of heavy minerals in the modern deposits of the Western Arctic Shelf: 1. < 3; 2. 3 to 10; 3. 10 to 30; 4. > 30.

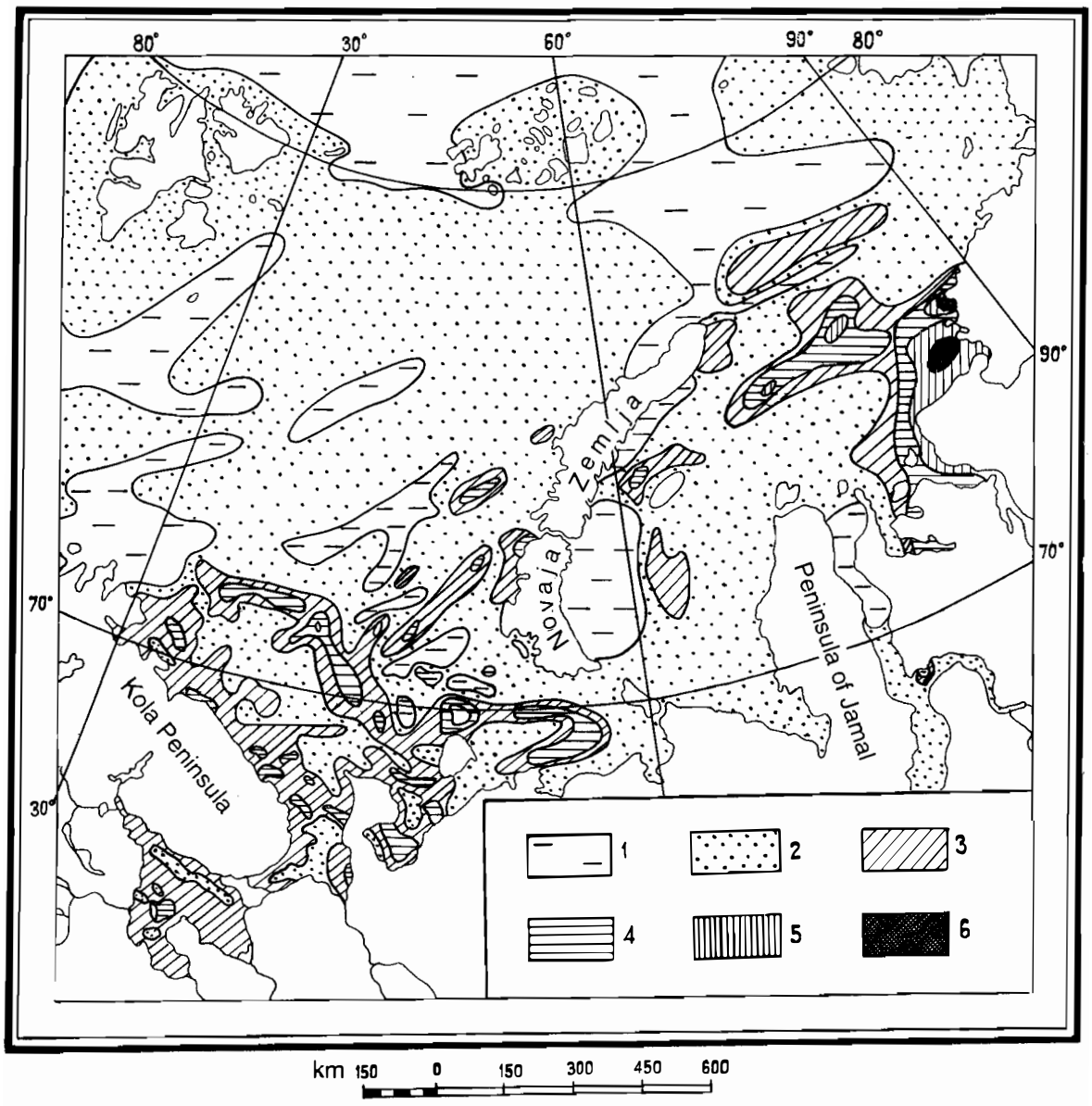

Fig. 4.9 The content (%) of black ore minerals in the modern deposits of the Western Arctic Shelf: 1. < 0.01; 2. 0.01 to 0.1; 3. 0.1 to 1; 4. 1 to 5; 5. 5 to 7; 6. > 7.

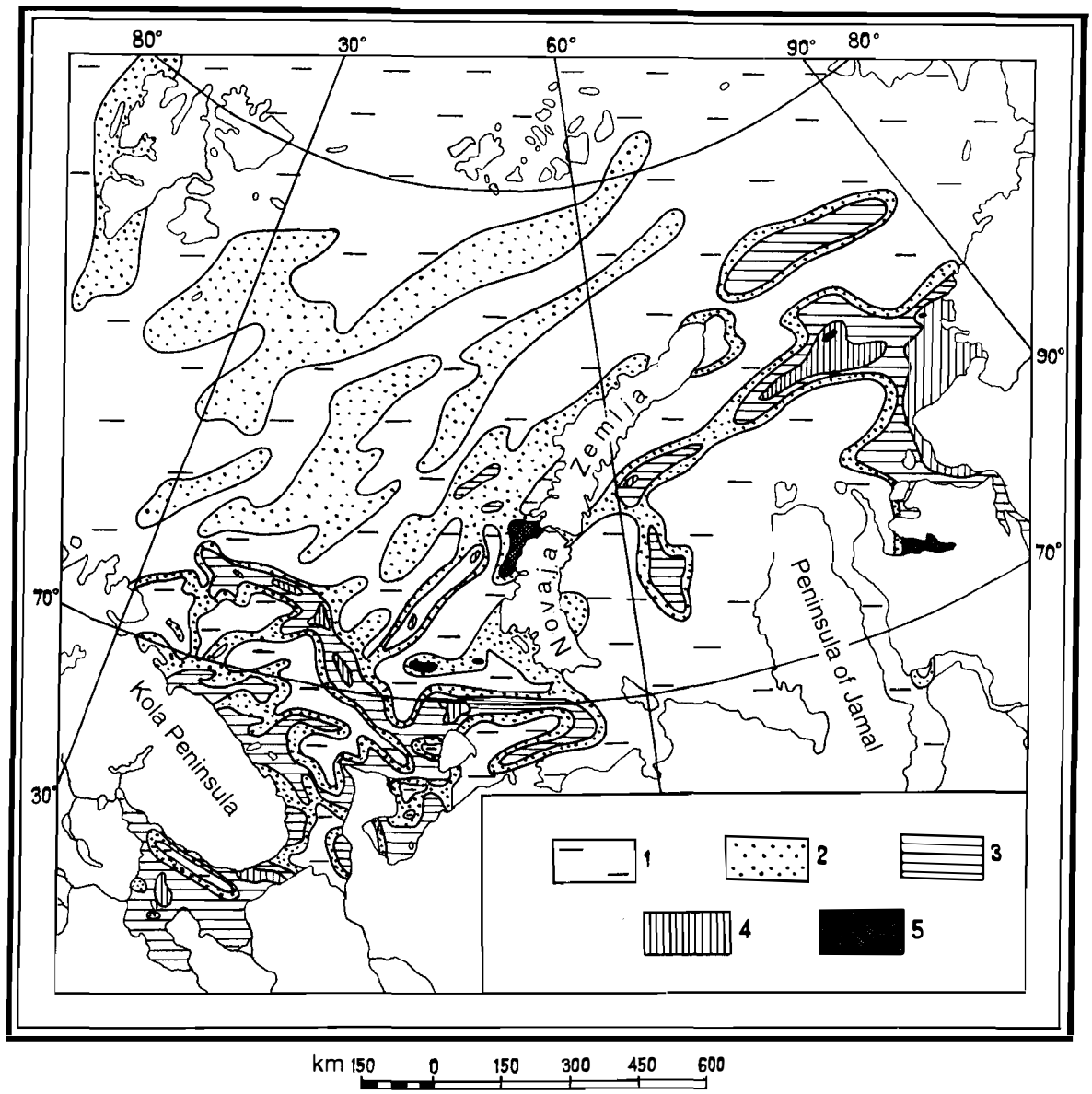

Fig. 4.10 The content (%) of titaniferous minerals (sphene, rutile, leucoxene, anatase, brucite) in the modern deposits of the Western Arctic Shelf: 1. < 0.01; 2. 0.01 to 0.1; 3. 0.1 to 1; 4. 1 to 2; 5. > 2.

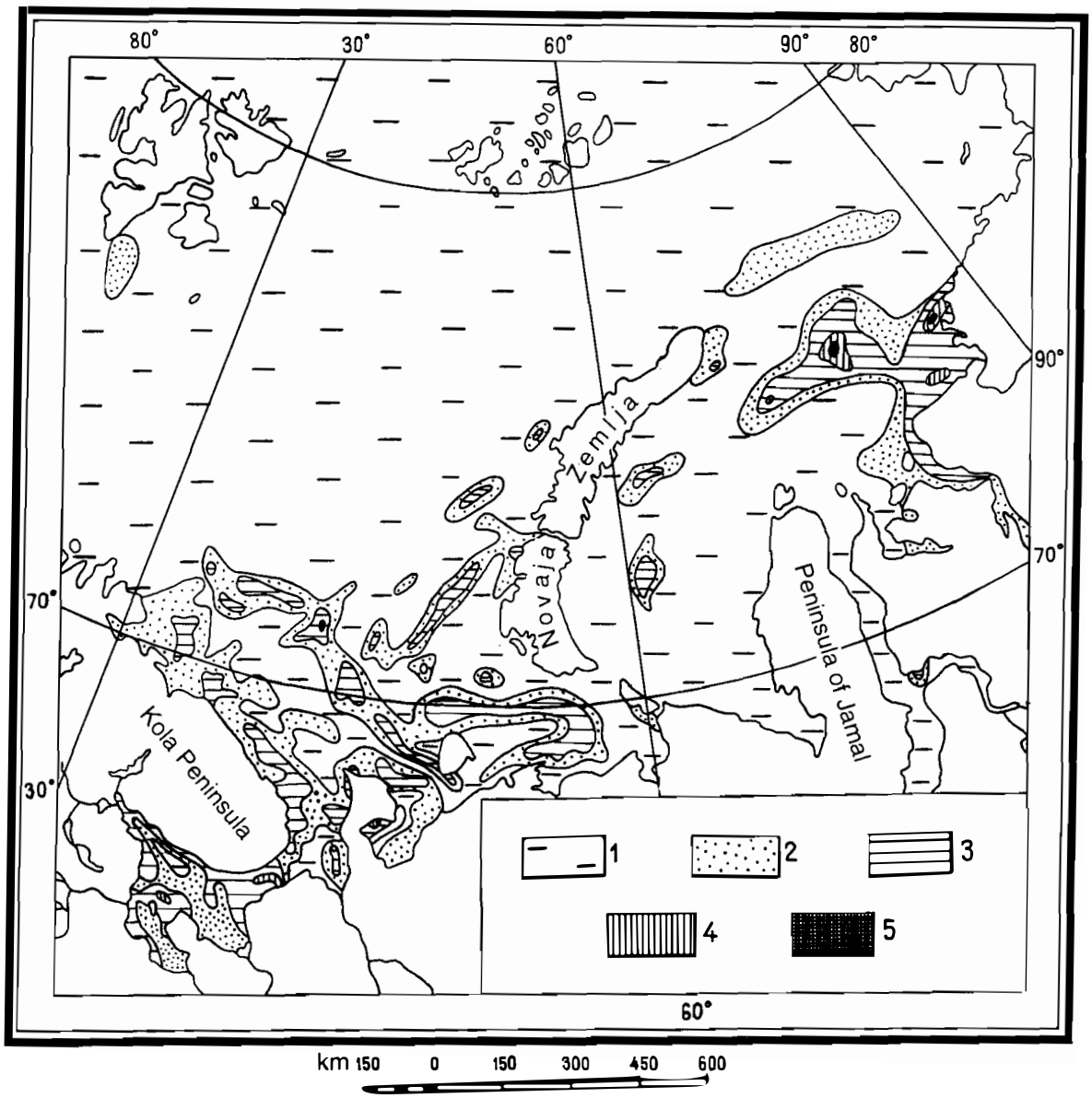

Fig. 4.11 The content (%) of zircon in the modern deposits of the Western Arctic Shelf: 1. < 0.01; 2. 0.01 to 0.1; 3. 0.1 to 1; 4. 1 to 3; 5. > 3.

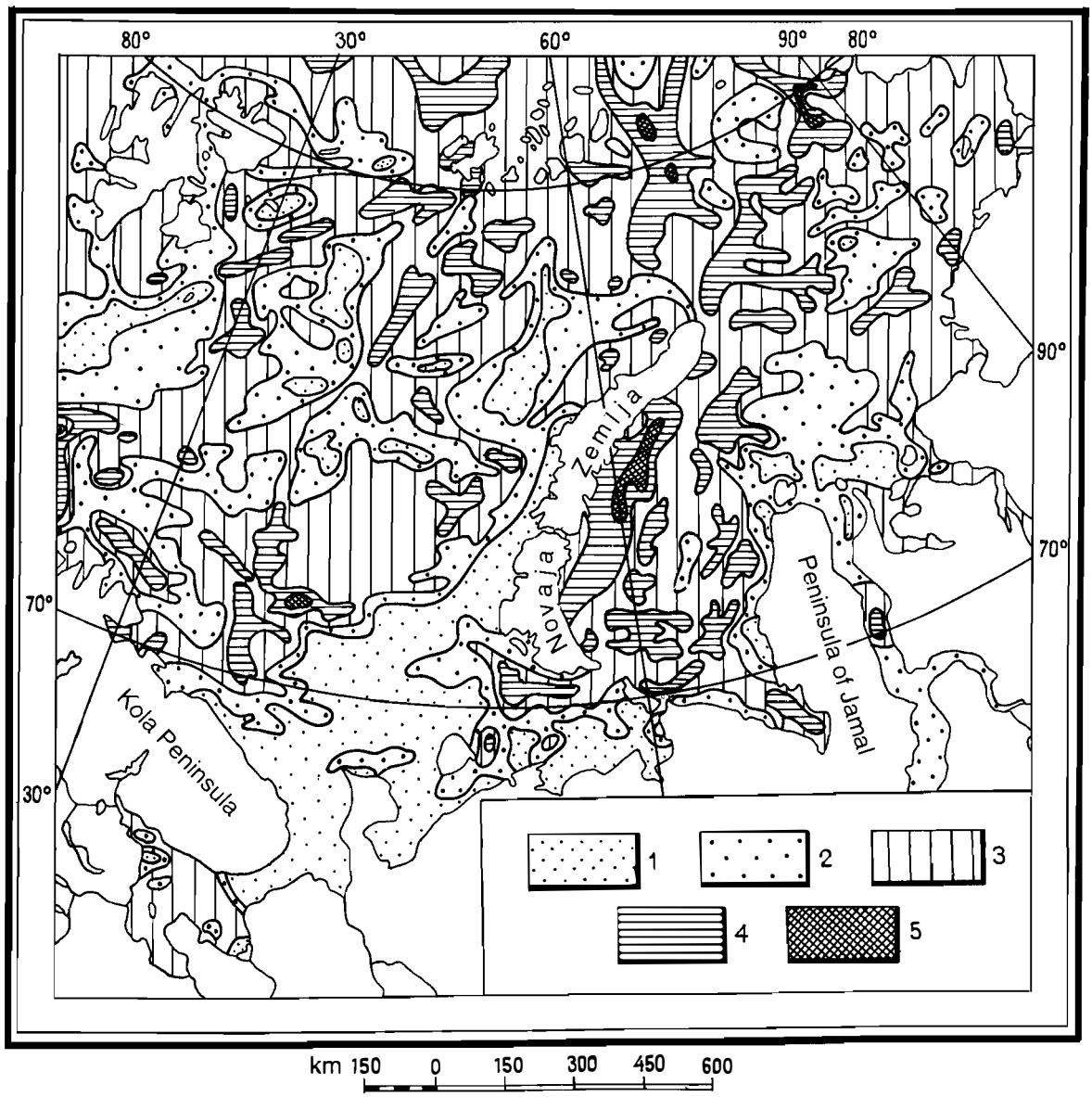

Fig. 4.12 The content (%) of the clay fraction in the modern deposits of the Western Arctic Shelf: 1. < 10; 2. 10 to 25; 3. 25 to 50; 4. 50 to 75; 5. > 75.

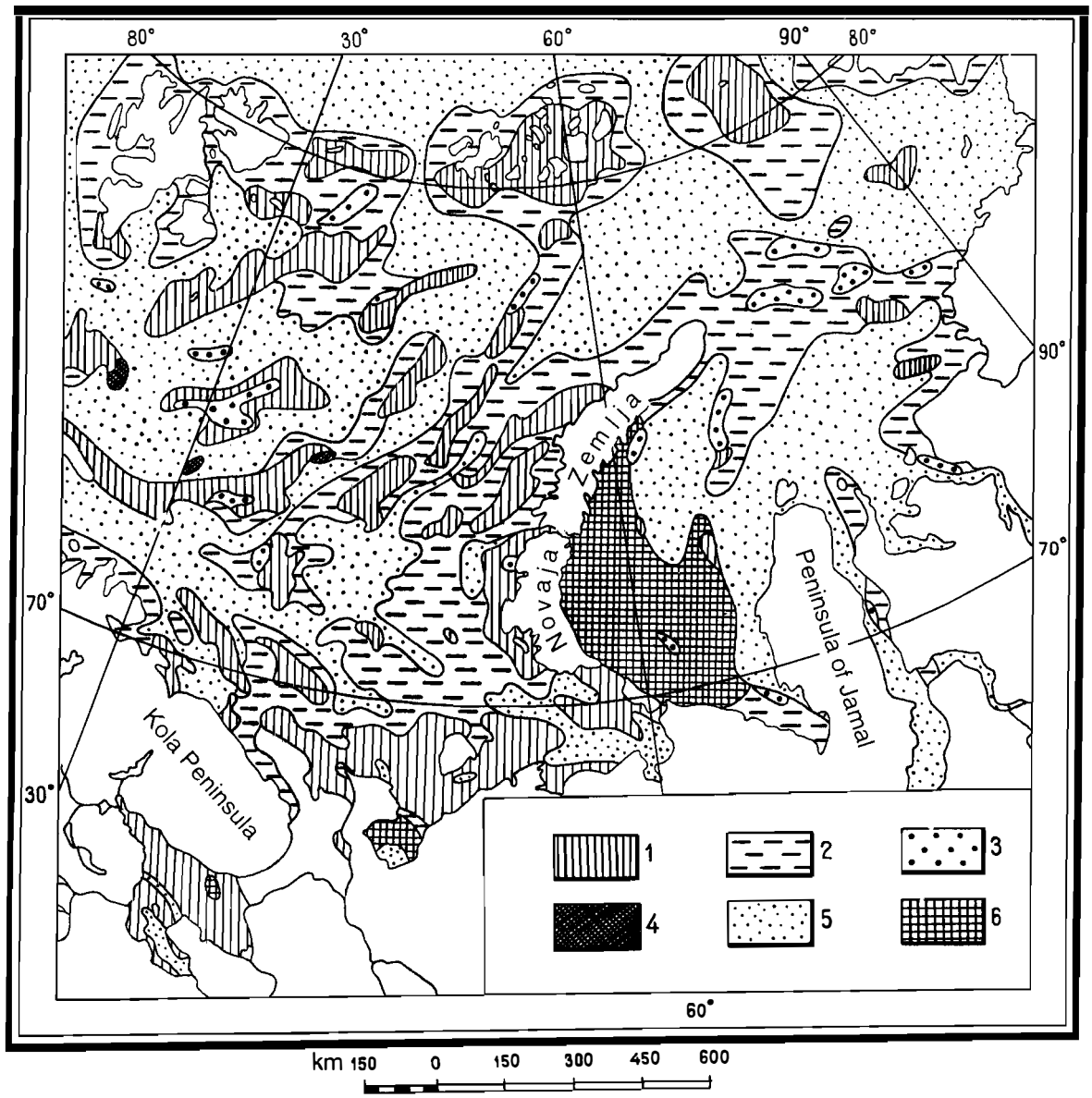

Fig. 4.13 The clay mineral composition in the clay fraction of the modern deposits of the Western Arctic Shelf: 1. montmorillonite and montmorillonite-illite; 2. chlorite and chlorite-illite; 3. montmorillonite-illite with kaolinite; 4. vermiculite-illite; 5. illite; 6. mixed chlorite-montmorillonite-illite.The content of the main clay minerals (illite, chlorite, montmorillonite, kaolinite) in relation to the total mass of the modern sediments is shown in Figure 4.14.

Fig. 4.14 The clay minerals (%) in the modern deposits of the Western Arctic Shelf.

4.4 Clay minerals

Clay minerals are only concentrated in the clay fraction, whose distribution in modern sediments of the Western Arctic Shelf is shown in Figure 4.12. The mineral composition of the clay fraction, investigated in 1075 samples using X-ray crystallography and thermic analyses, is shown in Table 4.4 and Figure 4.13.

Table 4.4 Distribution of clay mineral composition in the clay fraction of modern sediments (% by area)

Composition	*White Sea*	*Barents Sea*	*Kara Sea*
Monominerals			
Illite I	49.7	26.4	31.4
Montmorillonite M	13.3	0.9	–
Chlorite C	–	0.1	–
Kaolinite K	–	0.2	–
Biminerals			
Montmorillonite-Illite MI	32.8	25.5	21.0
Chlorite-Illite CI	–	31.6	40.9
Vermiculite-Illite VI	–	1.7	–
Kaolinite-Illite KI	–	2.8	–
Triminerals			
CMI	4.2	9.9	–
KMI	–	0.6	–
KCI	–	–	6.7

Illite generally seems to dominate the clay fraction of bottom sediments on the Western Arctic Shelf and is the only clay mineral in areas experiencing intensive recent sedimentation (see section 3.1). Because of bottom denudation and reworking of underlying rocks (especially Upper Palaeozoic and Mesozoic), montmorillonite is common where a thin veneer of Upper Cenozoic sediment is present. The presence and increased content of montmorillonite may often serve as a marker and approximate quantitative criterion for autochthonous components in modern sediments. The author believes that the presence of small areas carrying more kaolinite and vermiculite than normal indicates bottom denudation of ancient weathering crusts because these minerals cannot form in the severe conditions of cold Arctic seas. High concentrations of chlorite have been mapped in northern and northeastern parts of the shelf, including areas where neighbouring islands now have glaciers. Hence, this unstable clay mineral is regularly present where mechanical, not chemical, erosion prevails.

Mixed-layer clay minerals occur in no more than 5–15 % of the total mass of the clay fraction; mixed layers of montmorillonite (20–30 %) and illite (70–80 %) are found. The composition of mixed-layer minerals and their correspondence with areas that are transitional between autochthonous parts undergoing bottom abrasion and those experiencing stable accumulation show the predominance of aggradational processes in the alteration of clay minerals on the Barents Sea Shelf.

5. BIOGENIC COMPONENTS

The biogenic components of modern sediments on the Western Arctic Shelf are carbonate and siliceous remains and organic material originating from animals and plants. The total content of biogenic components in the sediments (Fig. 5.1) is usually only exceeded by the terrigenic components (Gurevich 1976).

5.1 Organic material

The map showing the distribution of organic carbon (Fig. 5.2) is based on analyses of bottom samples from 2078 stations. The content of dry organic material (OM) decomposed to the pelagic

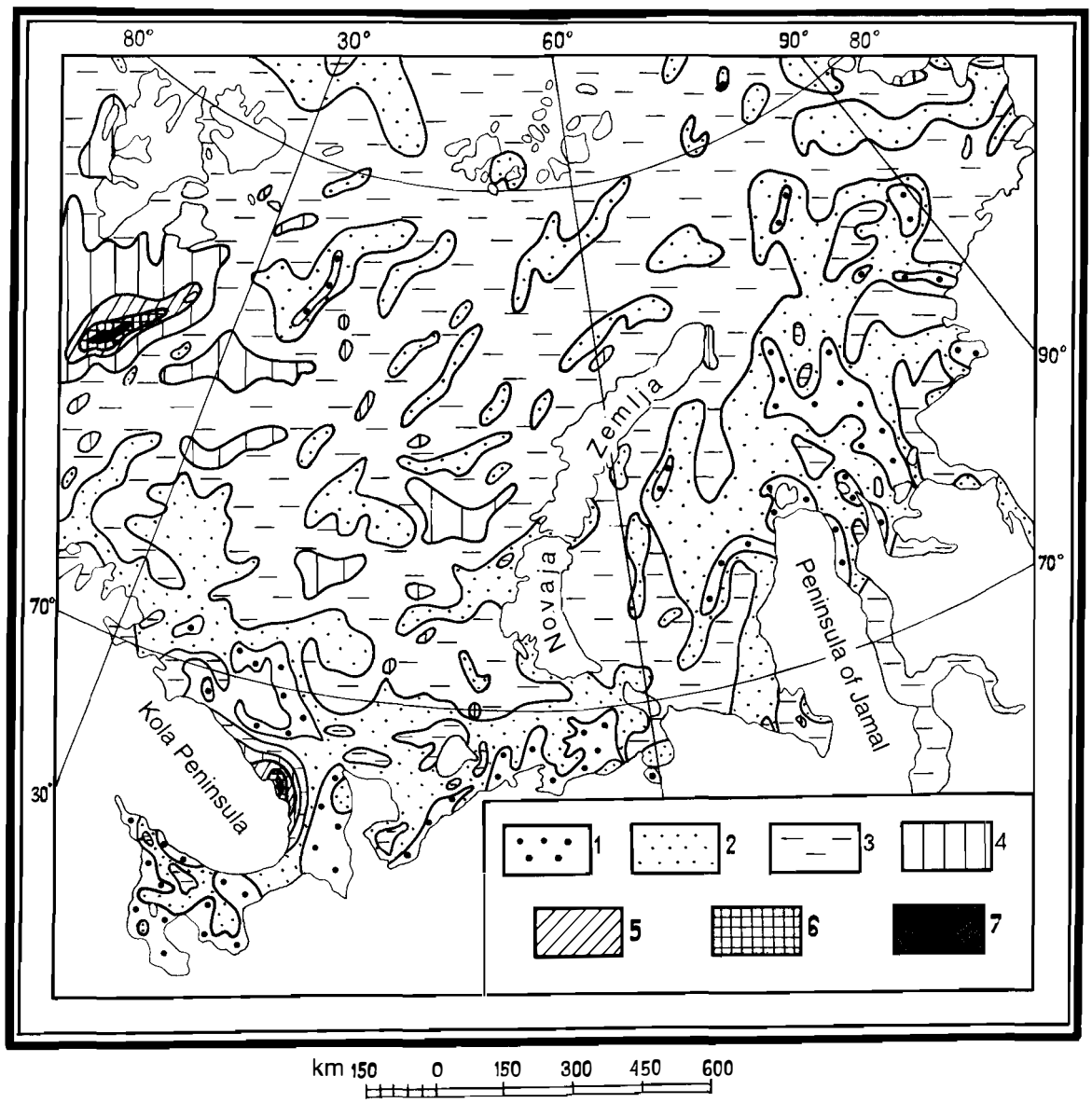

Fig. 5.1 The content (%) of biogenic components in modern deposits of the Western Arctic Shelf: 1. < 1; 2. 1 to 5; 3. 5 to 10; 4. 10 to 30; 5. 30 to 50; 6. 50 to 70; 7 > 70.

stage can be estimated using the relationship: OM = 1.82 C_{org}. The natural moisture in organic material is usually 50–70 % or more.

A significant proportion of the organic material of deposits in near-shore areas is humus compounds of vegetal origin. The distribution of humic acids is shown in Figure 5.3.

There is a very high content of sapropelic components in organic material near polar fronts. The background content of chloroformic bituminoids is less than 0.007 %, but this is enriched to 0.1–0.3 % in fine-grained sediments of frontal zones. In addition to syngenetic bituminoids, epigenetic bituminoids and bituminoids of mixed origin are also noted (Fig. 5.4).

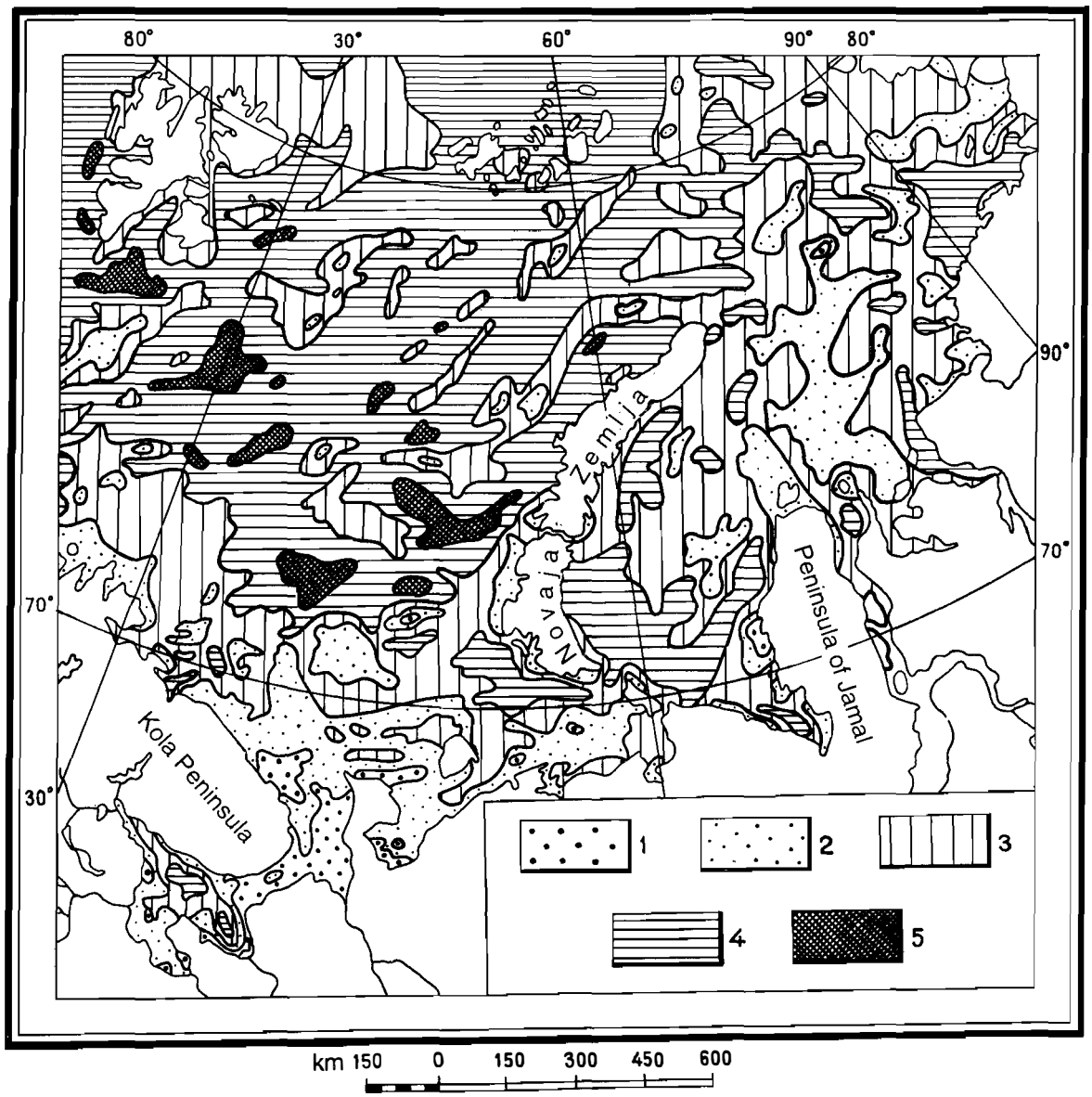

Fig. 5.2 The organic carbon (C_{org}) content (%) of the modern deposits of he Western Arctic Shelf: 1. < 0.1; 2. 0.1 to 0.5; 3. 0.5 to 1; 4. 1 to 2; 5. > 2.

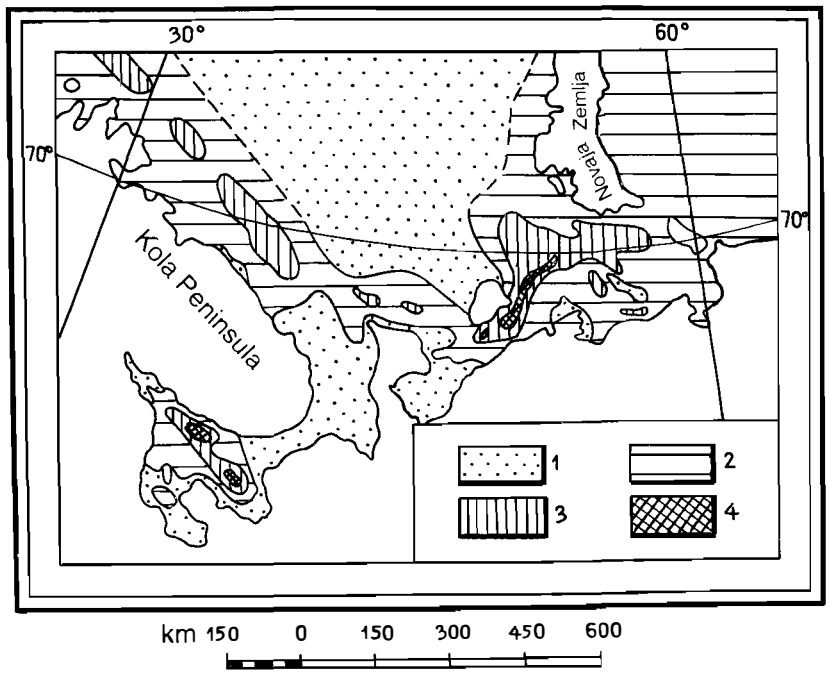

Fig. 5.3 The humic acids content (%) of the modern deposits of the southernmost Barents Sea and Kara Sea shelves: 1. < 0.1; 2. 0.1 to 0.5; 3. 0.5 to 1; 4. > 1.

5.2 Carbonates

$CaCO_3$ has been determined at 3005 stations. The biogenic carbonate content of the modern sediments is generally low (Fig. 5.5), and carbonate sedimentation is uncommon in polar regions in general. Across 65.3 % of the Western Arctic Shelf it measures no more than 1 %, and in 32.2 % of the area it ranges between 1 and 5 %. However, the $CaCO_3$ content increases to 25–50 % of the total mass of modern sediment in two provinces, Medvezjinsko-Nadezjdinskaya and Svyatonosskaya.

The Svyatonosskaya province of carbonate shell sands was discovered in 1974 (Yakovleva & Gurevich 1974). It is on the boundary between the White Sea and the Barents Sea, northeast of Cape Svyatoy Nos. The shell bed is about 120 km long and 40 km wide, and the water depth is 28–70 m. The bed varies in thickness from 0.5 to 3.6 m, averaging 1.5 m. The fauna is barnacles *Balanus crenatus* + *B. balanus* (about 90 %), molluscs (9 %) and bryozoans (0.55 %). The $CaCO_3$ content varies from 10 to 90 %, averaging 40–50 %. Intensive biogenic carbonate sedimentation is therefore capable of taking place near polar fronts on the Western Arctic Shelf. Such sedimentation is especially atypical because Cirripedia are not the most important lime-secreting organisms. The age range of this deposit, as determined by ^{14}C dating at two localities, is 790 ± 60 years (TA-1541, station 3, interval 0.1–0.5 m) to 1170 ± 60 years (TA-1543, station 3, interval 2.4–2.7 m), and 2340 ± 40 years (TA-1532, station 6, interval 0–0.5 m) to 2720 ± 40 years (TA-1533, station 6, interval 2.5–3.2 m). The sedimentation rate in the Svyatonosskaya province is therefore extremely high (up to 3–8 mm/year) and the biogenic carbonate sedimentation is of avalanche character.

The shell-sand resources in the Svyatonosskaya province exceed 300 million tons and are adequate to satisfy the needs of industrial poultry farms in Russia and neighbouring countries.

An estimate of the absolute age of Holocene carbonate deposition in this region is based on 97 ^{14}C determinations that form a fairly representative group irregularly distributed across several Holocene epochs (Table 5.2.1).

Table 5.2.1 shows that there were at least two peaks of carbonate formation during the Holocene. These were not due to climatic optima, as believed previously, but to the succeeding periods of deteriorating, increasingly cooler, climate such as the mid-Holocene Pereslavle interval and the Sedov stage. Holocene carbonates were often deposited during moderate sea-ice conditions – from 2 to 4 tenths of ice cover.

Table 5.2.1 Age of Holocene carbonates on the White Sea and Barents Sea shelves

Period, phase	*Age (1000 yr)*	*Duration (1000 yr)*	*Ice conditions (tenths)*	*Frequency of data*	
				percentage, %	*relative %/1000 yr*
Unnamed warming	10.3–9.6	0.7	2	1.1	1.6
Pereslavle interval	9.6–9.0	0.6	6	6.2	10.3
Mid-Holocene optimum					
phase 1 – increasing	9.0–7.5	1.5	2	11.4	7.6
phase 2 – culmination	7.5–3.0	4.5	0	27.7	6.2
phase 3 – decreasing	3.0–2.5	0.5	2	16.5	33.0
Sedov stage	2.5–1.5	1.0	4	16.5	16.5
Early Medieval warming	1.5–0.5	1.0	2	12.4	12.4
Little Ice Age	0.5–0.1	0.4	6	4.1	10.2
Modern warming	0.1–0.0	0.1	4	2.1	21.0

Using infrared methods, the author, in co-operation with O.A. Zalkind, has obtained data about the mineral composition of some common biogenic carbonates of the Western Arctic Shelf. These are shown in Table 5.2.2 and are related to species that commonly produce lime in modern sediments.

The most stable crystalline form of biogenic carbonates is anhydrous calcite. The hydrous form of calcite is more common in juveniles. Modern lithothamnion crusts are composed of hydrous calcite, but the content of carbonate with a dolomitic structure increases in mesotypical and, especially, palaeotypical species. The same tendency is noted for the bryozoan *Cellepora surcularis*. Dolomitisation of calcite obviously partly takes place during postmortem changes, through interaction with sea water in accordance with the Geidinger reaction. Sr, Ba, S and Se increase simultaneously. The dolomitisation process promotes the porosity of bryozoans and lithothamnion crusts. Shells of gastropods and many bivalves are composed of aragonite. Aragonite is partly substituted by calcite in fossilised detritus and palaeotypical shells. The Sr content simultaneously increases from 0.2 % (in aragonite) to 0.3–0.4 % (in calcite) of the total mass.

Hence, the mineralogical and chemical composition of biogenic carbonates is initially determined by the species of organisms producing the lime, but subsequently changes during and after their lifetime.

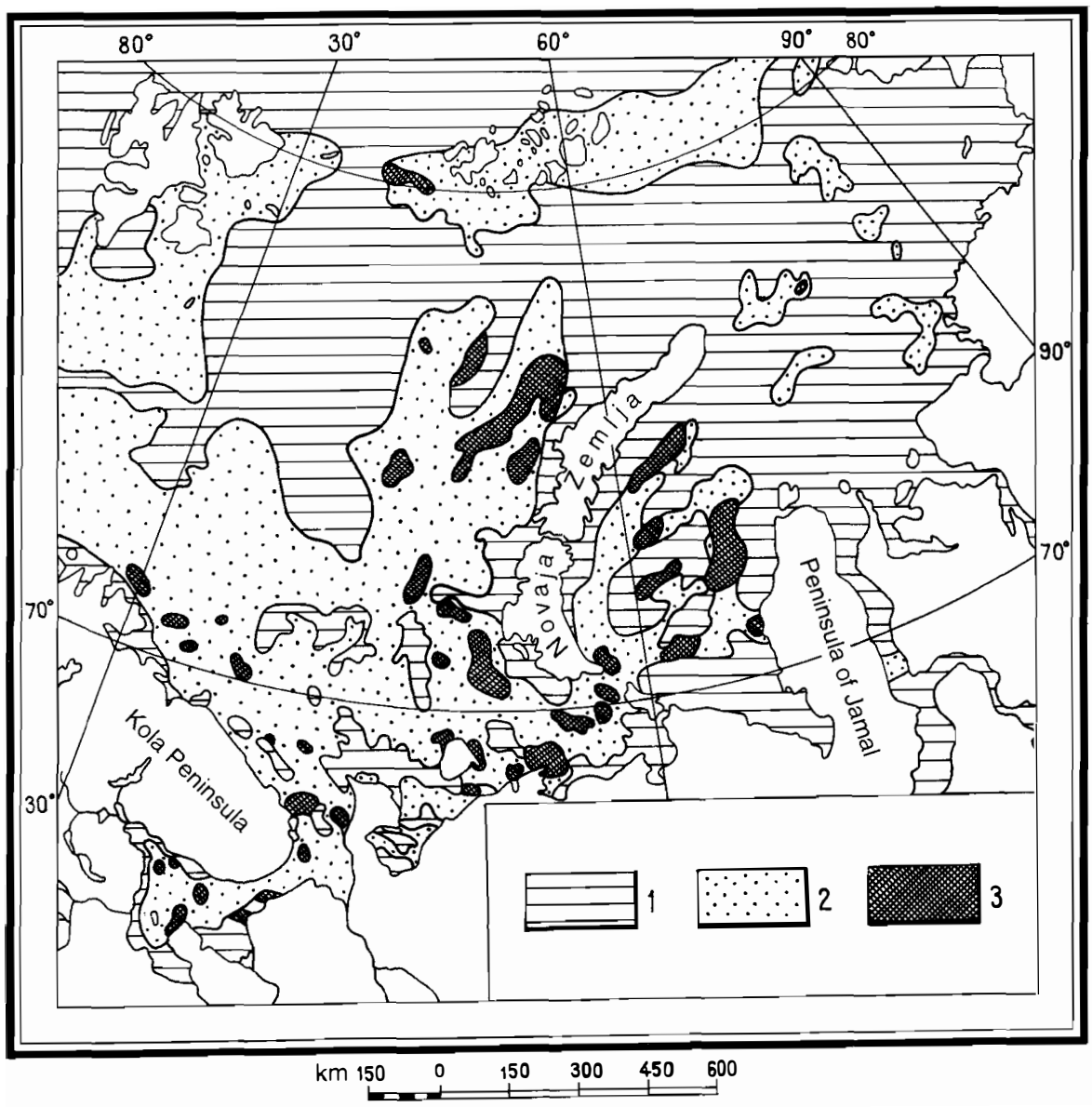

Fig. 5.4 Dominant types of chloroformic bituminoids A in the modern deposits of the Western Arctic Shelf: 1. syngenetic bituminoids; 2. mixed bituminoids; 3. epigenetic bituminoids.

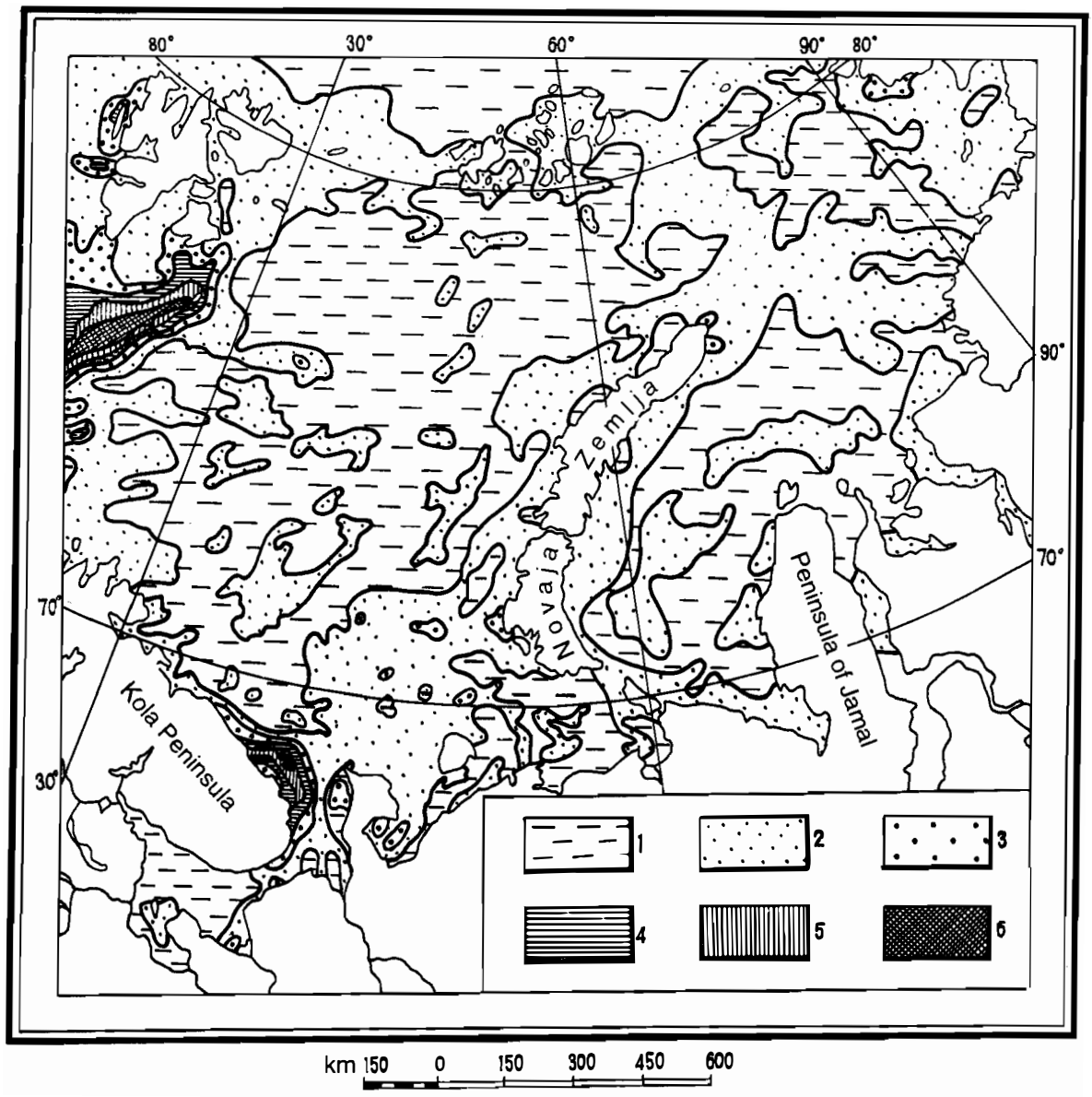

Fig. 5.5 The $CaCO_3$ content (%) of the modern deposits of the Western Arctic Shelf: 1. < 1, 2. 1 to 5; 3. 5 to 10; 4. 10 to 25; 5. 25 to 50; 6. > 50.

Table 5.2.2 Mineral composition of biogenic carbonates

Species	*Appearance*	*Mineral composition*
Balanus sp. *Chlamys islandica*	Palaeotypical, mesotypical	Calcite, anhydrous
Balanus crenatus B. balanus, Chlamys islandica	Cenotypical, juvenile	Calcite, hydrous
Strongylocentrotus droebachiensis	Cenotypical	Calcite, hydrous
Asterias rubens	Cenotypical	Calcite, hydrous with organic material
Lithothamnion sp.	Cenotypical	Calcite, hydrous
Lithothamnion sp.	Palaeotypical	Carbonate, hydrous with dolomite structure
*Cellepora surcul*aris	Cenotypical	Carbonate, hydrous with organic material
Buccinum undatum, Neptunea despecta, Modiolus modiolus, Hiatella arctica, Arctica islandica	Mesotypical	Aragonite
Mytilus edulis, Neptunea despecta	Palaeotypical	Aragonite and calcite

5.3 Siliceous components

The biogenic siliceous components of Western Arctic Shelf sediments are mainly represented by diatom shells and sponge spicules. White, glass-like, "thick felt" derived from spicules of siliceous sponges was noted several times in south-western areas of the Barents Sea. Increasing contents of amorphous silica ($SiO_{2amorph}$) (Fig. 5.6) reach 2–3 % or more of the total mass of modern deposits in these areas.

5.4 Spore and pollen components

Spores and pollen grains form a volumetrically insignificant part of the bottom sediments of the Western Arctic Shelf, but provide some indirect criteria for the origin of modern sediments. The maps showing their distribution are based on palynological investigations of 994 samples of modern sediments from 663 stations (Fig. 5.7A), including original data from 208 stations.

Six age assemblages are found: Palaeozoic (Fig. 5.7B), Permo-Triassic (Fig. 5.7C), Jurassic-Early Cretaceous (Fig. 5.8A), Late Cretaceous-Palaeocene (Fig. 5.8B), Eocene-Miocene (Fig. 5.8C) and Pliocene-Quaternary (Fig. 5.8D). The distribution of the various assemblages across the shelf is shown in Figure 5.9 and Table 5.4.

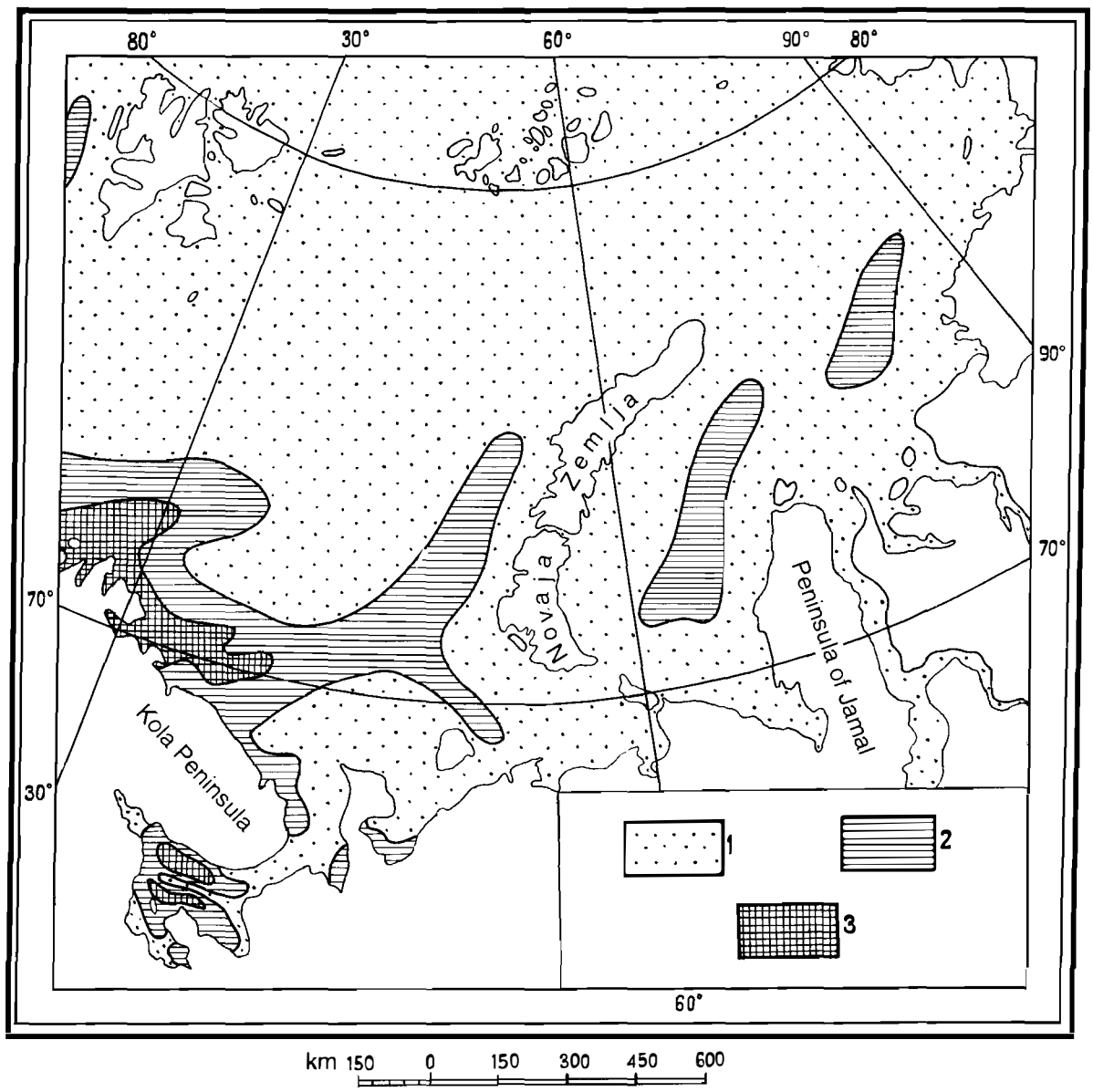

Fig. 5.6 Siliceous biogenic fragments in the modern deposits of the Western Arctic Shelf: 1. not found; 2. 0.5 to 1 %; 3. > 1 %.

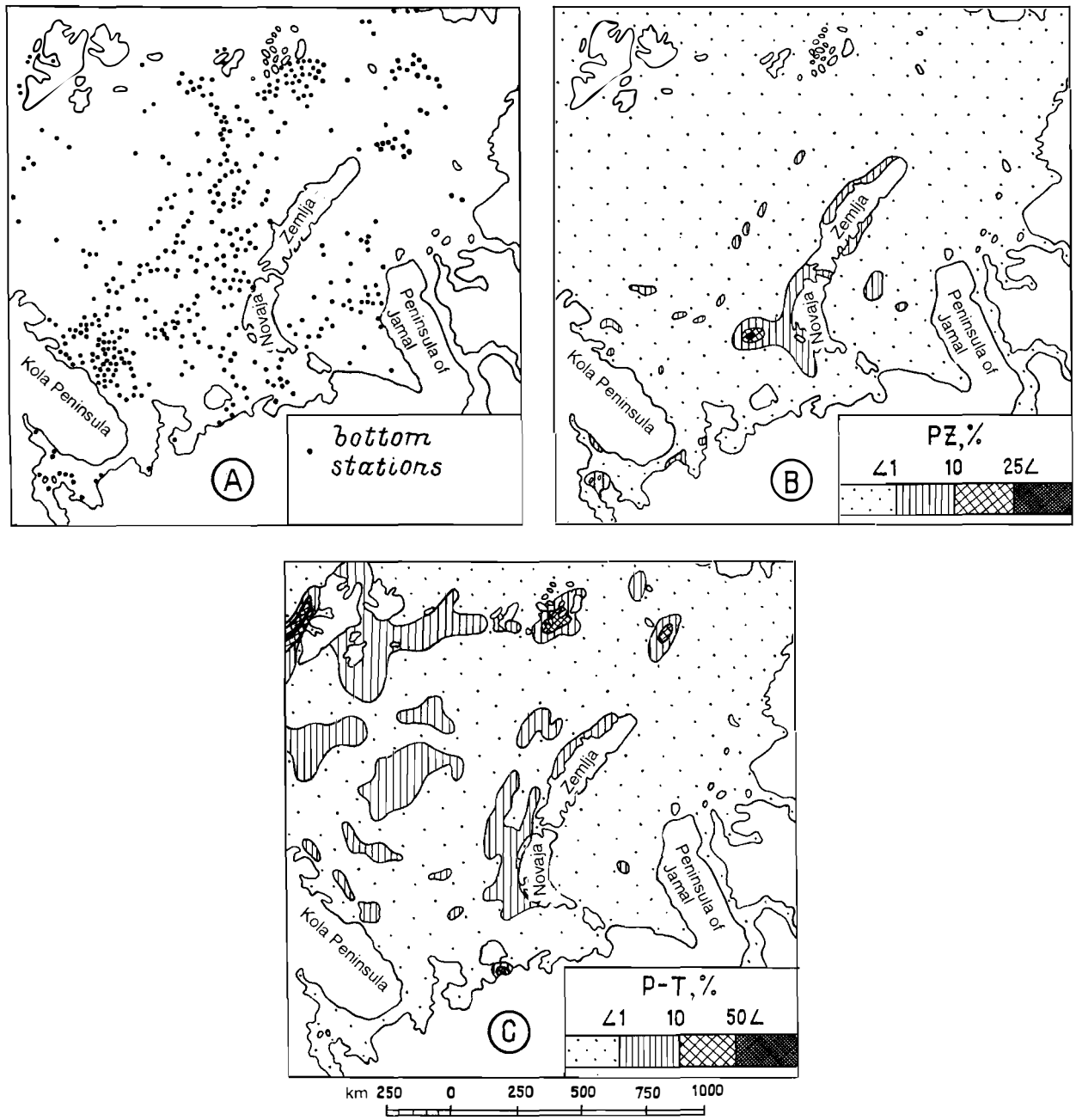

Fig. 5.7 Location of sampling sites for palynological analysis (A) and distribution of Palaeozoic (B) and Permo-Triassic miospores (C) in palynological spectra from modern deposits of the Western Arctic Shelf.

Table 5.4 Distribution of ages of palynological assemblages on the Western Arctic Shelf

Age of assemblage	*Shelf, % of total area*			
	White Sea	*Barents Sea*	*Kara Sea*	*Western Arctic*
Dominant (> 75% of grains)				
N_2Q (Pliocene-Quaternary)	38.1	12.8	26.8	19.0
P_2N_1 (Eocene-Miocene)	–	–	1.6	0.5
K_2P_1 (Late Cretaceous-Palaeocene)	–	0.3	18.1	5.5
JK_1 (Jurassic-Early Cretaceous)	25.6	65.4	30.7	52.2
P-T (Permo-Triassic)	–	0.5	–	1.1
PZ (Palaeozoic)	–	0.1	–	0.1
Transitional (25-75% of grains)				
JK_1-N_2Q	36.3	19.5	7.1	15.9
Mixed (10-50% of grains)				
K_2P_1-P_2N_1-N_2Q	–	–	4.3	1.3
JK_1-K_2P_1-N_2Q	–	0.9	10.4	3.6
Total number	100.0	99.5	99.0	99.2
Additional (1-10% of grains)				
P_2N_1	–	0.6	1.3	0.8
K_2P_1	–	1.4	0.4	1.0
PT	–	22.8	1.3	14.2
PZ	5.0	1.1	1.8	1.4

Modern palynological assemblages are only present and dominant (Fig. 5.10) in areas of intensive recent sedimentation where Quaternary deposits are more than 50 m thick. These are the Kandalaksha-Dvinskaya province in the White Sea, the Nordkapp, Malozemelskaya and Bolsheze melskaya provinces in the Barents Sea, and the Preyamalskaya province in the Kara Sea. However, reworked fossilised palynological assemblages dominate in modern sediments in vast areas where recent denudation and modern erosion of the sea floor prevail and the thickness of the unconsolidated cover is 5–10 m or less. Jurassic-Lower Cretaceous miospores are most widespread, occurring in central, eastern and northern parts of the Barents Sea and the northern part of the Kara Sea. Permo-Triassic miospores are widespread in the Svalbard and Medvezjinsko-Nadezjdinskaya provinces and near the continental slope of the Norwegian-Greenland Sea. Palaeogene-Miocene palynological assemblages dominate in many provinces of the Kara Sea (Baidaratskaya, Vaigachsko-Litkenskaya, Prednovozemelskaya, Enisey-Pyasin-skaya). Local areas where miospores of Permo-Triassic and Palaeozoic age are found form a chain along the southern and eastern margins of the Southern Barents Sea Synclinorium. Permo-Carboniferous miospores are recorded in small quantities almost everywhere near the shores of Novaya Zemlya. This is the main evidence for widespread modern autochthonous sediments on the Western Arctic Shelf, the origin of the sediments being erosion of underlying rocks.

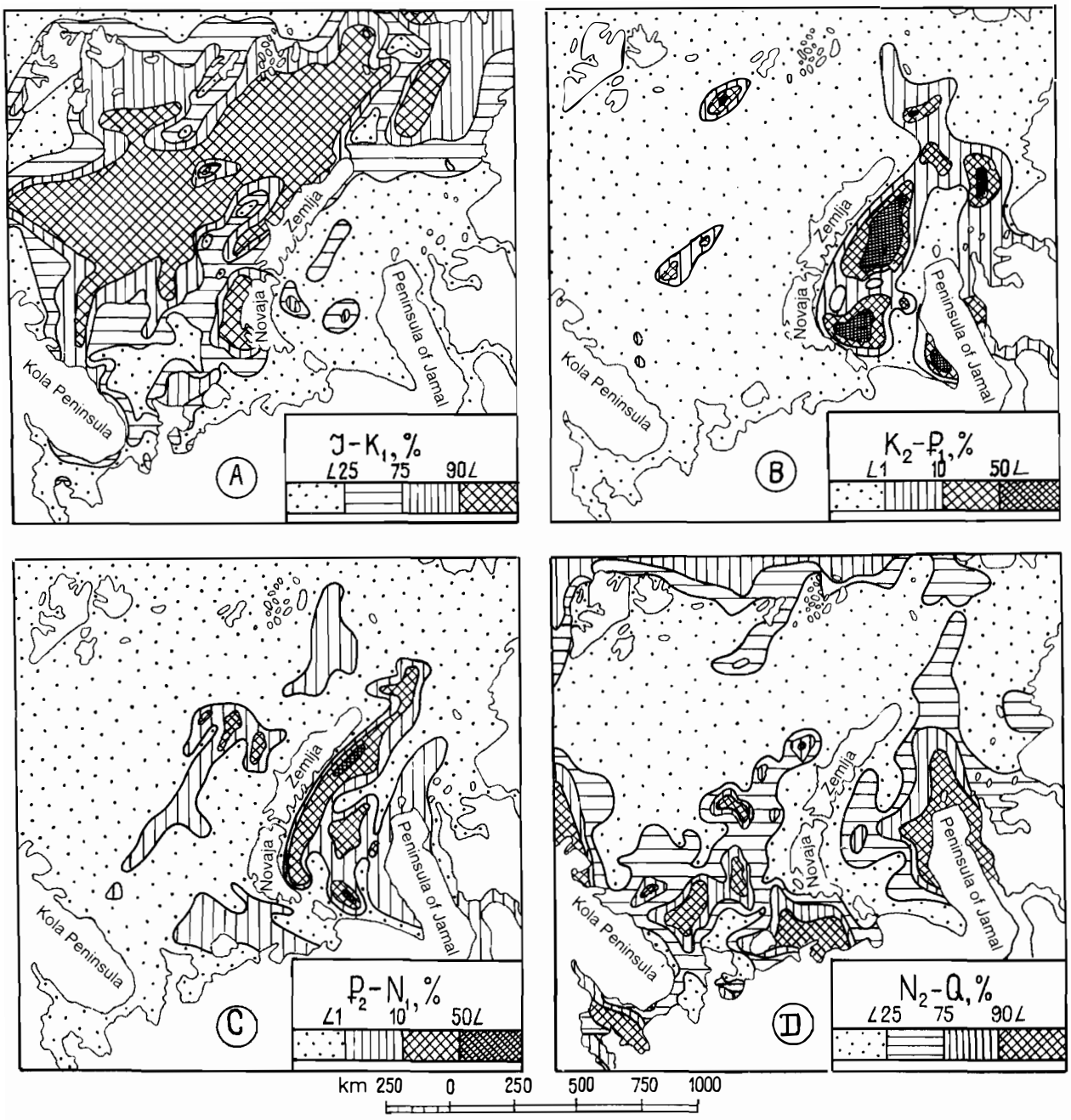

Fig. 5.8 Distribution of Jurassic-Early Cretaceous (A), Late Cretaceous-Palaeocene (B), Eocene-Miocene (C) and Pliocene-Quaternary (D) spores and pollen in palynological spectra from the modern deposits of the Western Arctic Shelf.

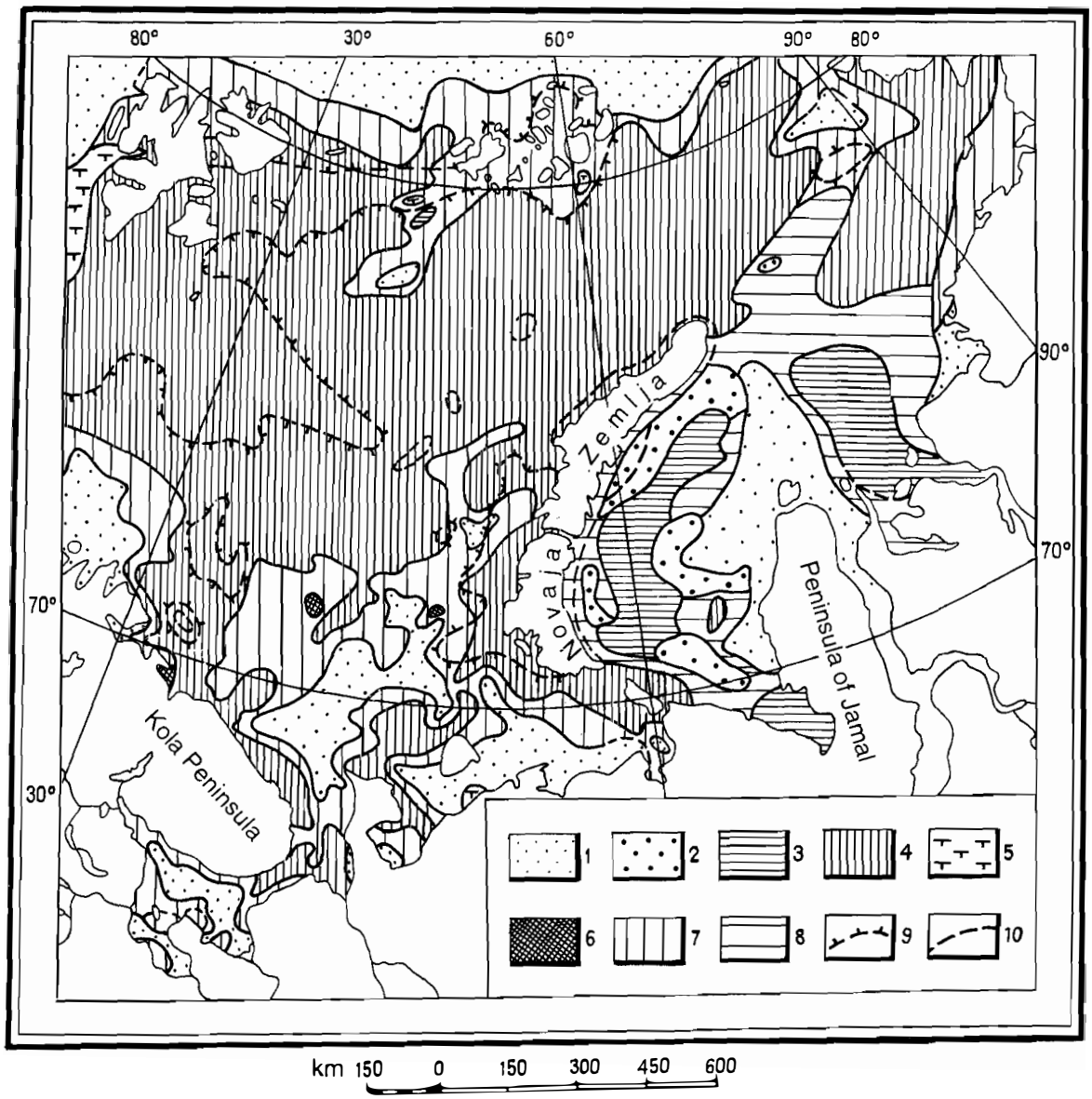

Fig. 5.9 Age of the palynological assemblages of the modern deposits of the Barents-Kara Shelf: 1. Pliocene-Quaternary (> 50 % N_2Q grains); 2. Eocene-Miocene (> 50 % P_2-N_1 grains); 3. Late Cretaceous-Palaeocene (> 50 % K_2-P_1 grains); 4. Jurassic-Early Cretaceous (> 50 % J-K_1 grains); 5. Permian-Triassic (> 50 % P-T grains); 6. Palaeozoic (> 50 % PZ grains); 7. Mixed Jurassic-Early Cretaceous-Quaternary; 8. Mixed Cretaceous-Paleocene-Quatermary; 9. limit for presence of Permo-Triassic spores; 10. limit for presence of Palaeozoic spores.

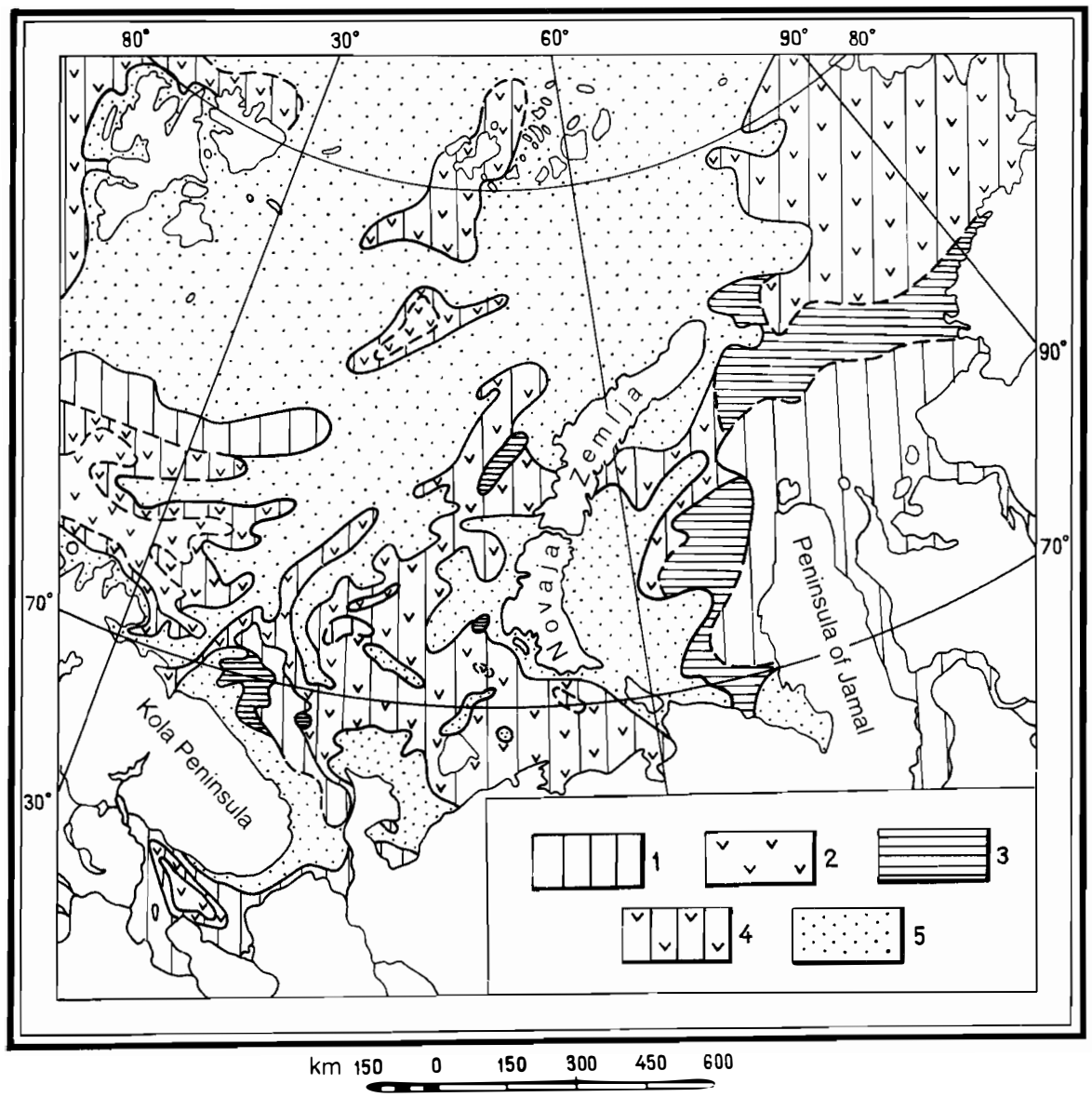

Fig. 5.10 Composition of the Pliocene-Quaternary palynological assemblages of the modern deposits of the Western Arctic Shelf: 1. wood; 2. spore; 3. wood-spore-nonwood; 4. spore-wood; 5. practically no modern pollen or spores (< 1 grain per 50 gm sediment).

6. CHEMOGENIC COMPONENTS

Chemogenic components form 0.5–40 % of the total mass of modern sediment on the Western Arctic Shelf; on average about 8 %. They are related to the diagenetic-galmirogenetic subtype (see section 8.4). Fe and Mn minerals are most significant.

6.1 Authigenic ferro and manganese forms

The composition and distribution of associations of authigenic ferriferous minerals is shown in Figure 6.1, compiled from mineralogical analyses of the silt and fine sand fractions. The distribution of carbonate, oxide and sulphide minerals conforms with the sedimentary environment. Carbonate minerals are dominant, or authigenic ferriferous components absent, in shallow-marine areas. Sulphides dominate in deep marine areas experiencing recent deposition of silt and clay. Glauconite grains are generally only present near exposures of Jurassic and Lower Cretaceous rocks. The majority of this glauconite is obviously reworked; its origin is therefore not authigenic, but autochthonous.

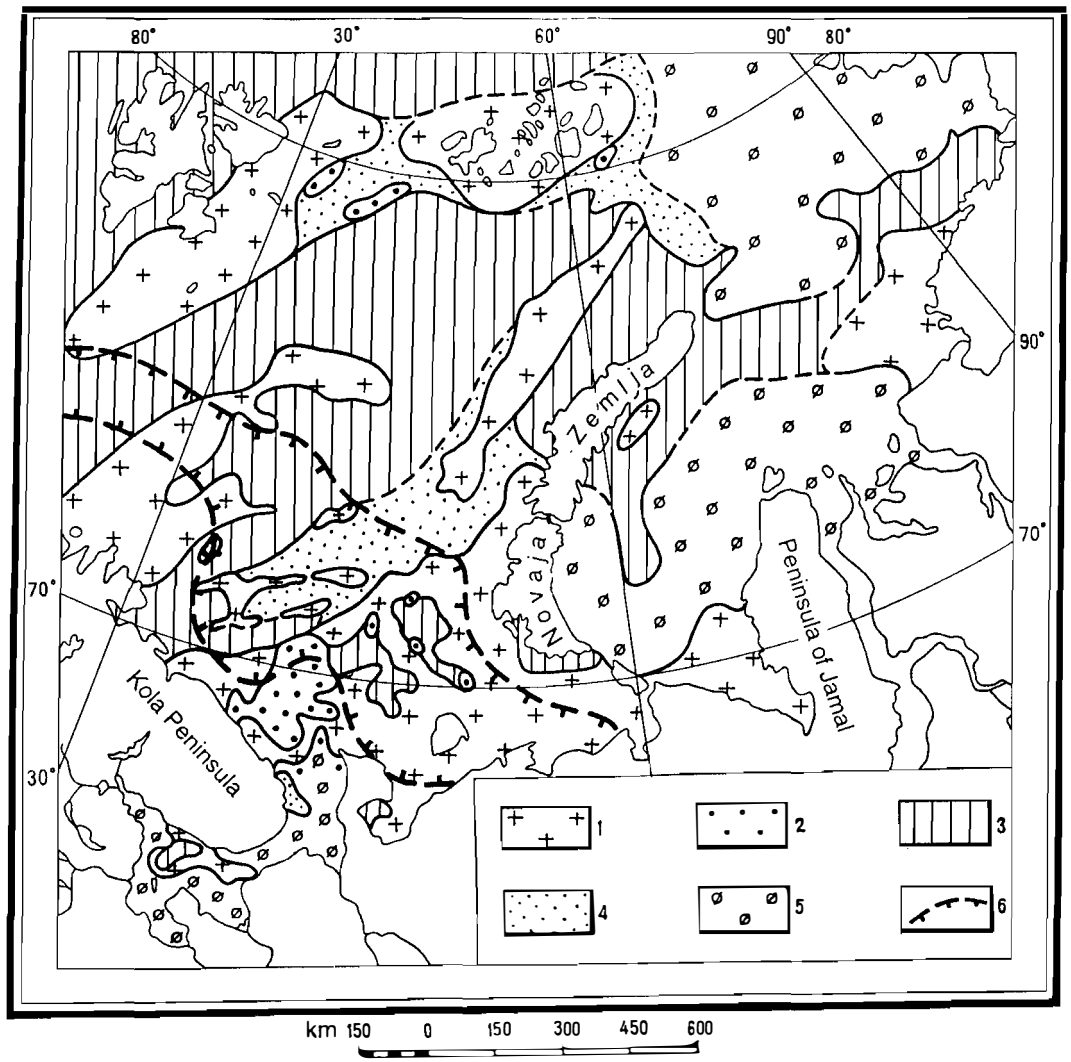

Fig. 6.1 Association of authigenic ferriferous minerals of the modern deposits of the Western Arctic Shelf: 1. carbonate (sum siderite and ankerite in a sample of authigenic ferriferous minerals exceeds 50 %); 2. oxides (sum haematite, hydrohaematite, hötite and limonite in a sample exceeds 50 %); 3. sulphides (sum iron pyrites, marcasite and hydrotroilite in a sample exceeds 50 %); 4. transition sulphide-carbonate; 5. authigenic ferriferous minerals not found (< 0.5 % in a heavy mineral suite sample); 6. boundaries of glauconite-bearing area (> 1 % in a light fraction sample).

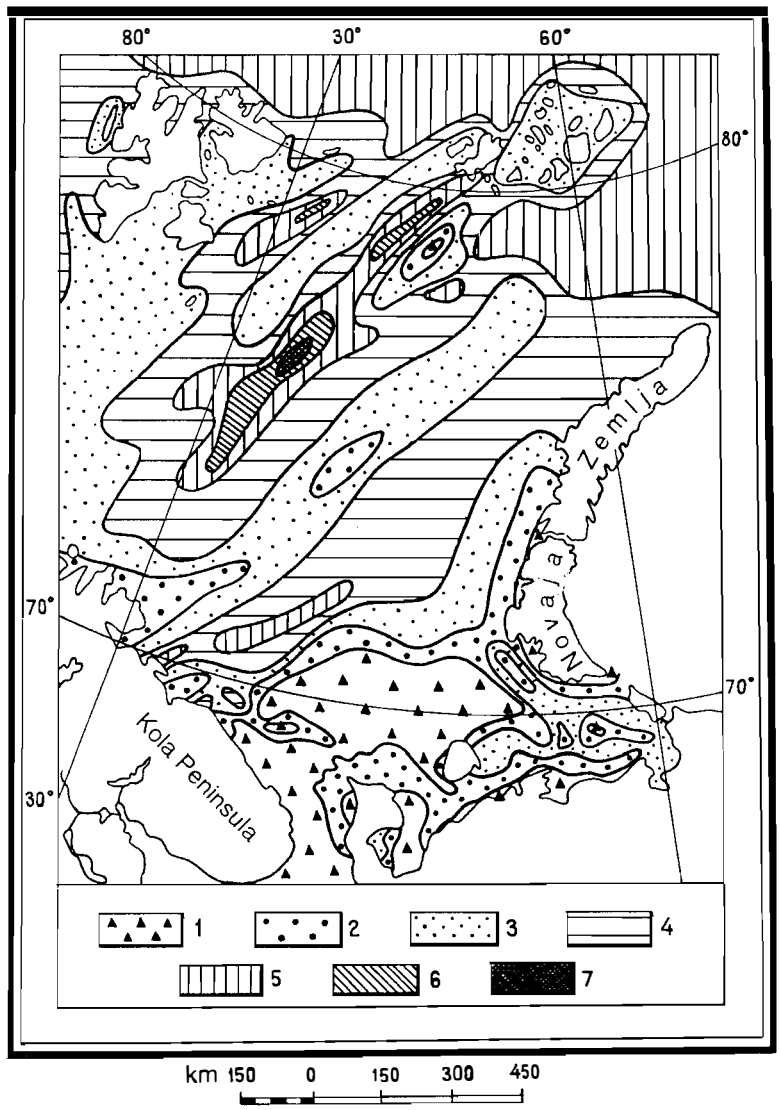

Fig. 6.2 The content (%) of iron (including Fe_2O_3) in the modern deposits of the Western Arctic Shelf: 1. < 2; 2. 2 to 3; 3. 3 to 5; 4. 5 to 7; 5. 7 to 10; 6. 10 to 15; 7. > 15.

The iron content (Fig. 6.2) varies widely, from 1 to 17 %, if Fe_2O_3 is included. High iron concentrations are usually due to the presence of pyrite, iron hydrosulphides, siderite and ankerite.

The distribution and concentration of manganese (Fig. 6.3) vary greatly. The highest content (at least 0.3–0.5 %) is found in areas where near-bottom water has a low temperature and this temperature has a low gradient (Fig. 2.4).

In contrast to oceanic concretions, the ferriferous and ferromanganese concretions and crusts in the deposits of these three seas (Fig. 6.4) do not contain significant quantities of heavy metals. The largest areas where ferromanganese concretions occur in shallow water are in the Kara Sea and the southern part of the Gorlo White Sea. The largest, disc-shaped concretions (diameter exceeding 7 cm), which contain about 10 % MnO, are also found there. Concretions in the Barents Sea have little manganese (Table 6.1).

When the reasons for the distribution of Fe-Mn concretions on the Western Arctic Shelf were assessed (Gurevich 1988), no proof of the concept of a geochemical boundary of "river-sea" type was found, nor for the notion of transport of metals along deep-seated faults. The best conditions for forming ferromanganese concretions include low speed of sedimentation, moderate near-bottom hydrodynamic activity of cool currents, enrichment of sediments by iron and manganese, and bioturbation.

Table 6.1 Composition of selected ferromanganese concretions

Content, %	*White Sea* *65°37'N* *39°13'E*	*Barents Sea* *74°49'N* *48°12'E*	*Kara Sea* *72°13'N* *65°02'E*
SiO_2	49.60	21.60	52.10
TiO_2	0.28	0.36	0.53
Al_2O_3	4.54	6.80	10.89
Fe_2O_3	10.28	40.90	7.19
MnO	12.67	0.84	9.96
MgO	1.94	4.60	2.43
CaO	1.49	3.60	1.01
Na_2O	2.58	0.50	2.69
K_2O	1.43	1.20	1.74
H_2O	10.07	2.40	not det.
P_2O_5	0.99	not det.	0.22
Sr	0.0100	0.0440	0.0260
Co	0.0010	0.0016	0.0020
Ni	0.0050	0.0056	0.0050
Cu	0.0020	0.0038	0.0048
V	0.0100	0.0089	0.0070
Cr	0.0100	0.0068	0.0074
Mo	0.0030	0.0019	0.0045
Pb	0.0010	0.0030	0.0027
U	0.0002	0.0009	0.0008
Th	0.0022	0.0020	0.0006

6.2 Metals

A significant portion of heavy metals is concentrated in fine sediment, the clay fraction, which is enriched with organic material. As an example, the distribution of uranium is shown in Figure 6.5. Increased concentrations of barium notably occur in small authigenic crystals of barytes, whose occurrence has been mapped along certain frontal zones. Areas of increased concentrations of barium (Figure 6.6) partly correspond to zones where sediments are enriched with manganese and phosphate.

6.3 Non-metals

An authigenic origin for phosphates (Fig. 6.7) and manganese-bearing material cannot explain all the connection between their distribution. X-ray diffraction studies revealed the presence of reddingite $(Mn,Fe)_3(PO_4)_23H_2O$ in some Fe-Mn concretions.

The distribution of sulphur (Fig. 6.8) is very remarkable. Areas with an abnormally high sulphur content (> 0.2–0.3 %) occur within the confines of a narrow, linear, northeast-trending zone. This zone of anomalies is an extension on the shelf of the Brøgger lineament, which has been traced along the Rhone, Rhine and Oslo grabens. We suggest that increased concentrations of sulphur can be explained by invoking upward transport of frigid hydrothermal solutions along faults to reach modern sediments.

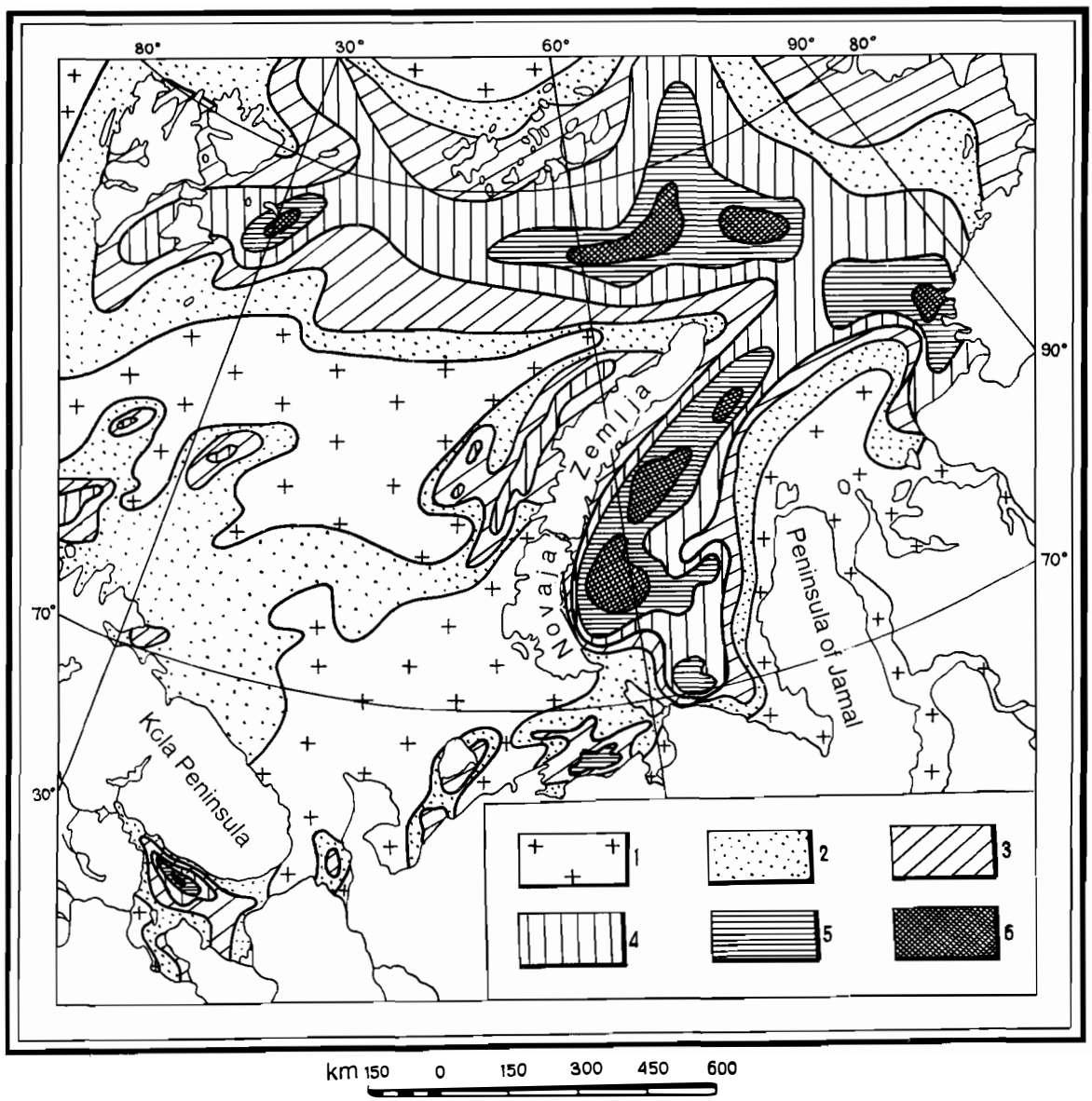

Fig. 6.3 The manganese content (%) of the modern deposits of the Western Arctic Shelf: 1. < 0.03; 2. 0.03 to 0.05; 3. 0.05 to 0.1; 4. 0.1 to 0.3; 5. 0.3 to 0.5; 6. > 0.5.

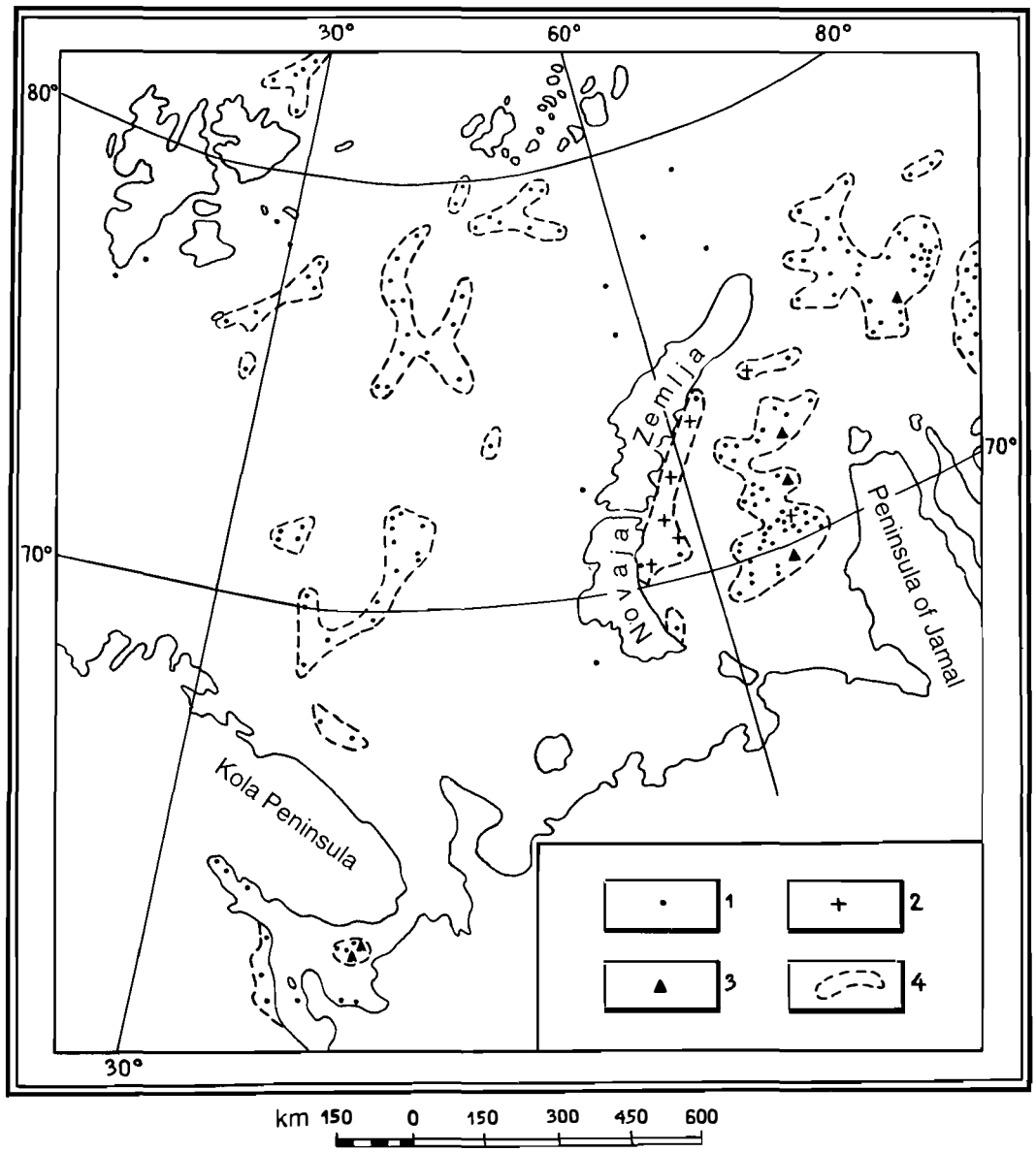

Fig. 6.4 Distribution of ferriferous and ferromanganese concretions (FMC) and crusts in the modern deposits of the Western Arctic Shelf: 1. microconcretions; 2. concretions and crusts; 3. 7–10 cm diam. and larger concretions (crusts); 4. areas containing FMC.

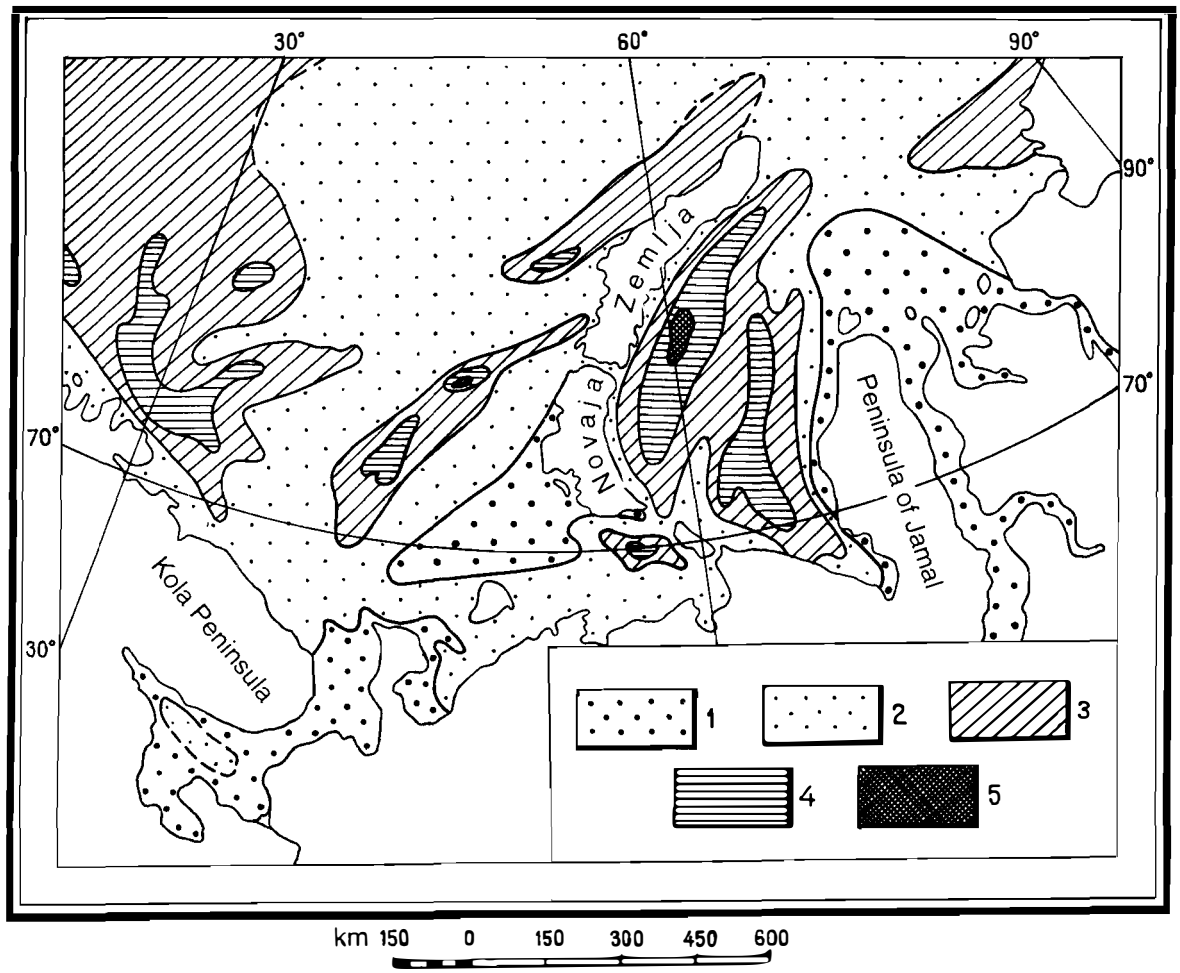

Fig. 6.5 The uranium content (% $U10^{-4}$) of the modern deposits of the Western Arctic Shelf: 1. < 1; 2. 1 to 5; 3. 5 to 7; 4. 7 to 10; 5. > 10.

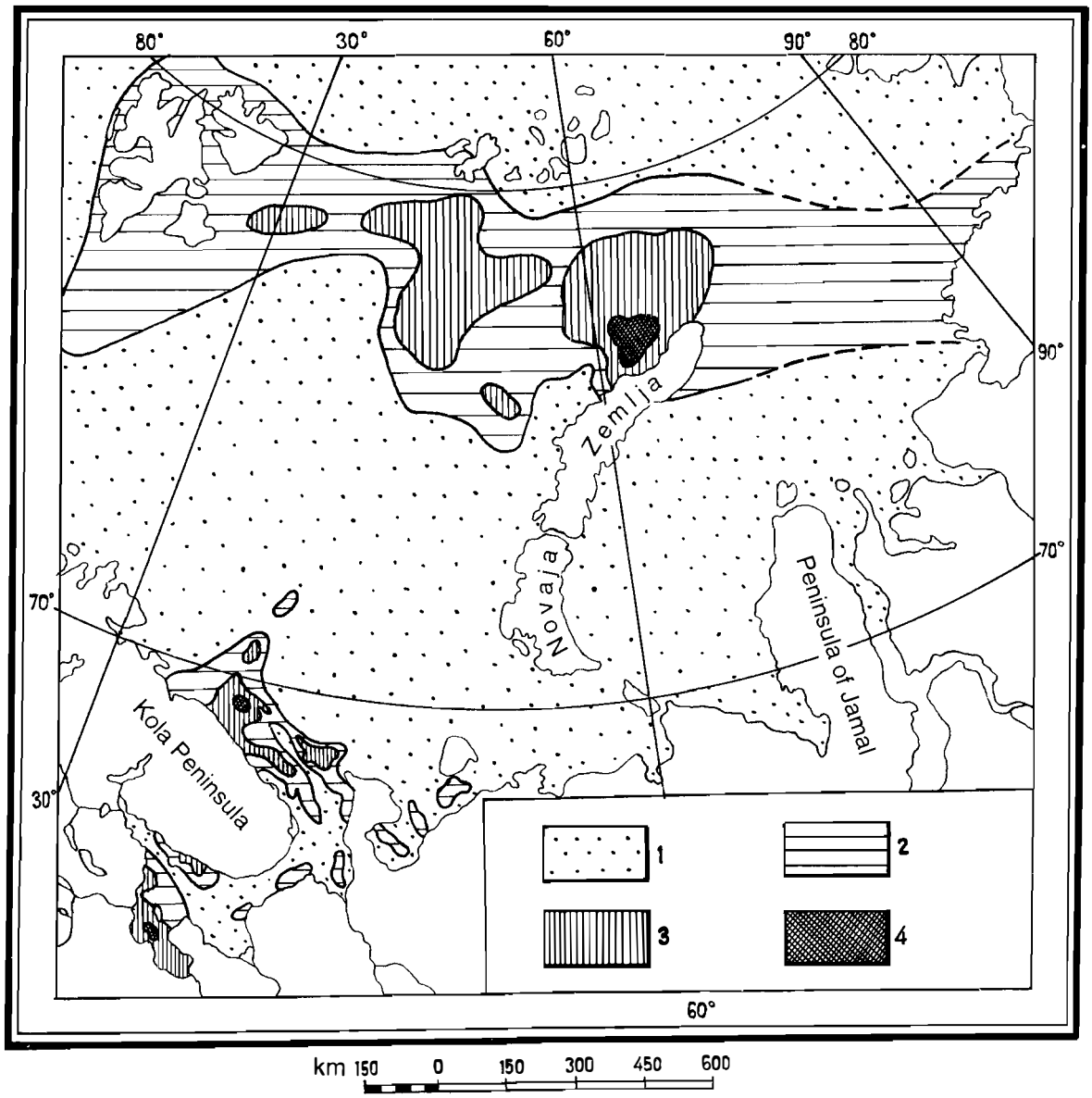

Fig. 6.6 The barium content (%) of the modern deposits of the Western Arctic Shelf: 1. < 0.05; 2. 0.05 to 0.1; 3. 0.1 to 0.2; 4. > 0.2.

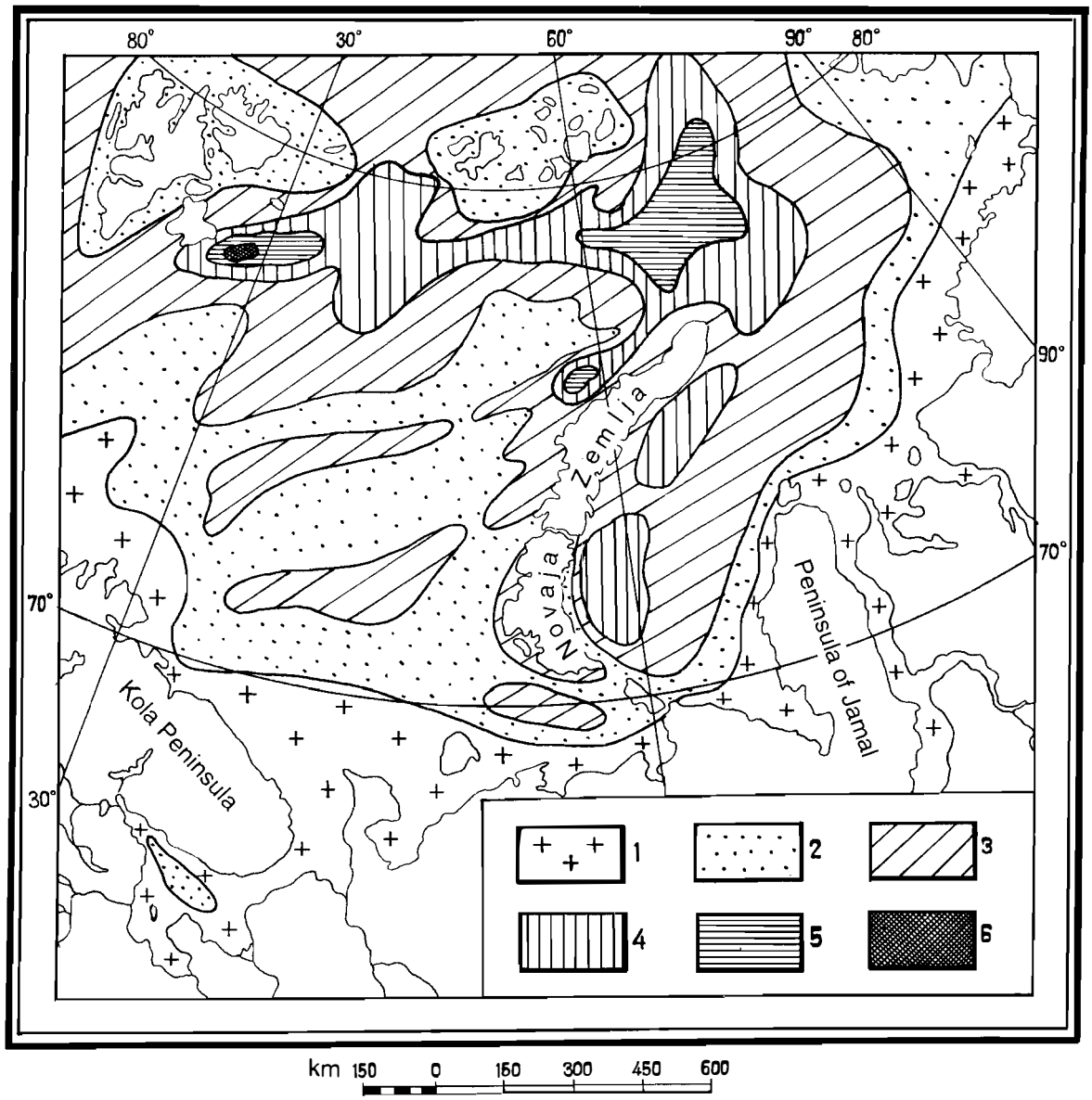

Fig. 6.7 The phosphate content (% P_2O_5) of the modern deposits of the Western Arctic Shelf: 1. < 0.1; 2. 0.1 to 0.15; 3. 0.15 to 0.2; 4. 0.2 to 0.3; 5 . 0.3 to 0.5; 6 – > 0.5.

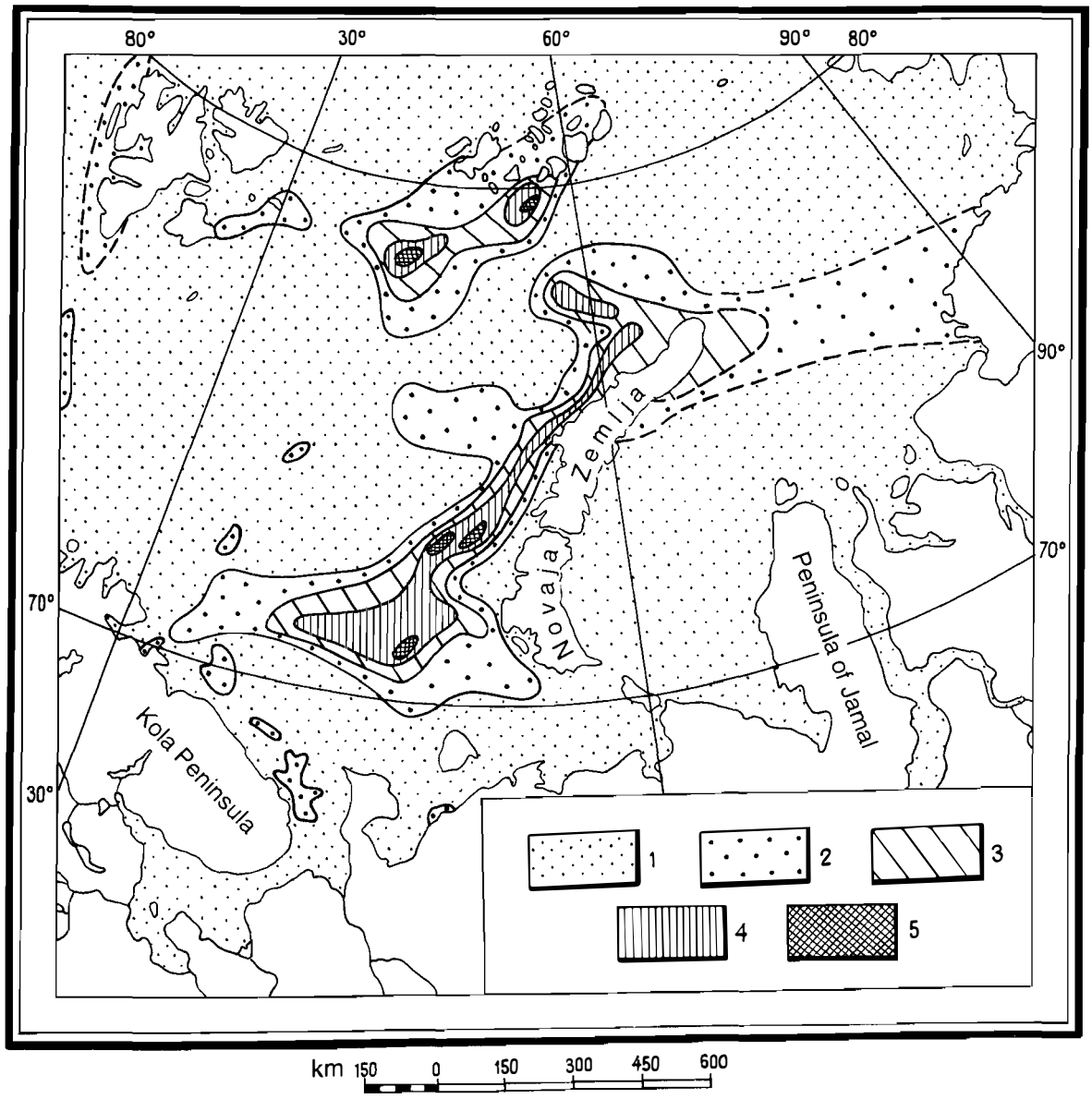

Fig. 6.8 The sulphur content (% total S) of the modern deposits of the Western Arctic Shelf: 1. < 0.1; 2. 0.1 to 0.2; 3. 0.2 to 0.3; 4. 0.3 to 0.4; 5. > 0.4.

7. TECHNOGENIC AND OTHER COMPONENTS

7.1 Volcanogenic forms

Basic pumice has frequently been found on sandy beaches on the Murman Coast of the Kola Peninsula. This material was probably transported from Iceland by the North Cape branch of the Gulf Stream. The author believes that the presence of volcanic glass in modern sediments of south-eastern, near-shore areas of the Barents Sea is due to the destruction of such allochthonous fragments of volcanic rocks. The content of volcanic glass may reach 0.5–2 % in these areas, and in some samples from near the shore it can increase to 3 % or more. Modern sediments of the White Sea and Kara Sea have not revealed obsidian or tachylite.

7.2 Cosmogenic fragments

The presence of solid, highly magnetic, well-polished spherical grains, 0.01–0.05 mm, rarely up to 0.2–0.5 mm, in size, were sometimes noted when the heavy fraction of sandy silt was being examined. We believe these metallic spherules to be meteoritic dust. The frequency of samples containing such meteoritic spherules ranges from 0.1 to 4.8 %, averaging about 1 % (or 0.003 % of the total weight of the heavy fraction). The highest frequency has been found where the Quaternary cover is thin or absent (e.g. near Spitsbergen). No spherules were found in samples from areas with stable sedimentation, but such spherules may have been discarded when 500 grains were being chosen for investigation.

7.3 Technogenic components

Technogenic components in modern sediments of the Western Arctic Shelf include aero-, hydro-, litho-, petro-, dendro-, agro-, zoo- and radiotechnogenic material (see section 8.4). Data on the composition and content of such material in the surface layer of recent deposits in the White Sea are shown in Table 7.3.

Table 7.3 Technogenic components in White Sea sediments

Components	*Unit*	*Content*	
		normal	*anomalous*
Aerotechnogenic			
Zinc	mg/kg	2–20	150–175
Lead	mg/kg	5–8	250–560
Hydrotechnogenic			
synthetic surface-active substances	mg/l	0	7–19
Lithotechnogenic			
detritus of coal, clinker	%	0	0.1–1
Petrotechnogenic			
oil hydrocarbons	mcg/g	50	350–750
polycyclic arenes	mcg/g	0.2	0.62
Dendrotechnogenic			
phenols	mcg/g	0.0	8–18
wood, bark	%	0	0.1–2
Agrotechnogenic chloro-organic compounds			
cyclic	ng/g	0.00	0.1–0.75
aromatic	ng/g	0.00	0.2–1.40
polybiphenyl	ng/g	0.00	0.7–8.1
Zootechnogenic			
nitrites	mg/kg	0.0	0.3–2.2
nitrates	mg/kg	0.0	0.5–5.8
phosphates	mg/kg	0–1	3–7

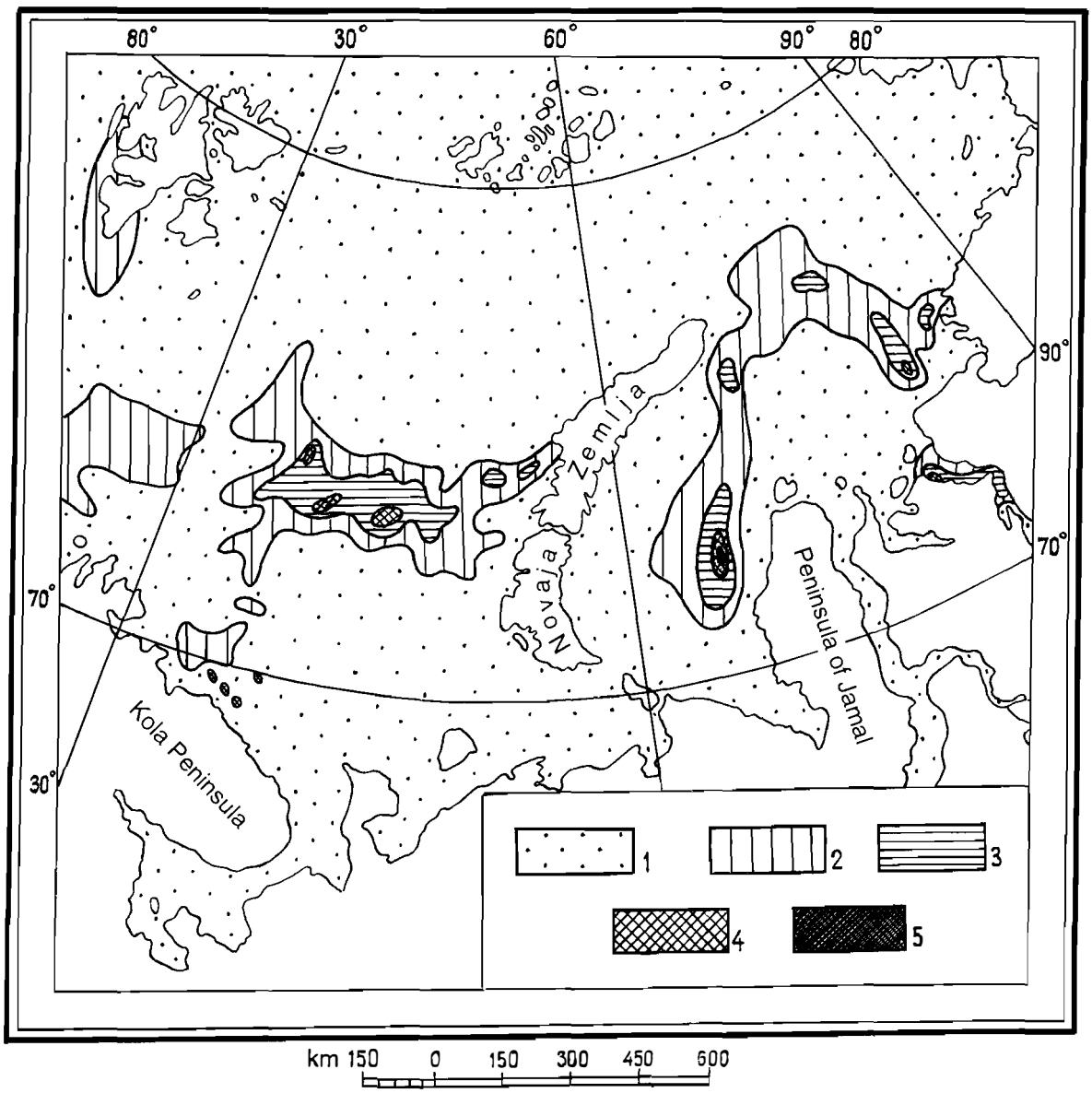

Fig. 7.1 The coal detritus content (%) of the modern deposits of the Western Arctic Shelf (in the 0.5–1 mm fraction of the minero-petrographical analysis data): 1. < 1; 2. 1 to 3; 3. 3 to 10; 4. 10 to 30; 5. > 30.

Kandalaksha Bay (especially near the town of Kandalaksha), areas near the mouths of the rivers Kem, Onega, Solza, Ponoy, etc., near-shore areas of the Terskiy and, especially, Letniy coasts of the White Sea, are the regions having the highest content of technogenic pollution. Sediments near the mouth of the Dvina and adjacent areas of Dvinsk Bay are less polluted than expected, probably because of the high depositional velocity of terrigenic particles, which reduces the relative content of technogenic components.

Figure 7.1 shows the distribution of coal detritus in modern sediments of the Barents Sea and Kara Sea. Some of the anomalies revealed are obviously technogenic in origin (e.g. areas in Enisey Bay). However, some in the Barents Sea may relate to bottom exposures of coal-bearing Mesozoic rocks, in which case these anomalies have an autochthonous origin.

Other technogenic components in sediments in the Barents Sea and Kara Sea, such as radionuclides (Fig. 7.2), are currently being investigated and information will be published later.

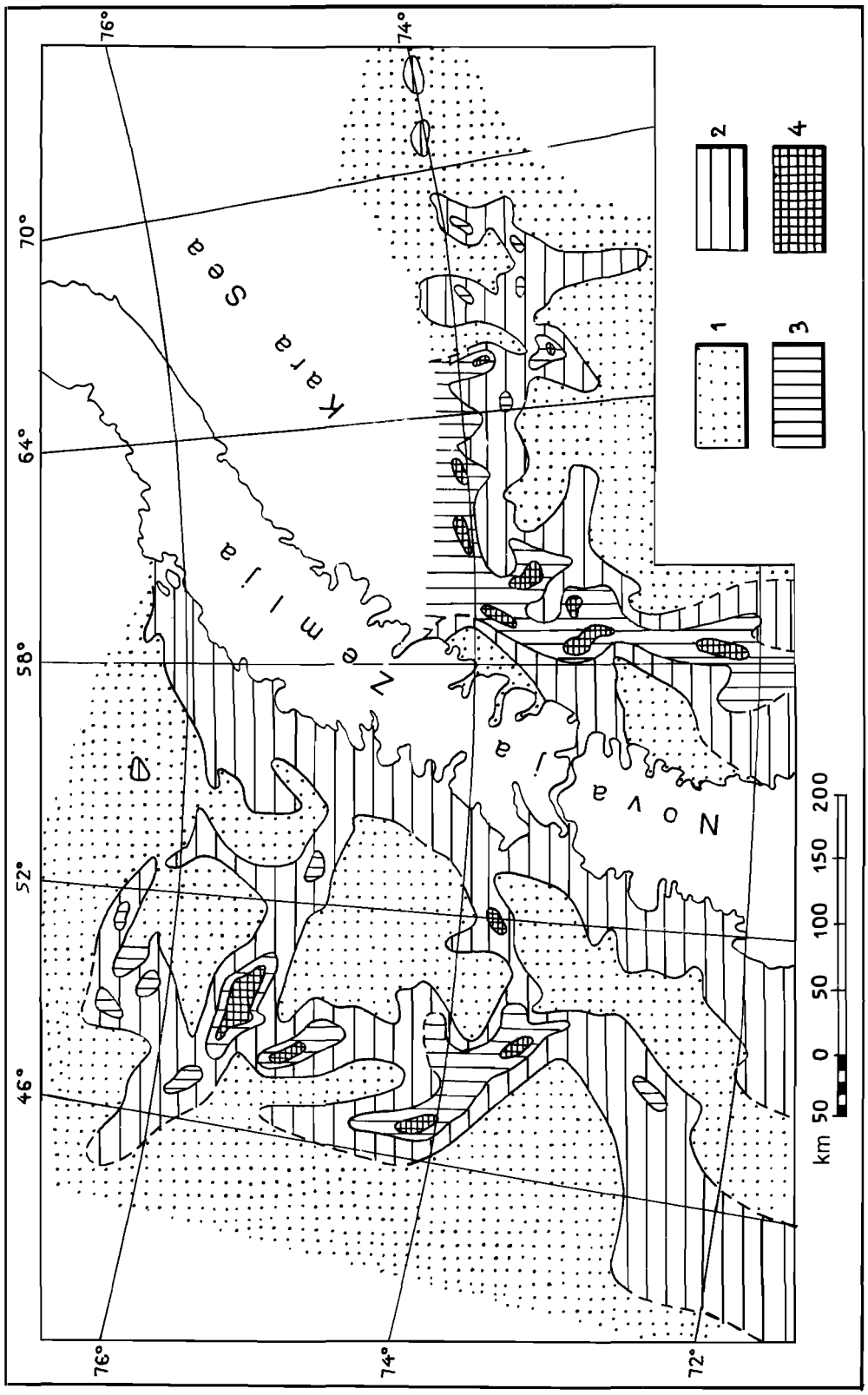

Fig. 7.2 The distribution of technogenic radionuclides $^{137}Cs \cdot 10^{-10}$ Ku/kg in the modern deposits of the eastern and western Novaya Zemlya archipelago: 1. < 5; 2. 5 to 10; 3. 10 to 15; 4. > 15.

8. SEDIMENTOLOGICAL AND SEDIMENTOGENETICAL CLASSIFICATION

The methods of sedimentological analysis and the ways of characterising the sediments have been maintained during the long-term investigations of modern sedimentation on the Western Arctic Shelf. The author hopes that some of these methods will be applicable in studies of other shelf regions.

8.1 Sedimentary regime

The regimes of marine and lacustrine sedimentation are defined by the interplay between erosion, denudation and accumulation. These processes take place against the background of tectonism in the form of uplift or subsidence of the bottom. During recent shelf sedimentation, there has clearly been a general tendency for tectonic subsidence, which has not been entirely compensated for by sedimentation. Shorelines, *a priori*, correspond to conditions of total sedimentary compensation.

The correspondence of some parameters that define the regime of recent sedimentation in epicontinental basins on the shelf will be considered on the basis of shallow seismic measurements (Fig. 8.1). Obviously, the water layer with average thickness h characterises relative non-compensation for subsidence through accumulation and denudation; unconsolidated sediments of the Quaternary cover, with average thickness m, result from the combined influence of accumulation and denudation; the relative difference between the pre-Quaternary relief and the local base of erosion, with an average value of ΔZ shows the range of the erosive processes. The normalised components of accumulation A, erosion E and non-compensation for subsidence H can be estimated according to the following:

$$A, \% = \frac{100m}{h+m+\Delta Z}\ ;\ E = \frac{100\Delta Z}{h+m+\Delta Z}\ ;\ H = \frac{100h}{h+m+\Delta Z}$$

The direction and relative range of denudation can be estimated as $D = A - E$. If $A > E$, the sedimentary regime can be judged to be accumulative-denudational, and if $A < E$, this regime is erosional-denudational.

A classification of sedimentary regimes in shelf regions is shown in Figure 8.2, and Figure 8.3 shows the recent sedimentary regime on the Western Arctic Shelf.

Factor analyses of sedimentological parameters (section 8.5) show that the sedimentary regime is the main factor and is responsible for most of the general pattern of modern sedimentation on the Arctic shelf of western Eurasia. Other evidence supporting this includes the numerous correlations between the sedimentary regime and geomorphological, lithological, biotic and other parameters (Figs. 8.4 and 8.5). Another important factor in sedimentation is hydrodynamic activity.

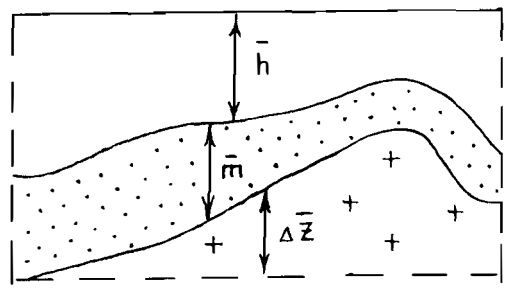

Fig. 8.1 Calculated parameters of a shallow-seismic profile: h. average depth of sea, m. average thickness of unconsolidated veneer, ΔZ. average altitude of pre-Quaternary relief.

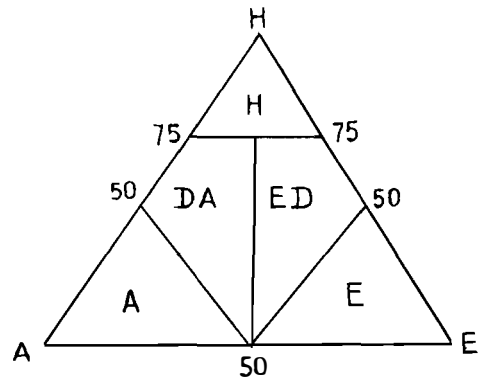

Fig. 8.2 Classification of sedimentary regimes in the Western Arctic Shelf provinces: A. accumulative regime; DA. denudate-accumulative regime with moderate compensation; ED. erosive-denudate regime with moderate compensation; E. erosional regime; H. regime lacking flexural compensation by the sediments.

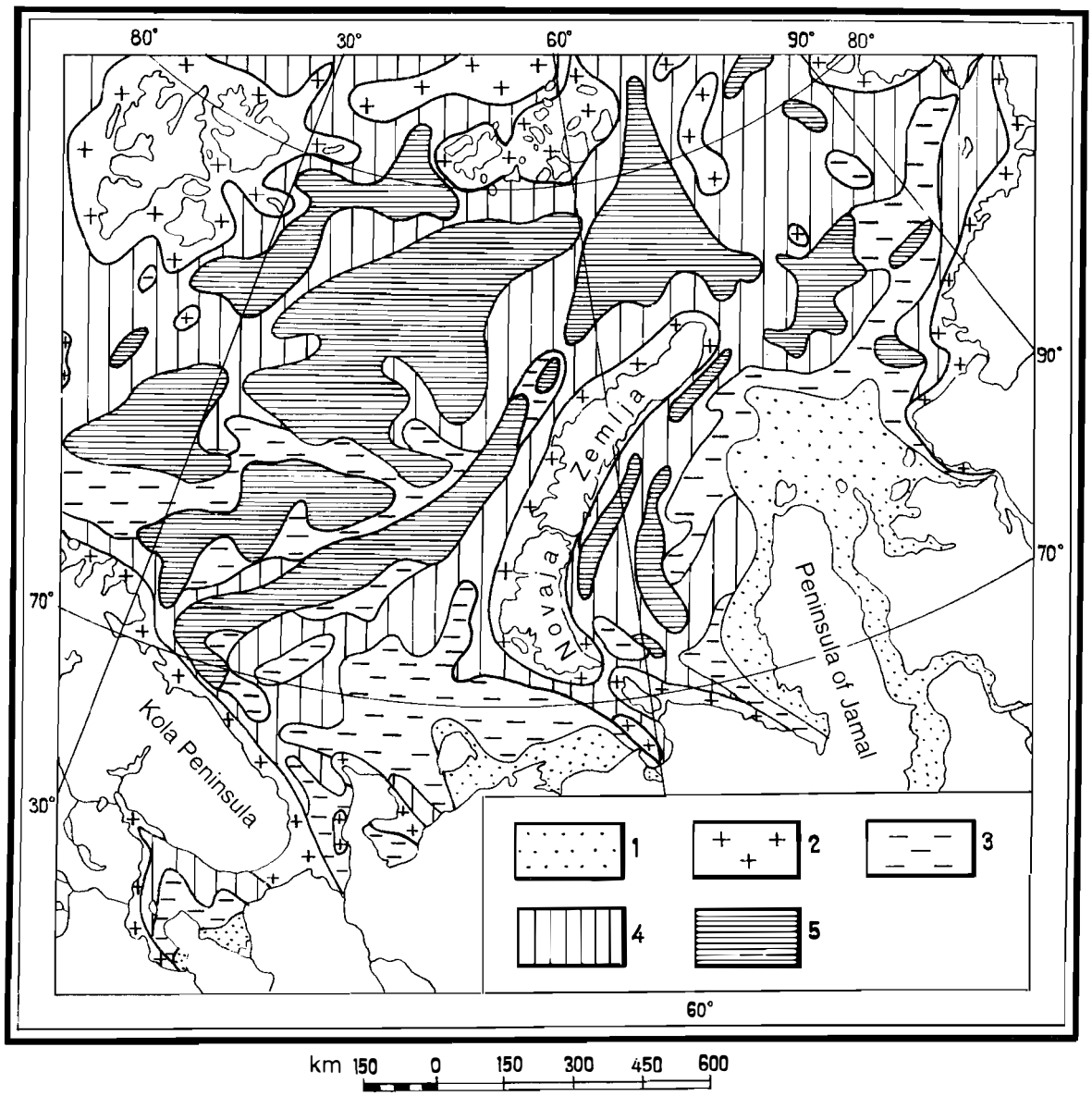

Fig. 8.3 Regimes of modern sedimentation on the Western Arctic Shelf: 1. accumulative; 2. erosive; 3. denudate-accumulative with moderate compensation; 4. erosive-denudate with moderate compensation; 5. regime lacking flexural compensation by the sediments.

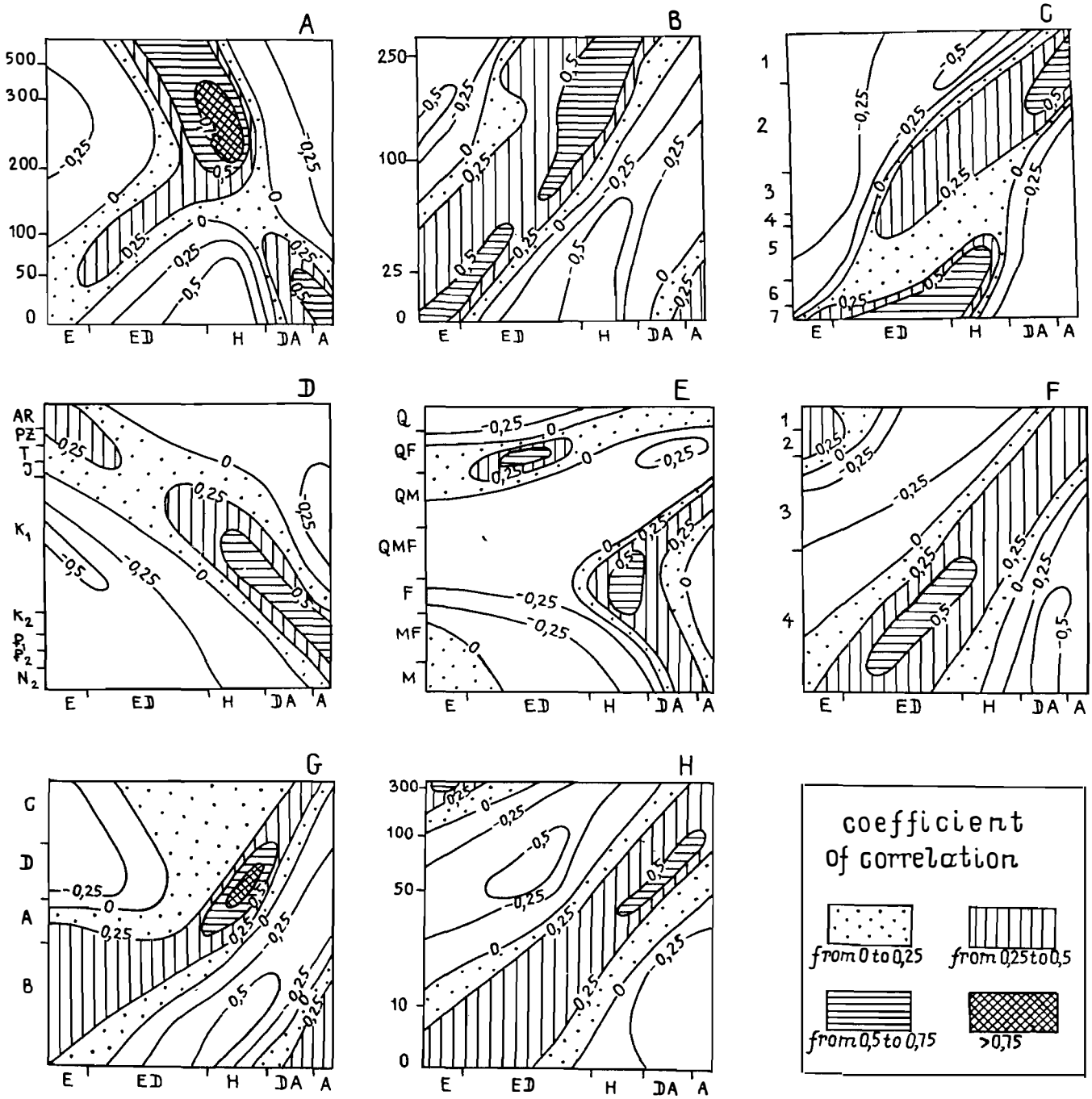

Fig. 8.4 Diagrams showing the correlation between the sedimentary regime and geomorphological, geological and biotic parameters on the Western Arctic Shelf: A. water depth, m; B. distance offshore, m; C. geomorphological location (1. offshore shallow-water areas; 2. submarine plains; 3. banks, plateaus and other highs; 4. slopes of category 3; 5. depressions; 6. troughs; 7. continental slopes); D. geological age of bedrock; E. composition of samples of bottom bedrock (M. metamorphic; F. Phanerozoic sediment; Q. Late Cenozoic); F. colour of bottom deposits (1. brown; 2. green; 3. yellow; 4. grey); G. trophic assemblages of benthos (A. sessile sestonophagous; B. mobile sestonophagous; C. collecting detritophagous; D . gulping detritophagous); H. total benthos biomass (g/m^2). Sedimentary regime: E. erosive; ED. erosive-denudate; DA. denudate-accumulative; A. accumulative; H. essentially lacking flexural compensation by sediments.

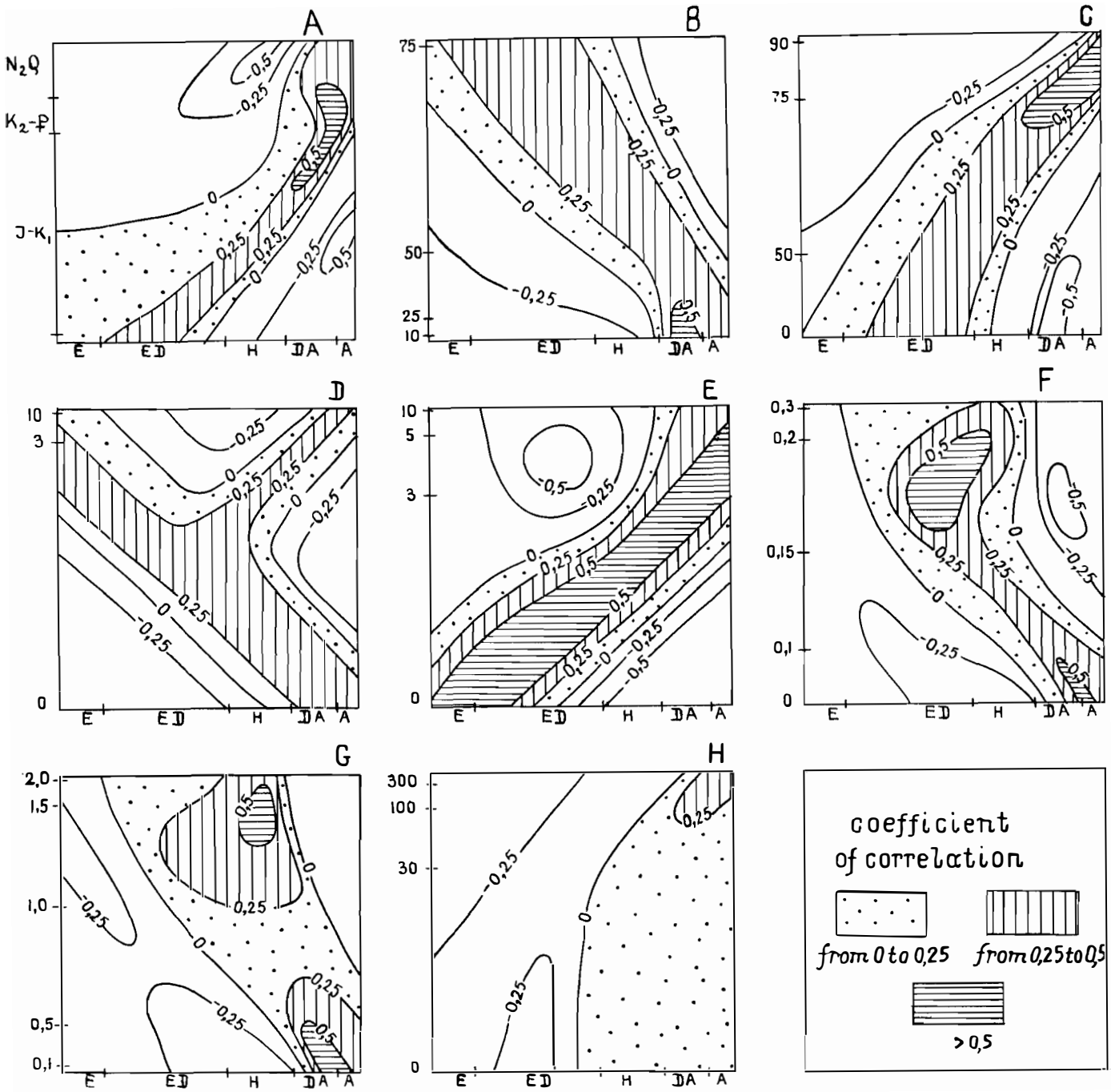

Fig. 8.5 Diagrams showing correlation between sedimentary regime and lithological-geochemical parameters on the Western Arctic Shelf: A. age structure of palynological assemblages in the modern deposits; B. content of silty fraction; C. quartz content (%) in a light-fraction sample; D. content (%) of heavy fraction; E. zircon content (%) in a heavy-fraction sample; F. phosphorus content (%); G. organic carbon content (%); H. methane content (% vol. $CH_4 \cdot 10^{-4}$); sedimentary regime: E. erosive; ED. erosive-denudate; DA. denudate-accumulative; A. accumulative; H. essentially lacking flexural compensation by sediments.

8.2 Dynamic classification

The dynamic conditions relating to the formation and alteration of bottom sediments depend upon the interplay between the hydrodynamic activity of the near-bottom water layer and the lithological properties of the deposits. To be able to examine the relationship between hydrodynamic and lithological parameters, Gurevich & Kazakov (1981) proposed that they should be expressed as single units. Extreme values for the velocity of near-bottom currents (V_{min} and V_{max}) could be used to estimate hydrodynamic activity, and values of average velocities for the breaking-up of deposits (V_{br}) and for sedimentation (V_{sed}) could be used to estimate the lithodynamic activity. The last two parameters are easily estimated using the following equations:

$$V_{br} = \sum_{i=1}^{n} V_{i\,br} \cdot P_i; \quad V_{sed} = \sum_{i=1}^{n} V_{i\,sed} \cdot P_i,$$

where n is the number of granulometrical fractions, $V_{i\,br}$ and $V_{i\,sed}$ are the values of these velocities according to the curves of Hjulstrøm, and P_i is the content of the i-granulometrical fraction (in parts of the unit).

When the extreme velocities of currents at a certain point on the bottom are compared with the sedimentary velocities at the same point, only 6 relationships are possible, representing the full range of conditions controlling sedimentation (Table 8.2). The sixth relationship implies complete erosion of the deposits and removal of the products of this erosion.

Table 8.2 Dynamic types of sedimentation

Dynamic type of sedimentation		*Terminal conditions index*	*Types of granulometrical cumulative curves form*
Sedimentation	$V_{sed} > V_{max}$	B	direct
Restricted sedimentation and transport	$V_{av} \geq V_{max} > V_{sed} \geq V_{min}$	C	concave
Restricted sedimentation, transport and erosion	$V_{max} > V_{av} > V_{sed} \geq V_{min}$	A	S-shaped
Transport	$V_{av} > V_{max} \geq V_{min} > V_{sed}$	D	convex
Restricted transport and erosion	$V_{max} > V_{av} \geq V_{min} > V_{sed}$	E F	bimodal, polymodal
Erosion	$V_{min} \geq V_{av}$		

The main types of cumulative curves of granulometric composition can be closely related to dynamic types of sedimentation if we use the example of deposition on the Western Arctic Shelf (Fig. 8.6). We recommend the use of the dynamic classification of bottom sediments as expressed by the shape of the cumulative curves of their granulometrical composition, which permits the prevailing dynamic type of sedimentation to be characterised approximately when modern and ancient sediments are being investigated (Gurevich & Kasakov 1988).

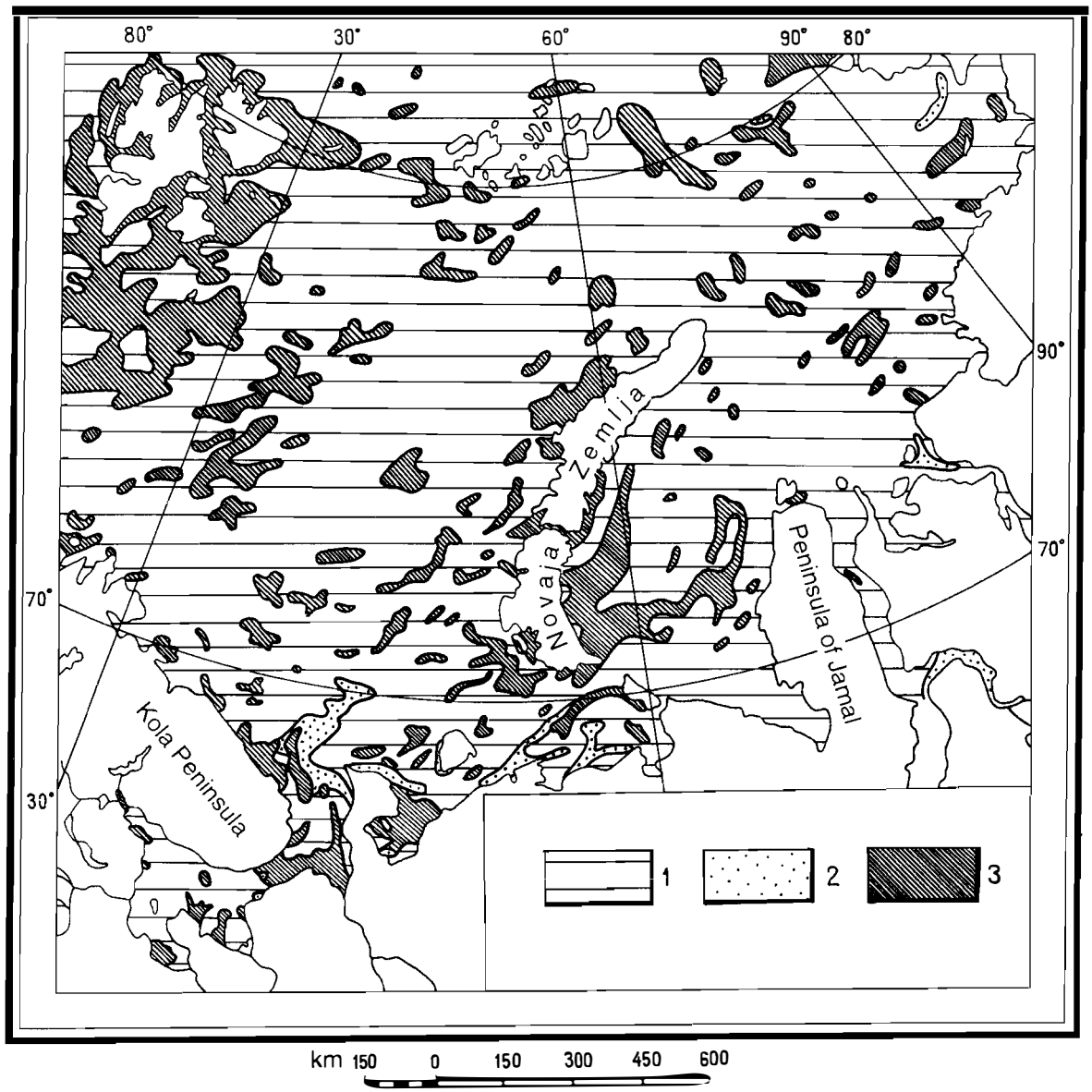

Fig. 8.6 Division of the modern deposits on the Western Arctic Shelf according to their sedimentation dynamics: 1. dominant accumulation under slightly and moderately unstable hydrodynamic activity, 2. transportation under moderate and high hydrodynamic activity, 3. dominant erosion under high hydrodynamic activity. Diagrams showing the close correlation between velocities of near-bottom currents and various parameters in the environment (Figs. 8.7 and 8.8) emphasise the extreme importance of hydrodynamic activity in the near-bottom layer as a factor in modern sedimentation.

8.3 Granulometrical classification

The author proposes that the position of a deposit in the granulometrical classification is determined by the number of size fractions forming the major part (> 75 %) of the total mass of the deposit. Following the system approach, the classification will, *a priori*, only include four granulometrical types of deposit:

- monogranular or pure type, consisting of one dominant group of fractions,
- bigranular or transitional type, consisting of two groups of fractions,
- trigranular or mixtites, consisting of three groups of fractions,
- polygranular or polymixtites, consisting of four or more groups of fractions.

Pure deposits are very rare. A systematic granulometrical classification must, in the opinion of the author, be based on adequate presentation of the fractions making up the deposit, as determined by laboratory investigation. The main groups are shown in the tetrahedra of Figure 8.9. The classification used is in Table 8.3.1.

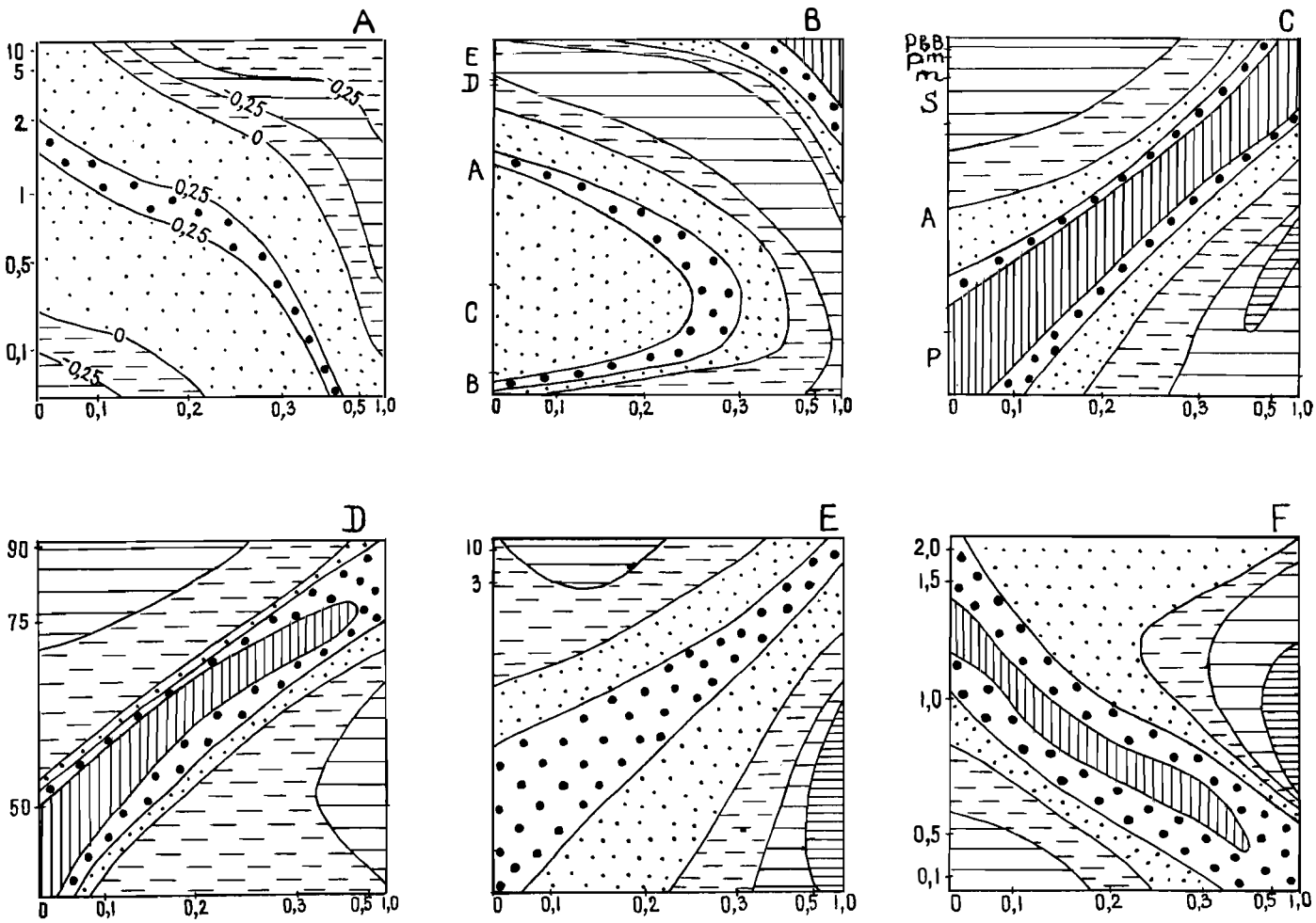

Fig. 8.7 Diagrams showing correlations between the lithological parameters of the modern deposits and the velocities of near-bottom currents (abscissa, m/s) on the Western Arctic Shelf: A. thickness of the modern deposits, m; B. dynamic classification of a deposit (A. with S-like cumulate; B. rectilinear; C. concave; D. convex; E. with bimodal cumulative granulometrical curve); C. granulometrical composition (C. clays, S. silts, S. sands, m. mixtites, pm. poly-mixtites, Pb and B. pebbles and boulders); D. quartz content (%) in light-fraction sample; E. content (%) of heavy fraction; F. C_{org} content (%).

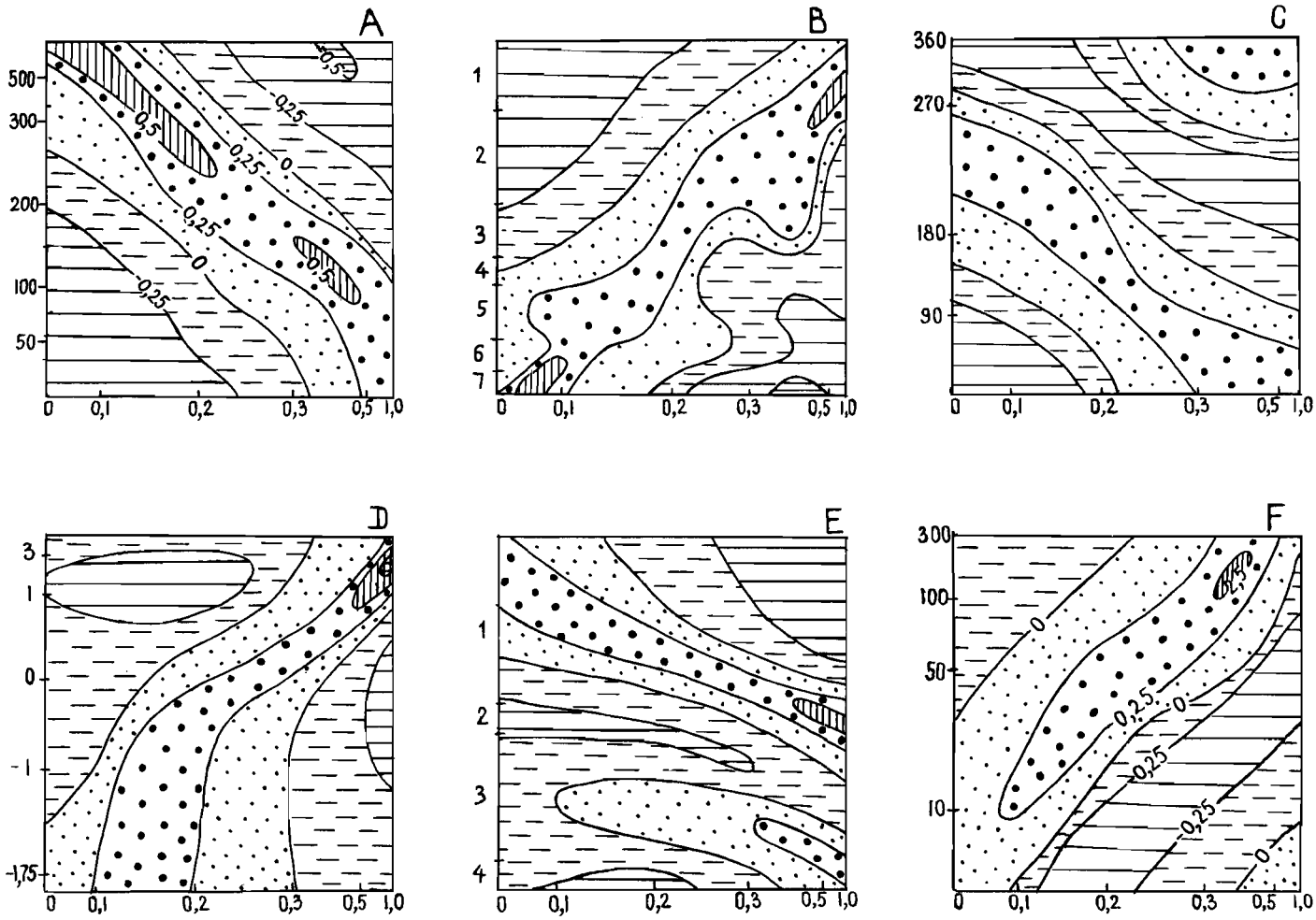

Fig. 8.8 Diagrams showing correlation between velocities of near-bottom currents (abscissa, m/s) and geomorphological, hydrological and biotic parameters on the Western Arctic Shelf: A. water depth, m; B. geomorphological location (1. offshore shallow-water areas; 2. submarine plains; 3. banks and other highs; 4. slopes of category 3; 5. depressions; 6. troughs; 7. continental slopes); C. directions of near-bottom currents, degree; D. near-bottom temperature (°C); E. colour of bottom deposits (1. brown; 2. yellow; 3. green; 4. grey); F. benthos biomass (g/m^2).

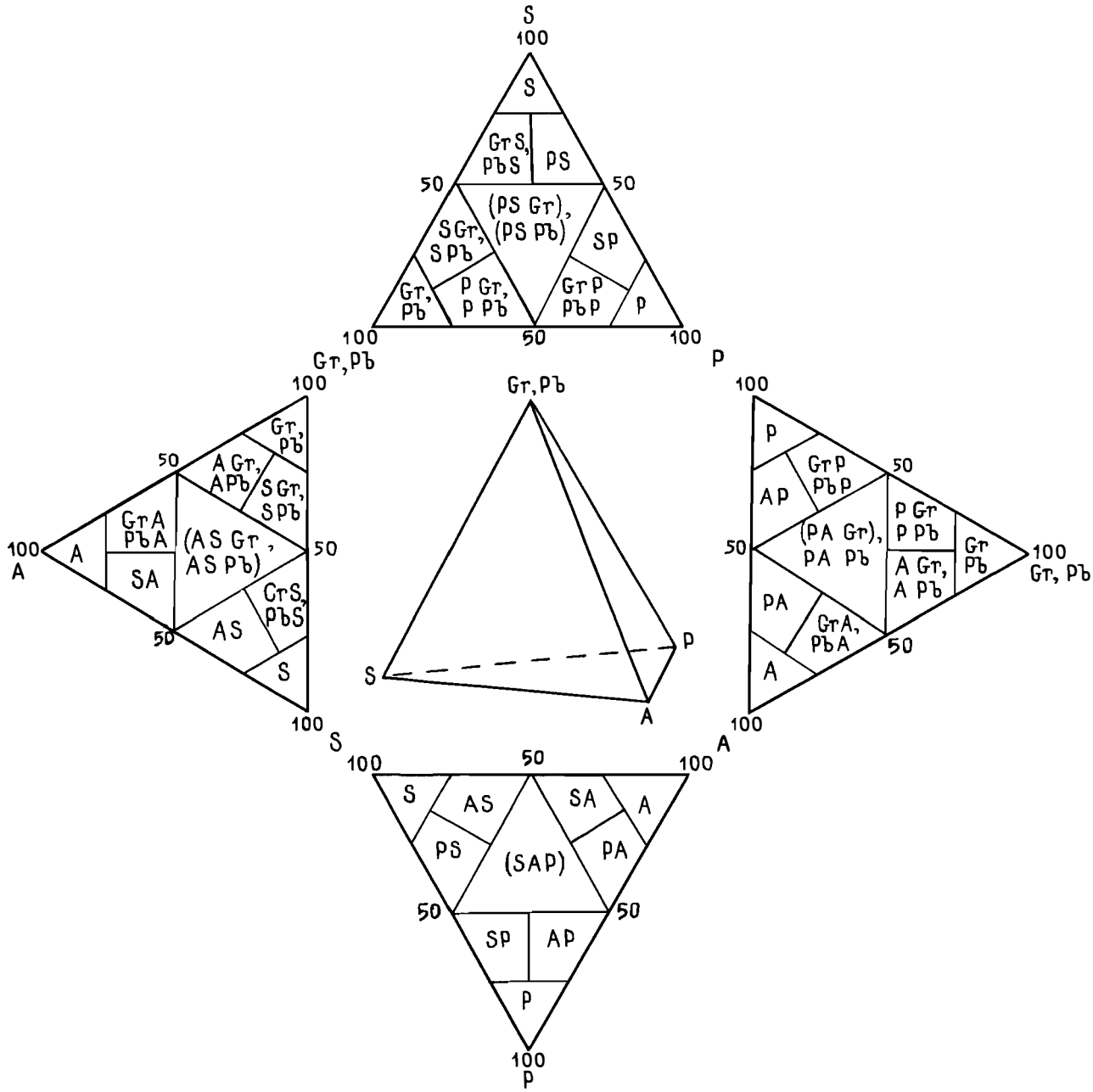

Fig. 8.9 Granulometrical tetrahedra to classify unconsolidated clastic and clayey deposits.

Table 8.3.1 Systematic granulometrical classification of clastic and clayey deposits

Unconsolidated sediments		*Cemented rocks*	
Monogranular or pure, consisting of one dominant group of fractions (> 75 %)			
Boulders	B	Bouldery conglomerate	[B]
Pebbles	Pb	Pebbly conglomerate	[Pb]
Crushed stone	Cr	Breccia	[Br]
Gravel	Gr	Gravelite	[Gr]
Sand	S	Sandstone	[S]
Silt	Si	Siltstone	[Si]
Clay	C	Claystone	[C]
Bigranular or transitional, consisting of one dominant (50–74.9 %) and one additional (49.9–25 %) group of fractions			
Boulders		Conglomerates	
pebbly	PbB	pebbly-bouldery	[PbB]
gravelly	GrB, etc.	gravelly-bouldery	[GrB], etc.
Pebbles			
gravelly	GrPb	gravelly-pebbly	[GrPb]
sandy	SPb, etc.	sandy-pebbly	[SPb], etc.
Gravels		Gravelites	
pebbly	PbGr	pebbly	[PbGr]
sandy	SGr, etc.	sandy	[Sgr], etc.
Sands		Sandstones	
gravelly	GrS	gravelly	[GrS]
silty	SiS	silty	[SiS]
clayey	CS, etc.	argillaceous	[CS], etc.
Silts		Siltstones	
sandy	SSi	sandy	[SSi]
clayey	CSi, etc.	argillaceous	[CSi], etc.
Clays		Argillites	
gravelly	GrC	gravelly	[GrC]
sandy	SC	sandy	[SC]
silty	SiC, etc.	silty	[SiC], etc.
Trigranular or mixtites, consisting of three groups of fractions (25-49.9 %)			
Mixtites		Mixtolithes	
sandy-silty-clayey	SSiC	sandy-silty-clayey	[SSiC
silty-sandy-gravelly	SiSGr, etc.	silty-sandy-gravelly	[SiSGr],
etc.			
Polygranular or polymixtites, consisting of four or more fractions (25-49.9 %), or combined (10-24.9 %) groups of fractions			
Polymixtites		Polymixtolithes	
gravelly	SSiCGr	gravelly	[SSiCGr]
pebbly-bouldery	SiCSBPb	pebbly-bouldery	[SiCSBPb],
etc.			

The systematic granulometrical classification proposed is appropriate for identifying clastic-clayey sediments with various fractional structures. The lithological map showing the modern sediments on the Western Arctic Shelf (Fig. 3.3) has been compiled using this classification.

When this classification is used it is usually not necessary to estimate the co-efficients of sorting of the deposits separately; this is defined directly by the grouping of the deposit in accordance with the terminology found in Table 8.3.2.

Table 8.3.2 Co-efficients of sediment sorting

Types and subtypes of sediments according to Gurevich (1986, 1990)	*Co-efficients of sorting*		*normalised entropy*	*Degree of sorting of sediments (according to Romanovsky 1988)*
	by Trask $S_0 = \sqrt{Q_3/Q_1}$	*by Inman* $\epsilon = \sqrt{Q_{84}/Q_{16}}$	*Hz*	
Monogranular				
extremely pure (90% from one dominant fraction)	1.17	1.28	0.07	Excellently sorted
very pure (90% from one dominant group of fractions)	1.58	2.00	0.15	Well sorted
pure (75% from one dominant group of fractions)	1.94	2.63	0.20	Well sorted
Bigranular				
transitional deposits consisting of dominant (> 50%) and additional (> 25%) groups of fractions	3.9	7.3	0.33	Moderately sorted
Trigranular				
mixtites consisting of three additional groups of fractions	7.6	20.0	0.53	Poorly sorted
Polygranular				
polymixtites consisting of four (> 10%) additional groups of fractions	14.2	52.5	0.76	Non-sorted
polymixtites consisting of five or more additional groups of fractions	28.2	146.0	0.93	Absolutely non-sorted

Remarks: the co-efficients of sorting for unimodal sediments are average values for modern basins. This granulometrical classification is adequate for terrigenic and other clastic sediments and rocks.

8.4 Classification according to genesis and dominant composition

Any marine deposit can first be grouped according to the origin of the initial material that was transported into the sedimentary basin. The genetic types distinguished (volcanogenic, lithogenic, biogenic, etc.) form a superior group called a system. In the classification proposed (Table 8.4.1), the genetic subtypes summarise our opinion about the source of the sedimentary material and how it was transported to become bottom sediment. The dominant composition is classified on the level of taxons of lower order: classes (clastic, clayey, carbonaceous, oxidic, etc.), subclasses (calcareous, siliceous, phosphatic, etc.) and species.

Terrigenic sediments are normal clastic or clayey deposits. They are usually in hydrodynamic and physical-chemical balance with natural conditions in the sedimentary basin. Palimpsestic sediments were formed *in situ* by erosion of the bottom and reworking of Upper Cenozoic pre-Holocene sediments. Autochthonous sediments or components were formed during erosion of more ancient sediments and rocks.

Autochthonous and palimpsestic sediments are widespread on the Western Arctic Shelf (Fig. 8.10). Estimates of the distribution of the main components in the classification based on genesis and dominant composition are shown in Table 8.4.2.

Technogenic sediments have been less thoroughly investigated and are more poorly classified than other components. The technogenic components of modern sediments are substances and objects entering the sedimentary basin, which are reworked products of industrial technology and waste resulting from the use of natural products. They are classified (Table 8.4.3) according to their origin and how they are transported, based on sedimentological studies carried out on the Western Arctic Shelf and in lakes in northern Russia.

Table 8.4.1 Outline of the classification of modern marine sediments according to their genesis and dominant composition

Genetic types	*Dominant composition*	
and subtypes	*Classes, subclasses*	*Characteristic varieties*
Volcanogenic	Pyroclastic	Tephra, ash, slaggy lava, volcanic glass
	Lavaclastic	Fragments of lavas and tuffs
Lithogenic		
Terrigenic	Fragmented silici-clastic	Boulders, pebbles, gravel, sands, silts
	Clayey illitic, etc.	Clays and subcolloidal clays
Autochthonous-	Clastic palimpsestic	Boulders, pebbles, gravel, sands, silts (incl. grains of unstable rocks and minerals)
	Clayey montmorillon-itic, kaolinitic, etc.	Clays
Biogenic		
Benthic	Siliceous oxide	Skeletons of sponges and diatoms
	Ferrous oxide	Ferrous tracks of worms
	Carbonate	Coral, bryozoan and algal reefs. Lithothamnion crusts. Shells of molluscs, foraminifera, barnacles, echinoderms. Tracks of worms and their fragments
	Organic chitinous	Worm tracks, fragments of crayfish tests and hydrozoans, conchiolin covers of molluscs

Genetic types and subtypes	*Dominant composition* *Classes, subclasses*	*Characteristic varieties*
Planktonic	Siliceous oxide	Skeletons of diatoms and radiolarians Diatomites
	Carbonate	Skeletons of pterodans and coccoliths. Chalk
Sestonic	Clayey	Pellets
	Siliceous oxide	Siliceous cryptogenic detritus. Gaize
	Carbonate	Limey cryptogenic detritus
	Organic sapropel	Lipides and other components of sapropels
	Organic humosous	Lignin and other humus materials
Nektonic	Phosphate	Bones of fish and marine mammals Sharks' teeth
	Carbonate	Fish otoliths
Epinaphthenic	Organic bituminoids	Paraffins, naphthenates and other epibituminoids
Chemogenic		
Hydrothermal-enterogenic	Sulphidic polymetallic	Metal-bearing mud and other sediments
	Ferrous, manganese and cobaltic oxides	Concretions and crusts
Diagenetic-halmyrogenic	Siliceous oxide	Siliceous collomorphic concretions and inclusions Diatomaceous soil
	Ferrous and manganese oxides	Hydroxidic ferromanganese concretions, crusts and films
	Siliceous zeolitic	Phillipsitic and other films and inclusions
	Carbonate	Concretions and crusts of siderite and ankerite. Concretions of calcite, aragonite and glendonite
	Sulphatic	Concretions of gypsum and barytes Celestite inclusions
	Phosphatic	Concretions of phosphorite; vivianite, reddingite and arsenoclasite inclusions
	Sulphidic ferrous	Concretions of pyrite and marcasite Inclusions of hydrotroilite and melnicovite
	Native non-metallic	Fragments of native sulphur
Hydrogenic	Gaseous water	Hydrocarbonaceous gas hydrates Dissolved and adsorbed gases
	Cryogenic water	Inclusions of ice
	Salinised water	Dissolved and adsorbed ionic-salinised assemblages
Halogenic	Carbonate	Precipitated neo-composites of lime and dolomite
	Sulphatic	Precipitated gypsum, anhydrite and mirabilite
	Chloridic	Precipitated halite, sylvite, carnallite and bischofite
	Boratic	Neo-composites of hydroboracite and pandermite
Cosmogenic		
Meteoritogenic	Siliceous chondrites	Chondrite spherules
	Native metallic	Ferro-nickel spherules
Tectitogenic	Siliceous glassy	Glassy spherules
Polygenic		Deep-water "red clays", etc.
Technogenic	(see Table 8.4.3)	

Table 8.4.2 The main components in the classification based on the genesis and dominant composition of modern sediments on the Western Arctic Shelf

Main genetic components, % of mass	*Distribution on the shelf, % of area*			
	White Sea	*Barents Sea*	*Kara Sea*	*Entire Western Arctic*
Volcanogenic (volc. glass)				
< 1	–	62.3	–	61.0
1–2	–	27.6	–	26.7
2–3	–	10.4	–	10.1
> 3	–	1.0	–	0.9
Lithogenic siliciclastic and clay (insoluble residue)				
< 60	–	0.8	–	0.4
60–75	2.7	20.8	15.8	17.2
75–90	33.6	59.4	70.2	61.7
90–95	29.3	10.7	7.4	10.9
> 95	34.4	8.3	6.6	9.8
Chemogenic				
< 1	17.0	9.9	6.0	9.0
1–10	59.0	38.7	30.3	37.3
10–25	21.5	33.0	56.9	41.3
25–40	2.5	18.2	6.8	12.3
> 40	–	0.2	–	0.1
Biogenic carbonate ($CaCO_3$)				
< 1	79.7	70.8	55.8	65.3
1–5	11.0	26.8	44.0	32.2
5–10	3.6	1.5	0.2	1.2
10–25	1.6	0.8	–	0.6
25–50	2.9	0.4	–	0.5
> 50	1.2	0.1	–	0.2
Biogenic siliceous (SiO_2 amorphous)				
< 1	82.6	85.4	100.0	87.0
> 1	17.4	14.6	–	13.0

Table 8.4.3 Classification of the technogenic components of modern sedimentary basins

Subtype	*Components and sources of pollution*	*Recommended analyses*
Aerotechnogenic	Aerosols from industrial smoke, vehicle emissions, "acid precipitation"	Heavy metal (lead, cop per, zinc, vanadium, cadmium, etc.), sulphate, bromine
Hydrotechnogenic	Industrial salinised water flows. Flows of synthetic surfaceactive substances, flotation reagents. Dumping of poisonous substances	As above Detergents, xanthogenate, dithiophosphate
Lithotechnogenic	Bottom sediments from water-suspension flows resulting from construction work, deposition, extraction and enrichment of useful substances. Clinker, coal, tailings, glass, brick, concrete, drilling sludge	Aerial photography, visual and mineralogical-petro-graphical investi-gations of technogenic inclusions
Petrotechnogenic	Technogenic bituminous components of oil, inflammable lubricants, resins, asphaltenes	Bituminoids, oil products, polycyclic arenes (benzo-pyrene, etc.)
Dendrotechnogenic	Wood, bark, lignin	Visual descriptions; phenols, triphenilene
Agrotechnogenic	Pesticides, herbicides, insecticides, fungicides	Chlorinated hydrocarbons: cyclic, aromatic, cyclodienics, etc.
	Chemical fertilisers	Nitrates, phosphates, potassium
Zootechnogenic	Flows from pigsties, poultry farms, urban sewage	Nitrites, nitrates, ammonium, phosphates, sulphohydrogen, intestinal bacilli, pathogenic microflora
Radiotechnogenic	Radioactive dust, products of nuclear industry	Artificial long-term radio-nuclides (^{137}Cs, ^{134}Cs, ^{90}Sr, etc.)
Xenotechnogenic	Metallic constructions, polymers, etc.	Aerial photography, TV surveying of technogenic constructions; visual descriptions; determination of chlorinated biphenyls and other xenobiotics
Polytechnogenic technologies	Combined products and wastes from industrial methods	Integral estimates of pollution by biotesting

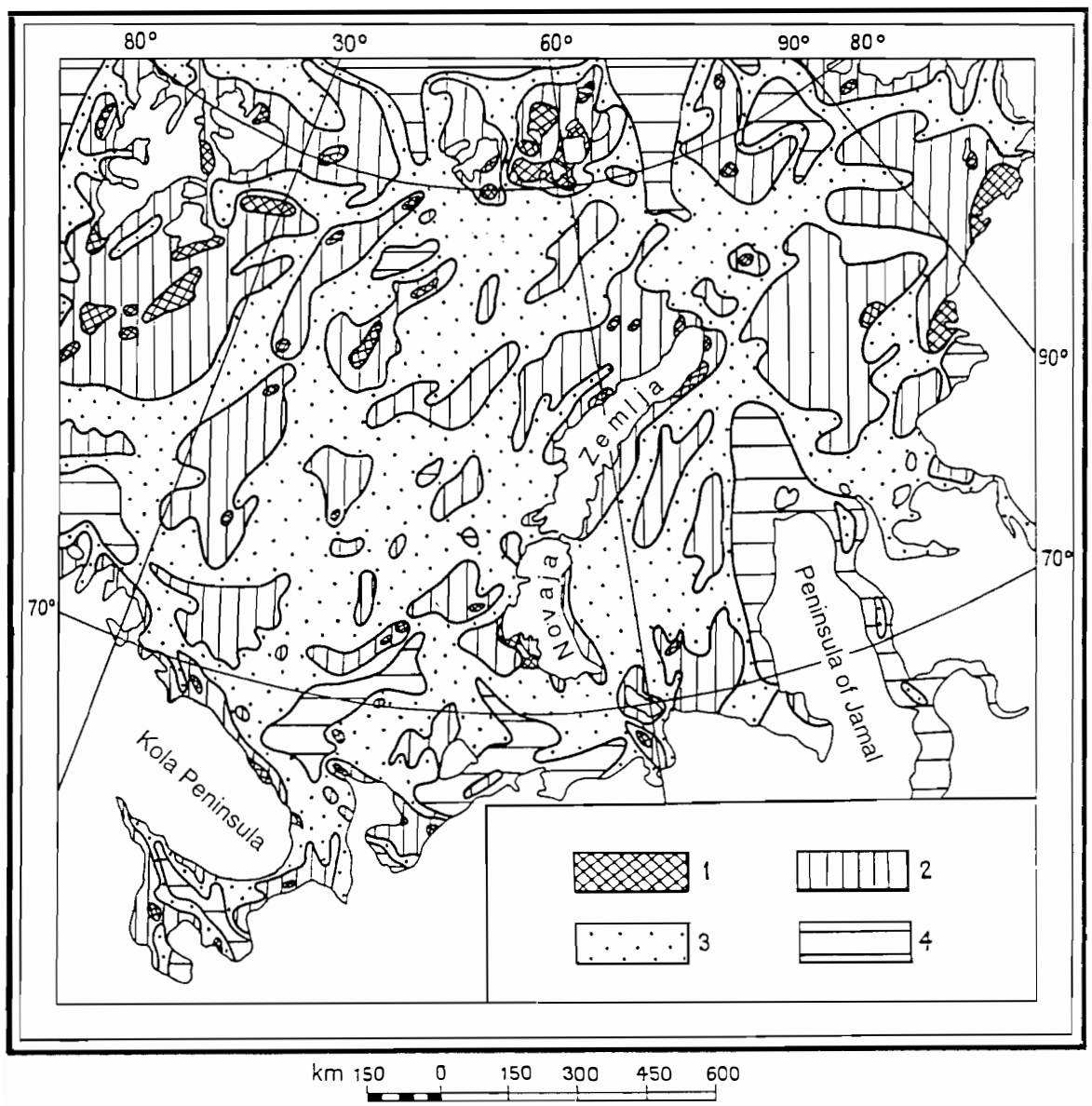

Fig. 8.10 Dominant types of lithogenic components in the modern deposits of the Western Arctic Shelf: 1. autochthonous-palimpsestic; 2. terrigenic-palimpsestic; 3. chiefly terrigenic; 4. solely terrigenic.

8.5 Sedimentological factors

All the hydrographical, lithological-geochemical and other sedimentological characteristics obtained (67 items in all) were analysed using a Q-factor analysis computer program to classify and group them into provinces of modern sedimentation. More than 84 % of the entire sedimentological system of the Western Arctic Shelf is defined by only two factors. The first, responsible for 54.9 % of the system, is the regime of recent sedimentation, and the second, determining 29.7 % of the system, is the hydrodynamic activity in the sedimentary basin. These principal factors were considered in sections 8.1 and 8.2. The scheme used for dividing the Western Arctic Shelf into regions is shown in Figure 8.11. Figure 8.12 illustrates the outline of the classification of conditions and regimes of modern sedimentation.

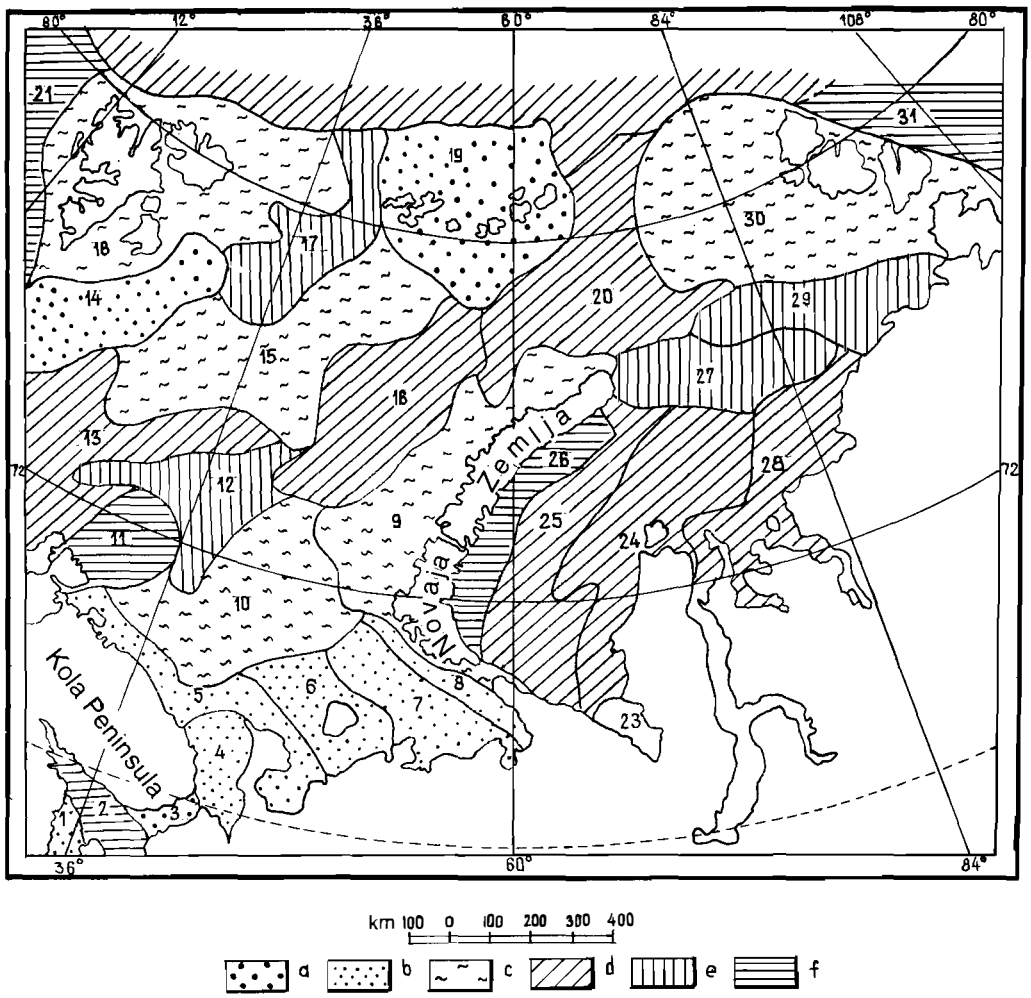

Fig. 8.11 Division of the Western Arctic Shelf into provinces of modern sedimentation using Q-factor statistical analysis of a variety of sedimentological data. a, b, c, d, e, f - dominant regimes of modern sedimentation (see Fig. 8.12). Sedimentary provinces: 1. Onega; 2. Kandalaksha; 3. Gorlo; 4. Mezen; 5. Kanin-Ribachy; 6. Malozemelskaya; 7. Bolshezemelskaya; 8. Korotayha; 9. Novaya Zemlya-Admiralteystwo; 10. South Barents; 11. Varanger; 12. Central Barents; 13. Nordkapp; 14. Medvezhy-Nadyezhda; 15. Eldholm-Victoria; 16. North Barents; 17. Franz-Persey; 18. Svalbard; 19. Vilchek; 20. Svyatoanninskaya; 21. Norway-Greenland; 22. North slope; 23. Baydaratskaya; 24. Preyamal; 25. East Litcke; 26. Prenovaya Zemlya; 27. Izvestinskaya; 28. Enisey-Pyasinskaya; 29. Nordensheldskaya; 30. North Kara; 31. Laptev.

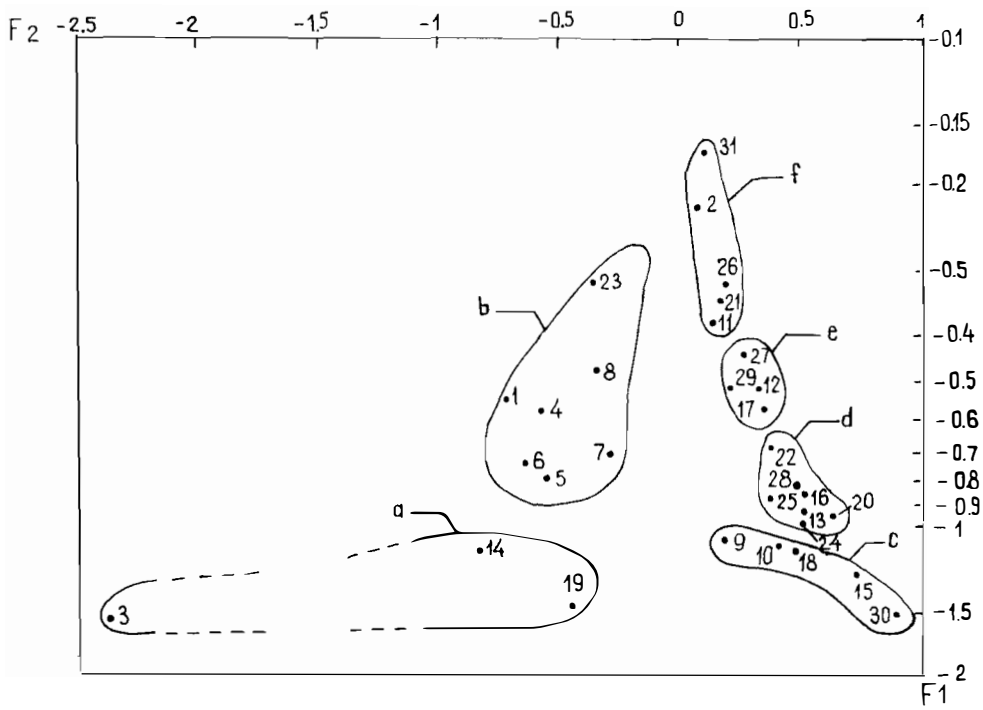

Fig. 8.12 Classification of regimes of modern sedimentation on the Western Arctic Shelf using data from Q-factor analysis of 67 lithological factors. Sedimentogenetic regimes: a. sedimentation in very shallow offshore areas with weak neotectonic and very intensive hydrodynamic activity; b. sedimentation in relatively shallow-water offshore areas with moderate neotectonic and high hydrodynamic activity; c. sedimentation on primary plains and plateaus with weak neotectonic and hydrodynamic activity, d. sedimentation in depressions and troughs with moderate neotectonic and weak hydrodynamic activity; e. sedimentation on submarine highs with significant neotectonic and moderate hydrodynamic activity; f. sedimentation on steeply sloping areas with high neotectonic and significant hydrodynamic activity. Figure 8.11 gives the locations and names of the sedimentary provinces.

9. GEO-ECOLOGY

Because the impact of modern sedimentary processes on the distribution and ecology of bottom assemblages varies a great deal (Matishov & Pavlova 1990), only some geo-ecological aspects relating to our own observations will be considered here.

9.1 Macrozoobenthos

The benthos of the Western Arctic Shelf was investigated at more than 5000 stations, where bottom sampling, dredging and submarine photosurveying were carried out (Gurevich & Kazakov 1989). These methods principally allowed a scheme to be devised showing the distribution of the main parameters of the macrozoobenthos (Table 9.1.1).

The distribution of the benthos biomass in the area is shown in Figure 9.1. Limited areas are occupied by potentially commercially viable invertebrates and their reserves have been estimated.

The resources provided by accumulations of Iceland scallops *Chlamys islandica* are estimated to be 62.8 thousand tons, common mussels *Mytilus edulis* and horse mussels *Modiolus modiolus* 42.8 thousand tons, and green sea urchins *Strongylocentrotus droebachiensis* 546.0 thousand tons.

The use of elaborate methods of graphical systematic analysis for isocorrelating in "indicative" space (Gurevich 1990a) enabled an estimation of the roles of sedimentological and other factors in determining the distribution of commercially viable invertebrate bioresources (Table 9.1.2).

9.2 Microbiological activity of sediments

Trunova, Gurevich & Izgoreva (1976) investigated the antibiotic effect of spore-forming bacteria from bottom sediments of the Barents Sea and White Sea (195 stations). 55 active clones of spore-forming bacteria, mainly *Bacillus micoides* and *B. glutinosus*, were studied while they were affecting test microbes (Salmonella, Shigella, staphylococci and enterococci). The bacilli chiefly affected the Shigella and Salmonella, completely stopping their activity. Staphylococci can only be stopped by 6 clones of *Bacillus glutinosus*. Enterococci are the most resistant.

The upper surface-active layer deposits have maximum antibiotic activity. Clastic gravelly and sandy deposits, as well as fine clayey deposits, contain almost no spores of active clones. Maximum antibiotic activity is a characteristic feature of silty deposits in areas with a moderate hydrodynamic regime forming in the southwestern part of the Barents Sea under the influence of the near-shore and Nordkapp branches of the Gulf Stream.

9.3 Biotesting

The distribution of certain technogenic components of modern sediments is outlined in section 7.3, and their classification is dealt with in section 8.4. The total biotic influence of technogenic pollution was estimated in 1991 by biotesting the near-bottom waters using a culture of the Ciliate *Tetrahymena piriformis*. Figure 9.2 is a schematic map showing the quality of near-bottom waters compiled by the author from data obtained by Dr. S.V. Sumin at 74 stations in the White Sea, Kara Sea and the southern part of the Barents Sea. Polluted deposits and waters are found in the near-shore zone, especially the mouths of the large rivers near major urban agglomerations.

9.4 Geo-ecological potential

The natural potential of the sea floor includes the resources of the bottom sediments, the bottom landscape and the beach landscape. Fig. 9.3 shows a classification of such resources on the Western Arctic Shelf, mainly determined on the basis of sedimentological techniques and geo-ecological mapping.

Table 9.1.1 Parameters for the distribution of the macrozoobenthos on the floor of the Western Arctic Shelf

Parameters	*% of shelf area*		
	White Sea	*Barents Sea*	*Kara Sea*
Biomass of benthos, g/m^2			
< 1	3.6	14.6	5.6
1–10	34.8	22.4	36.5
10–100	54.0	46.3	50.7
100–300	6.9	12.9	6.7
300–1000	0.7	3.6	0.5
> 1000	0.0	0.2	0.0
Variability of benthos, number of forms of benthic organisms per m^2			
< 5	5.0	20.5	13.9
5–10	28.2	33.2	32.7
10–20	57.8	33.0	49.1
20–30	0.8	12.3	3.6
30–40	0.2	0.9	0.6
> 40	0.0	0.1	0.1
Trophic groups			
immobile sestonophagous	46.1	12.0	1.5
mobile sestonophagous	51.9	18.0	35.6
collecting detritophagous	0.0	22.9	56.4
non-collecting detritophagous	2.0	17.9	6.5
omnivorous organisms	0.0	1.1	0.0
mixed groups	0.0	23.1	0.0

Table 9.1.2 Sedimentological and other factors determining the distribution of bioresources on the Western Arctic Shelf

Factors	***Connection with bioresources*** *Character of monotonous connection*	*Maximum correlations*	*Optimum values of factors*
1. Bituminosity of sediments (%)	positive	0.73	2–5
2. Type of bituminoids	positive	0.70	mixed bituminoids
3. Authigenic ferruginous minerals	positive	0.74	carbonates
4. Geomorphological position	–	0.71	bottom plains
5. Variability of benthos, number of species	positive	0.72	> 20
6. Colour of sediments	positive	0.63	green
7. Content of clay fraction, %	negative	0.59	< 10
8. Gradient of velocity of near-bottom currents (m/sec per 100 km)	positive	0.56	about 1
9. Salinity (°/oo)	positive	0.54	33–35
10. Regime of sedimentation	positive	0.53	denudational-accumulative
11. Depth of the sea (m)	negative	0.50	50–100
12. Temperature gradient (°C/100 km)	positive	0.49	4–5
13. Temperature of the bottom (°C)	–	0.49	0 to +1
14. Trophic groups	bimodal	0.47	sessile sestonophagous carnivores
15. Distance from shoreline (km)	–	0.42	25–50
16. Velocity of near-bottom currents (m/sec)	positive	0.42	0.3–0.5
17. Biogenic carbonates in sediments (%)	–	0.41	> 25
18. Content of $C_{organic}$ (%)	bimodal	0.37	< 0.5 and > 2
19. Content of sand (%)	positive	0.34	50
20. Granulometrical size	–	0.29	pebbles, sand

The data obtained may be useful for choosing areas that are favourable for accumulating commercially viable invertebrates, and for optimising the location of facilities for mariculture.

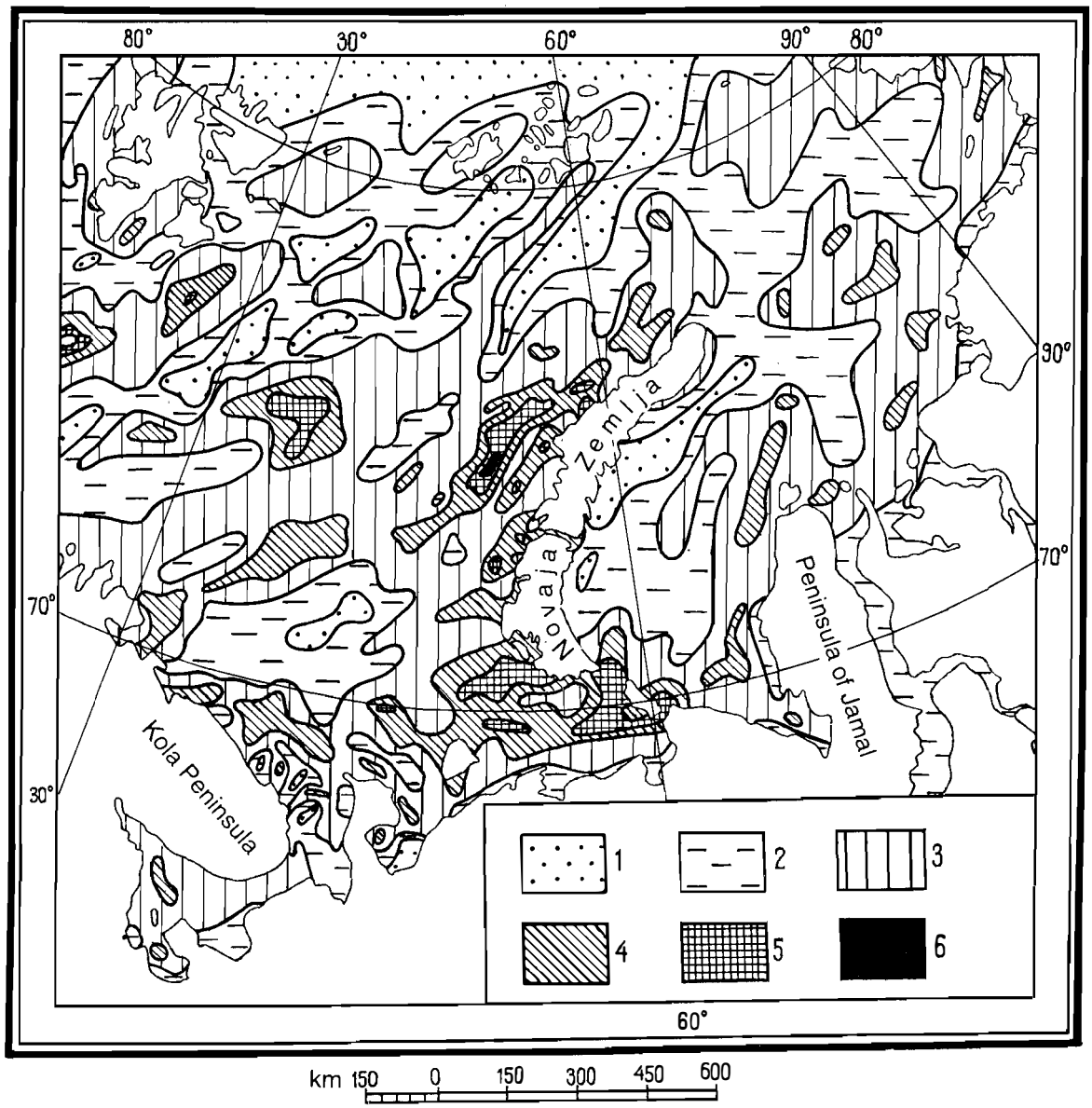

Fig. 9.1 The biomass of the benthos (g/m^2) on the Western Arctic Shelf: 1. < 1; 2. 1 to 10; 3. 10 to 100; 4. 100 to 300; 5. 300 to 1000; 6. > 1000.

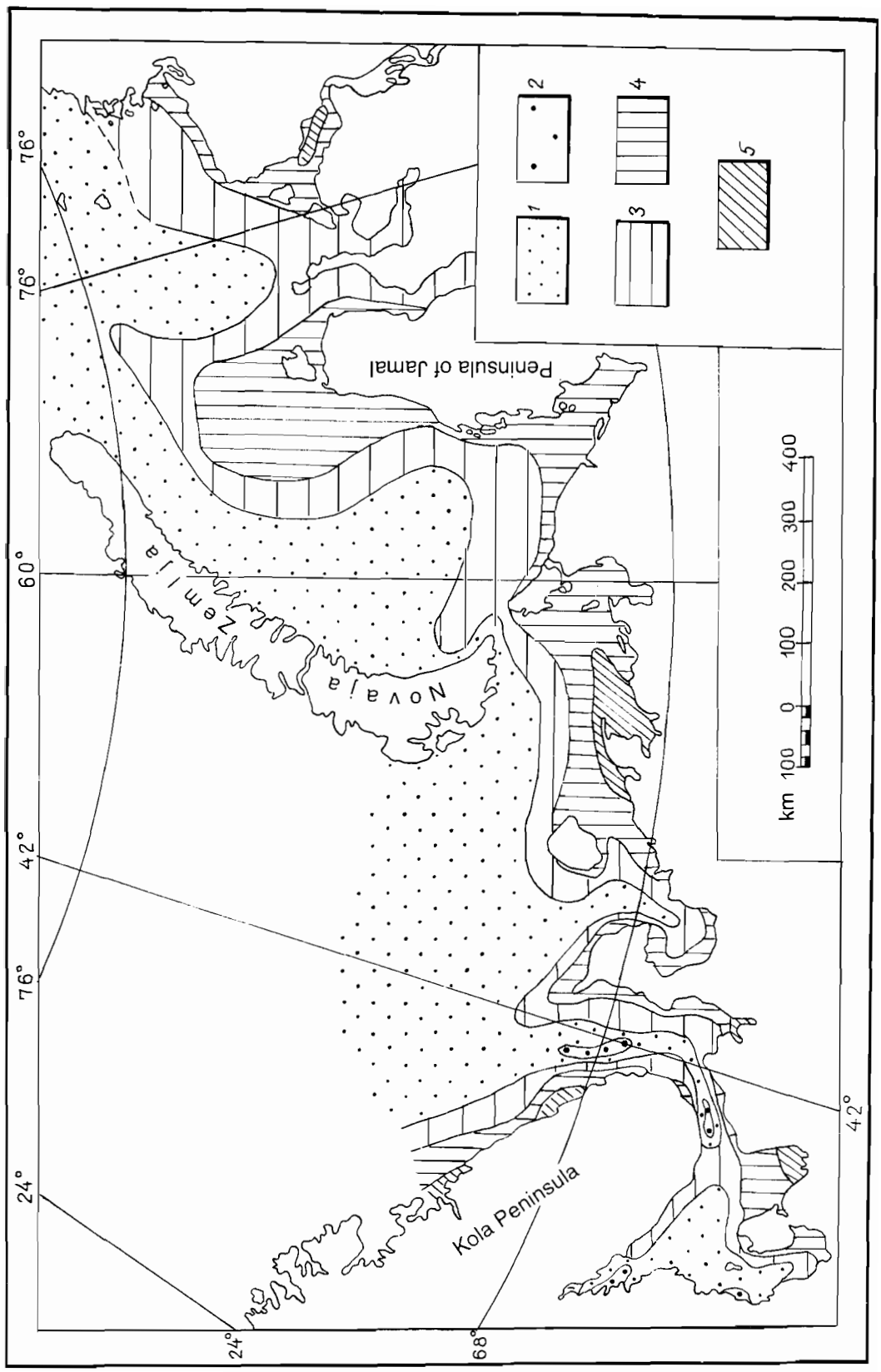

Fig. 9.2 Biotesting of the quality of near-bottom marine water on the Western Arctic Shelf based on three-day cultures of the Ciliate *Tetrahymena piriformis*, clone GL: 1. high quality (growth inhibition < minus 10 %); 2. relatively high quality, only weak organic pollution (no growth inhibition); 3. moderate quality (growth inhibition minus 10 % to minus 25 %); 4. poor quality (growth inhibition minus 25 % to minus 50 %); 5. extremely poor quality (growth inhibition exceeded minus 50 %).

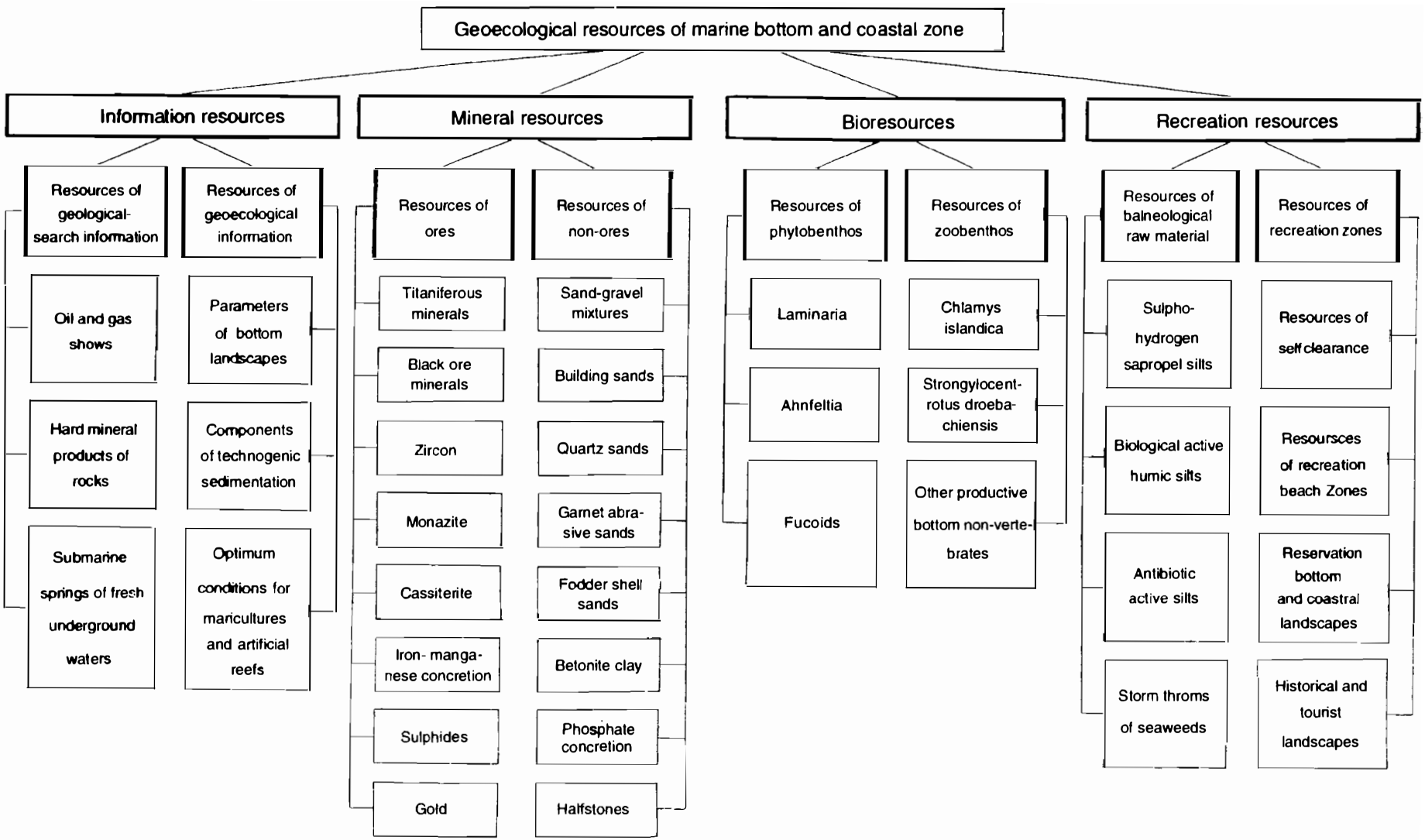

Fig. 9.3 Classification of the components of the natural geo-ecological resources of the sea floor and coastal zone (based on data from the Western Arctic Shelf).

CONCLUSIONS

1. Lithogenic, siliciclastic and clayey deposits dominate the modern sediments of the Western Arctic Shelf. They comprise two types: far-transported, entirely terrigenic sediments, and autochthonous-palimpsestic deposits that are located *in situ* or have only been transported a short distance. The allochthonous, terrigenic sediments have a regional type of distribution, whereas the autochthonous-palimpsestic sediments have a local distribution, their composition corresponding with that of the underlying rocks in every respect (petrographical-mineralogical, geochemical, palynological, etc.).

2. Biogenic carbonate sedimentation is not, in general, a characteristic feature of the Western Arctic Shelf, but near the polar front boundaries there are marked zones of carbonate sedimentation of avalanche-like character. The main lime-secreting organisms are barnacles *Balanus* sp., which is atypical because *Cirripedia* are not usually sediment-forming organisms.

3. The main factors of modern sedimentation are the recent sedimentary regime and the hydrodynamic activity of the near-bottom water layer. These account for 84 % of the sedimentological parameters and other environmental features, including the distribution of the macrobenthos and commercially viable invertebrates.

4. Maps showing the sedimentological and other characteristics of the environment are the parametrical and conceptual bases for predicting the mineral, biological and other natural resources of the Barents Sea, White Sea and Kara Sea.

5. New systems for classifying sediments (dynamic, granulometrical, genetic, and using the content of technogenic components, etc.) have been evolved during the investigations of modern sedimentation on the Western Arctic Shelf. The author hopes these will be useful in investigations of modern sedimentation in other seas.

ACKNOWLEDGEMENTS

The author is grateful to his wife, Dr. Tamilla V. Yakovleva, for various technical and scientific assistance in her capacity as a marine geologist. He is also indebted to his friend Dr. Jury G. Samoilovich for assisting in translating the text into English and to Richard Binns M.Sc. for greatly improving the English and preparing the manuscript for publication. The author considers it a great honour to have the opportunity of publishing his work through the Norwegian Polar Institute and is sincerely grateful to Dr. Anders Solheim and the administrative staff of the institute for their considerate attention and great assistance.

REFERENCES

Dibner, V.D. 1978: Morphostructura shelfa Barentseva morya. Nedre, St. Petersburg, 211 p.

Gurevich, V.I. 1976: Issledovaniya organogennyh komponentov v donnyh otlozheniyah juzhnoiy chasti Barentseva i Belogo moreiy. *In*: *Biologiya Barentseva i Belogo moreiy,* 93–102. Isd. KF AN SSSR, Apatity.

Gurevich, V.I. 1986: Metodicheskie rekomendatsii po granulometricheskomy klassifitsirovaniju osadkov. Isd. PGO Sevmorgeologiya, St. Petersburg, 18 pp.

Gurevich, V.I. 1988: Sedimentologicheskie faktory raspredeleniya ZHMK na Zapadno-Arkticheskom shelfe. *In*: *Geologiya i geohimiy zhelezo-margantsevyh konkretsiy Mirovogo okeana,* 81–92. Isd. PGO Sevmorgeologiya, St. Petersburg.

Gurevich, V.I. 1990a: Metod sistemnoiy kartograficheskoiy korrelyatsii. *In*: *Prognozirovanie tverdyh poleznyh iskopaemyh v Mirovom okeane* (na osnove EVM), 43–51. Isd. PGO Sevmorgeologiya, St. Petersburg.

Gurevich, V.I. 1990b: Prikladnaya sedimentologiya i Geoekologiya. Uchebnoe posobie. Isd. Len. Gorn. Inst. 64 pp.

Gurevich, V.I. & V.B. Hasankaev, 1974: K teorii rasprostranenija donnogo kamennogo materiala v morskih osadkah i o metodah izuchesniya DKM. *In*: *Geograf. aspekty problemy osadkoobrazo- vaniya v basseiynah Barentseva i Belogo moreiy,* 70–91. Isd. Sev. filiala Geograf. obshch., St. Petersburg.

Gurevich, V.I. & L.G. Pavlova, 1974: Physiko-chimicheskie parametry donnyh otlozheniy Belogo morja. *In*: *Geograf. aspekty problemy osadkoobrazovaniya v basseiynah Barentseva i Belogo moreiy,* 142–158. Isd. Sev. filiala Geograf. obshch., St. Petersburg.

Gurevich, V.I. & T.V. Yakovleva, 1976: Moshchnost ryhlyh otlozheniy i dochetvertichniy relief v Voronke i Gorle Belogo morya. *In*: *Geomorfologiya i geologiya chetvertichnogo perioda Severa Evropeiyskoiy chasti SSSR,* 38–46. Isd. Karelskogo filiala AN SSSR, Petrozavodsk.

Gurevich, V.I. & N.I. Kazakov, 1981: Sostav i fatsialnodinamicheskie tipy donnyh otlozheniy juzhnoiy chasti Barentseva morya. *In*: *Litologia i paleogeografiya Barentseva i Karskogo moreiy,* 41–54. Isd. NIIGA, St. Petersburg.

Gurevich, V.I. & N.I. Kazakov, 1988: Analiz fatsialnodinamicheskih factorov sedimentatsii (na primaere Voronki Belogo morya). *In*: *Geologicheskie i geograficheskie problemy osvoeniya prirodnyh resursov severnyh moreiy,* 52–62. Isd. Sev. filiala Geograf. obshch. SSSR, Murmansk.

Gurevich, V.I. & N.I. Kazakov, 1989: Vremennye metodicheskie rekomendatsii po landshaftnoekologicheskomu kartirovaniju pri geologicheskoiy siemke shelfa. Isd. PGO Sevmorgeologiya, St. Petersburg. 41 pp.

Gurevich, V.I. & E.E. Musatov, 1988: Pozdnekaiynozoiyskaya sedimentatsiya i strukturnyiy plan osadochnoho chehla na Zapadno-Arkticheskom shelfe. *In*: *Geologiya i mineralno-syrievye resursy Evropeiyskogo Severo-Vostoka SSSR,* 49–50. Tezisy dokl. na Vses. konf. Isd. Komi nauchnogo tsentra Ur O AN SSSR, Syktyvkar.

Gurevich, V.I. & N.P. Vlasova, 1983: Moshchnost ryhlyh otlozheniiy i intensivnost posdnekaiynozoiyskoiy sedimentatsii v juzhnoiy chasti Barentseva shelfa. *In*: *Osadkonakoplenie v shelfovyh zonah, 76–81. Isd. PGO Sevmorgeologiya, St. Petersburg.*

Gurevich V.I., B.G. Lopatin & E.E. Musatov, 1984: Fotoanomalii na kosmicheskih snimkah Zapadno-Arkticheskogo shelfa. *In*: *Kosmo-geologicheskie metody issledovaniya v Arktike,* 94–108. Isd. PGO Sevmorgeologiya, St. Petersburg.

Klenova, M.V. 1960: Geologiya Barentseva morya. ISD AN SSSR, Moscow, 365 pp.

Lopatin, B.G. & V.I. Gurevich, 1990: Instruktsiya po organizatsii i proizvodstvu melkomasshtabnoiy geoecologicheskoiy siemki shelfa i sostavleniju Gosudarstvennoiy geologicheskoiy karty shelfa SSSR masshtaba 1:1 000 000. Isd. PGO Sevmor- geologiya, St. Petersburg, 98 pp.

Matishov, G.G. & L.G. Pavlova, 1990: Obshchaya ekologiya i paleogeografiya polyarnyh okeanov. Nauka, St. Petersburg, 223 pp.

Nevesskiy, E.N., V.S. Medvedev & V.V. Kalinenko, 1977: Beloe more. Sedimentogenez i istoriya razvitiya v golotsene. Nauka. Moscow, 234 pp.

Romanovskiiy, S.I. 1988: Fisicheskaya sedimentologiya. Nauka, St. Petersburg, 238 pp.

Solheim, A. & Y. Kristoffersen, 1984: Sediments above the upper regional unconformity: thickness, seismic stratigraphy and outline of the glacial history. Norsk Polarinstitutt Skrifter 179B, 3–26.

Trunova, O.N., V.I. Gurevich & T.I. Izgoreva, 1976: Ob antibioticheskoiy aktivnosti sporoobrazujushchih bakteriy is donnyh otlozheniy Barentseva i Belogo moreiy. *In*: *Vliyanie zagryazniteleiy na morskie organizmy, 27–30.* Isd. KF AN SSSR, Apatity.

Yakovleva, T.V. & V.I. Gurevich, 1974: Rakushechnye otlozheniya Voronki Belogo morya. *In: Donnye otlozheniya i biogeotsenozy Barentseva i Belogo moreiy,* 3–22. Isd. KF AN SSSR, Apatity.